A STUDY INTO THE EFFECT OF RBM5 EXPRESSION ON A SMALL CELL LUNG CANCER CELL LINE

by

Justin Gaston Roy

A thesis submitted in partial fulfillment
of the requirements for the degree of
Master of Science (MSc) in Chemical Sciences

The School of Graduate Studies
Laurentian University
Sudbury, Ontario, Canada

THESIS DEFENCE COMMITTEE/COMITÉ DE SOUTENANCE DE THÈSE
Laurentian Université/Université Laurentienne
Faculty of Graduate Studies/Faculté des études supérieures

Title of Thesis Titre de la thèse	A STUDY INTO THE EFFECT OF RBM5 EXPRESSION ON A SMALL CELL LUNG CANCER CELL LINE
Name of Candidate Nom du candidat	Roy, Justin
Degree Diplôme	Master of Science
Department/Program Département/Programme	Chemical Sciences
Date of Defence Date de la soutenance	July 28, 2016

APPROVED/APPROUVÉ

Thesis Examiners/Examinateurs de thèse:

Dr. Leslie Sutherland
(Supervisor/Directeur(trice) de thèse)

Dr. Eric Gauthier
(Committee member/Membre du comité)

Dr. Amadeo Parissenti
(Committee member/Membre du comité)

Dr. Paola Marignani
(External Examiner/Examinateur externe)

Approved for the Faculty of Graduate Studies
Approuvé pour la Faculté des études supérieures
Dr. Shelley Watson
Madame Shelley Watson
Acting Dean, Faculty of Graduate Studies
Doyen intérimaire, Faculté des études supérieures

ACCESSIBILITY CLAUSE AND PERMISSION TO USE

I, **Justin Roy**, hereby grant to Laurentian University and/or its agents the non-exclusive license to archive and make accessible my thesis, dissertation, or project report in whole or in part in all forms of media, now or for the duration of my copyright ownership. I retain all other ownership rights to the copyright of the thesis, dissertation or project report. I also reserve the right to use in future works (such as articles or books) all or part of this thesis, dissertation, or project report. I further agree that permission for copying of this thesis in any manner, in whole or in part, for scholarly purposes may be granted by the professor or professors who supervised my thesis work or, in their absence, by the Head of the Department in which my thesis work was done. It is understood that any copying or publication or use of this thesis or parts thereof for financial gain shall not be allowed without my written permission. It is also understood that this copy is being made available in this form by the authority of the copyright owner solely for the purpose of private study and research and may not be copied or reproduced except as permitted by the copyright laws without written authority from the copyright owner.

Abstract

RNA Binding Motif domain protein 5 (RBM5) has been described as a lung cancer tumour suppressor gene. It influences the cell cycle, apoptosis, and the alternative splicing of various genes. In this study, the function of RBM5 was examined in a small cell lung cancer cell line, GLC20, in which RBM5 is deleted. GLC20 sublines expressing RBM5 were used for this study. It was observed that increased RBM5 expression associated with an increase in GLC20 cell death in the presence of cisplatin and a decrease in GLC20 cell proliferation. Increased RBM5 expression also resulted in a decrease in the EC_{50} of GLC20 cells towards cisplatin. The type of cell death triggered by both RBM5 expression and cisplatin treatment was observed to be apoptosis. Increased RBM5 expression resulted in changes in RBM10 alternative splicing. These results suggest that RBM5 expression may be important in the development of small cell lung cancer.

Keywords

RBM5, small cell lung cancer, cisplatin, GLC20, apoptosis, proliferation, cell death, RBM10, tumour suppressor

Acknowledgments

To begin, I would first like to thank my supervisor Dr. Leslie Sutherland who gave me the opportunity to work in her lab. Throughout my Master's you have taught me nearly everything I know in research, from how to do the simplest of tasks to reviewing papers for publication to helping me with my organization and writing. Your willingness to allow me to try to solve my own problems in the lab, and then stepping in when help needed was greatly appreciated. In addition, your dedication to the lab, your students, and proper research is unrivaled and something I am truly grateful of. I thank you for your mentorship and guidance in successfully completing my Master's degree and becoming the researcher and person I am today.

I would like to also thank my committee members, Dr. Amadeo Parissenti and Dr. Eric Gauthier for their time and commitment through numerous committee meetings. You time and input during my Master's was truly helpful and appreciated.

A big thank you goes to all Sutherland Lab members, specifically Benjamin Koenderink, Sarah Hunt and Julie Loiselle. I thank you all for teaching me different techniques within the lab and helping me get started. I also thank you for all the guidance and help you gave me when experiments didn't work or when I didn't know what step to take next. Benjamin also provided some Western blot analysis in Figure 14 biological replicate 1. In addition, I would like to thank all of those at the Health Sciences Northern Research Institute, especially all members of the Sutherland Lab group over the years. You all listened to me when times were tough and had a laugh with me when times went well.

Lastly, I dedicate this to all those in my family who have suffered cancer, including my brother. I hope that my research and research like it eventually lead to better discovery and treatment.

Table of Contents

List of Tables

List of Figures

List of abbreviations

°C – degree Celsius

µg – microgram

µL – microgram

µM – micromolar

7-AAD – 7-aminoactinomycin D

A – ampere

BAX – BCL-like protein 4

bp – base pair

BR – biological replicate

c-FLIP – FLICE-like inhibitory protein

d – deionized

DMSO – dimethylsulfoxide

EC50 – half-maximal effective concentration

EDTA - ethylenediaminetetraacetic acid

EGFR – epidermal growth factor receptor

EGTA - ethylene glycol-bis(2-aminoethylether)-N,N,N′,N′-tetraacetic acid

ES - extensive stage

g – g-force or relative centrifugal force

GAPDH – glyceraldehyde 3-phosphate dehydrogenase

h – hour

HER-2/NEU – human epidermal growth factor receptor 2

HRP – horseradish peroxidase

IC50 – half-maximal inhibitory concentration

KD – knockdown

LS – limited stage

LUCA15 – Lung Cancer 15

LUST - Luca 15 Specific Transcript

min – minute

mL – millilitre

ms – millisecond

MTT - 3-(4,5-dimethylthiazol-2-yl)-2,5-diphenyltetrazolium bromide

NSCLC – non small cell lung cancer

n.s – not significant

OCRE – octamer repeat

PARP – Poly (ADP ribose) polymerase

PCR – polymerase chain reaction

PTEN - Phosphatase and tensin homolog

PVDF - polyvinylidene fluoride membrane

RB – retinoblastoma protein

RBM – RNA binding motif

RBM10v1/v2 – RBM10 variant 1 and variant 2

RNP – ribonucleoprotein domain

RRM – RNA recognition motif

s – second

SCLC – small cell lung cancer

shRNA – short hairpin RNA

TAE - Tri-Acetate-EDTA

TARP syndrome – Talipes equinovarus, Atrial septal defect, Rbonin Sequence, and Persistent left superior vena cava)

TNF – tumour necrosis factor

TRAIL – TNF-related apoptosis-inducing ligand

U - unit

V – volt

v1 – Variant 1

v2 – Variant 2

Chapter 1

1 Introduction

1.1 RBM5

The RNA Binding Motif protein 5 gene, otherwise known as *RBM5*, codes for an RNA binding protein and is located on the short arm of chromosome 3 [1,2]. *RBM5* was first cloned and identified as *LUCA-15* (Lung Cancer gene 15) in 1996, and it was found within a region that is commonly deleted in lung cancers, 3p21.3 [1,3]. Since 1996, it was cloned three others times: as *H37* [4] and *RBM5* [5] in 1999, and as *LUCA15* in 2000 [6].

The *RBM5* gene is comprised of approximately 30,000 base pairs that are transcribed into an mRNA transcript that is approximately 3,000 bases long. This transcript contains 25 exons and possesses an open reading frame that codes for a protein of 815 amino acids [2] (Figure 1). Three alternative-spliced variants of RBM5 have been identified. A frameshift caused by the exclusion of exon 6, resulting in a premature stop codon, gives rise to a transcript named RBM5Δexon6 [7]. Secondly, the addition of introns 5 and 6 results in a premature stop codon in intron 5, resulting in a transcript named RBM5+5+6 [6,8]. Lastly the inclusion of intron 6 results in a premature stop codon within the mRNA, and yields a transcript named RBM5+6 [5,6,8,9]. RBM5 also has an anti-sense product referred to as LUST. LUST (Luca 15 Specific Transcript) spans (exons included) a 1.4 kb region ranging from intron 6 to intron 4 of the RBM5 gene [10]. This study focuses solely on full-length RBM5 and its function.

The RBM5 protein has a predicted size of 90 kDa [5]. This was confirmed *in vitro*, in 1999, through the incorporation of ^{35}S-methionine through a transcription/translation system [4]. On electrophoresis gels, RBM5 isolated from cells has a molecular weight of between 100-120 kDa

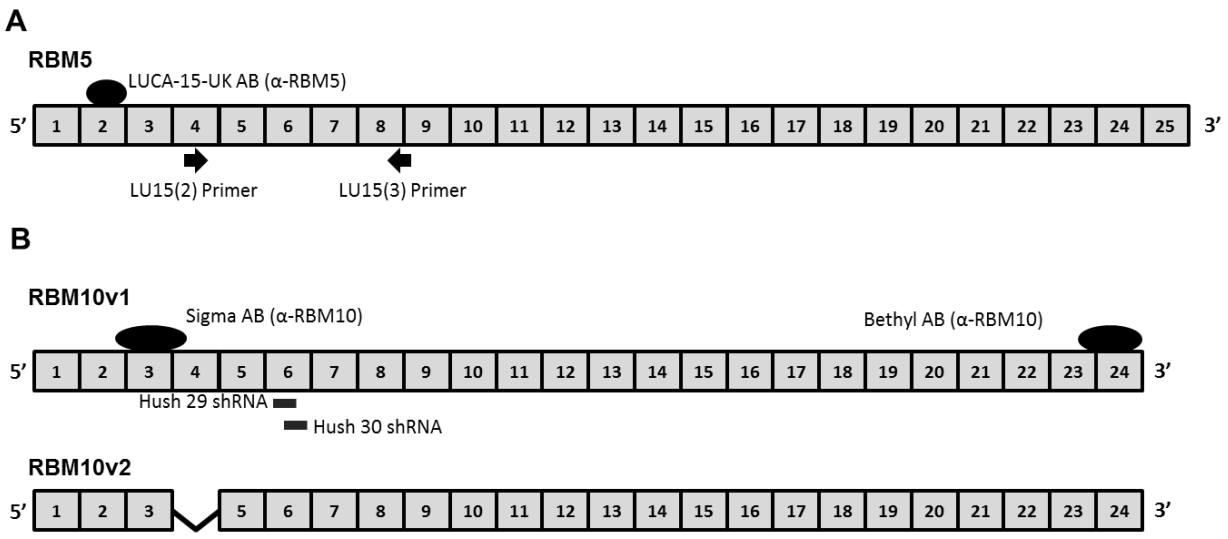

Figure 1. Schematic representation of the exons of RBM5 and RBM10v1/v2. Reported transcripts for both (A) RBM5 and (B) RBM10v1/v2. Exons are represented by grey boxes outlined in black. Box sizes are not representative of actual exon size. Black ovals represent approximate location of the epitopes recognized by the antibodies used in this study. Black lines with arrows represent the approximate location of RBM5 primers used in this study. Solid black lines represent the approximate location of shRNA RBM10 targets, which were not variant specific. Corresponding names of antibodies, primers and shRNA are listed next to their approximate location. Figure was adapted from ref #29.

[8,11]. The RBM5 protein has been shown to be reversibly phosphorylated, possibly indicating a method by which RBM5 function is regulated (to be discussed later) [12].

RBM5 shows amino acid sequence homology with two other functionally related proteins, RBM6 and RBM10 Variants 1 and 2 (RBM10v1 and RBM10v2, respectively). RBM6, also located within the 3p21.3 region, shares ~30% sequence homology with RBM5 [2,5]. RBM10, located on the X chromosome at Xp11.23 [13], shares sequence homology with RBM5 with RBM10v1 (49%) and RBM10v2 (53%) [2]. These values increase to 60% and 64%, respectively, when exons 4, 9 and 16 are removed [2]. This shared sequence similarity is thought to be a mechanism of regulation of RBM5 [14] and may demonstrate the importance of RBM5 expression.

1.1.1 Expression

Full length RBM5 is ubiquitously expressed throughout all primary tissue and non-tumour cell lines in humans. RBM5 is most highly expressed in heart and skeletal muscle tissue and in the pancreas, as detected by Northern blot analysis [8,9,15,16]. RBM5 was also shown to be expressed at low levels in the liver [9,15]. Most RBM5 expression studies have been performed in tumour cell lines and tissues. In 2002, it was shown that RBM5 was downregulated 82% at the mRNA level and 73% at the protein level in primary non-small cell lung cancer (NSCLC) tissue when compared to normal tissue [16]. These findings have been confirmed in two additional studies [17,18]. In addition, it has been shown that RBM5 is downregulated in HRAS(G12V) transformed Rat-1 cells [6]. Other reports have noted that there is also a decrease in RBM5 expression in vestibular schwannomas [19], cancerous prostatic tissue [20], biliary tract cancers [21], pancreatic ductal adenocarcinoma [22], and stage III ovarian carcinomas [23], compared to normal tissue. RBM5 expression decreases in a cisplatin-resistant A549 lung adenocarcinoma cell line relative to a non-resistant A549 cell line [24]. The *RBM5* gene has also been observed to be deleted in three small cell lung cancer (SCLC) cell lines [15,16,25]. In contrast RBM5 mRNA was upregulated, when the human epidermal growth factor receptor 2 (Her-2) was overexpressed in MCF-7 breast cancer cells and CaOv-3 ovarian cancer cells [4]. In non Her-2 over-expressing breast cancer samples a positive correlation between Her-2 and RBM5 expression has been noted [4,26]. It was conversely reported that RBM5 mRNA was downregulated in breast cancer samples with no reference to Her-2 expression, suggesting RBM5 expression levels may be regulated through the activity of extracellular growth factors, such as Her-2 [6].

In other biological systems, RBM5 was found to be upregulated after both traumatic mouse brain and rat spinal injuries [27,28]. During skeletal and cardiac muscle differentiation, RBM5 protein

expression decreased over time [29]. RBM5 expression was also found to be different between the adult and the fetal thymus; expression increased in the adult thymus, suggesting it may be developmentally regulated [9]. The observed changes in RBM5 expression indicate that RBM5 levels may be highly regulated in cells and that its function is important in various biological systems.

1.1.2 Regulation

As reviewed in Sutherland et al, 2010, RBM5 regulation is poorly understood [25]. Interestingly, it appears as though RBM5 expression is highly regulated in lung cancers, as it is consistently downregulated [15]. RBM5 shares similarities in structural motifs with its functional homologues RBM6 and RBM10v1 and v2 [2,5]. This duplication of similar functioning genes to different parts of the genome (3p21.3 and Xp11.23) has been suggested to be of evolutionary importance to ensure proper regulation of RBM5 or RBM5-like protein expression [5,14]. Loss of heterozygosity of a common 370 kb portion of 3p21.3, which includes *RBM5*, was observed in over 95% of SCLC and over 70% of NSCLC suggesting that the reduction of RBM5 expression, and possible other genes located in the deleted region, leads to the development of lung cancers [1,15,25,30,31,32]. Few mutations in *RBM5* have been noted [5,33]. Promoter hypermethylation studies to date do not suggest that the promoter of *RBM5* is methylated [34], however, as noted in Sutherland et al [25], more studies are needed to make this conclusion. Recently, the promoter of *RBM5* was shown to be mutated in melanoma samples, suggesting a possible mechanism of regulation or that the mutations reduced promoter function [35].

The size of the RBM5 protein is roughly 90 kDa [4,5] but it is typically detected in SDS-PAGE electrophoresis at between 100 kDa and 120 kDa [11]. RBM5 is not N-glycosylated, but has been shown to be reversibly phosphorylated [12]. This phosphorylation appears to regulate the ability of

RBM5 to promote apoptosis, as it is phosphorylated in unstressed TF-1 human erythroleukemia cells but is dephosphorylated in serum-starved cells undergoing apoptosis [12]. RBM5 expression appears to be regulated in instances of chemotherapy drug-resistance as its expression decreases in cisplatin-resistant A549 cells [24]. RBM5 has also been observed to be downregulated by a RAS-activating mutation HRAS(G12V) [6]; however, it does not appear to be regulated by EGFR, which is upstream of RAS [36]. One can note, at least in the literature that RBM5 protein expression and function regulation is not very well understood.

Recently, it was shown that a functional homologue of RBM5, RBM10, might be involved in RBM5 expression regulation. RBM10 knockdown correlated with an increase in RBM5 protein expression in SHSY5Y neuroblastoma cells [27]. In a separate study, RBM10 protein bound to RBM5 pre-mRNA in HEK293 (human embryonic kidney cells), suggesting a possible mechanism for the regulation of the alternative splicing of RBM5 [37]. Lastly, it appears that RBM5 protein expression is regulated in skeletal and cardiac muscle differentiation, as its expression decreases during differentiation [29]. In summary, RBM5 expression appears to be highly regulated; however to date the mechanism for its regulation is poorly understood.

1.1.3 Function

In the past 15 years, much research has been undertaken in order to better understand the role of *RBM5* in different biological systems. *RBM5* is one of nine genes within a 17 gene signature associated with metastasis that are downregulated in various human solid tumours (including lung) [38]. In addition, RBM5 may inhibit Wnt signaling, a key player in tumour cell metastasis, as RBM5 knockdown in A549, Calu-6, BEAS-2B, H1299, and MCF-10A cells was associated with an increase in β-catenin protein expression and Rac1 protein activation [39]. The same study further established that low RBM5 expression in primary lung tumour samples from patients

correlated with increased lymph node metastasis [39]. A similar study in 2013 suggested that low RBM5 expression in pancreatic cancer is associated with increased lymph node metastasis [22]. These studies suggest, as reviewed by Dr. Sutherland in 2010 [25], that the downregulation of RBM5 protein may be a key component for progression of lung and other cancers.

RBM5 expression correlates negatively with the expression of other cancer-related genes suggesting that RBM5 plays a role in various signaling pathways. RBM5 mRNA was downregulated in Rat-1 rat embryonic fibroblast cells that express HRAS, a RAS mutant that is constitutively activated [6]. RAS mutations are noted in over 30% of lung cancers [40]. RBM5 expression negatively correlated with increases in EGFR and KRAS expression in NSCLC tissue samples, and increases in KRAS expression in pancreatic cancers, further suggesting that loss of RBM5 expression is required for cancer progression [18,22]. Another study performed in A549 adenocarcinoma cells demonstrated that RBM5 overexpression resulted in a decrease in EGFR mRNA and protein expression [41]. In A549 cells treated with cigarette smoke extracts, RBM5 protein and mRNA expression decreased as Wnt and β-catenin protein expression increased [42]. The same study demonstrated that RBM5 overexpression resulted in a decrease in Wnt and β-catenin protein, similar to what was shown in the Oh et al paper [39]. These results suggest that RBM5 regulates the Wnt signaling pathway upstream of Wnt and β-catenin [42]. *RBM5* is one of six genes needed for expression of AHR (aryl hydrocarbon receptor), whose expression, when dysregulated, can be carcinogenic [43]. These results further suggest that RBM5 may regulate signaling pathways such as Wnt/β-catenin or EGFR/RAS, and loss of RBM5 is required for cancer progression.

Apoptosis is a type of energy-dependent programmed cell death characterized by many different morphological events [44,45]. There are many other modes of cell death, such as necrosis and

autophagy; this study focused on apoptosis as RBM5 is a known modulator of apoptosis [46]. Apoptosis is defined by morphological events such as the shrinkage and blebbing of cells, chromatin condensation, loss of adhesion and the eventual phagocytosis by surrounding macrophages [44,45,47-49]. In addition, apoptosis can also be characterized by various biochemical markers including caspase activation and cleavage, poly (ADP-ribose) polymerase proteolysis, ATP consumption, loss of membrane asymmetry (phosphatidylserine flipping) and DNA fragmentation [45,48]. It is generally understood that apoptosis is activated through one of two major pathways, depending on the type of stressor [47]. These pathways are the intrinsic or mitochondria-based pathway and the extrinsic or death receptor pathway. Both pathways result in activation of pro-apoptotic proteins, followed by the initiation of morphological changes [47,48,50].

Most RBM5 research has been investigating the role of this protein in the cell cycle and in apoptosis. RBM5 sensitizes Jurkat human T lymphoblastoid cells to Fas ligand, TNF-α, and TRAIL death receptor ligand-mediated apoptosis and also sensitizes MCF-7 human breast adenocarcinoma cells to TNF-α mediated apoptosis [11,51]. A microarray study performed on a human leukemic cell line, CEM-C7, found that overexpressing RBM5 resulted in a change in expression of 35 genes involved in cell proliferation and apoptosis [52]. In the same cell line, overexpression of RBM5 resulted in a decrease in cell growth, and G_1 cell cycle arrest [7], which was also noted in A549 cells [17,53]. Overexpression of RBM5 also suppressed cell growth of human fibrosarcoma HT108 cells [6], A549 cells [17,53], RBM5 null MCF-7 cells [16], A9 mouse non-malignant fibrosarcoma cells [16], NSCLC H1299 cells [54] and PC-3 prostate cancer cells [20]. RBM5 overexpression also suppressed lung tumour growth [16,17]. In contrast, RBM5 does not appear to

affect the growth of all cancer cell lines as overexpression of RBM5 had no effect on Jurkat cell proliferation [11] and non-malignant HBL-100 immortalized human cells [16].

RBM5 appears to modulate apoptosis through various processes. Increased RBM5 expression in A549 adenocarcinoma cells resulted in reduced cell proliferation and cell cycle arrest in G_1 phase [17,53]. In the same cells, increased RBM5 expression promoted an increase in apoptosis via increased cytochrome c release, increased expression of the pro-apoptotic BAX protein, increased cleavage of the pro-apoptotic forms of Caspases 9 and 3, while downregulating Cyclin A expression and phosphorylated RB [53]. Increased chromatin condensation and DNA fragmentation was also observed [53]. Another study using A549 cells confirmed these results and demonstrated a decrease in protein expression of the anti-apoptotic BCL-2 and an increase in apoptosis observed through increased PARP cleavage and increased Annexin-V binding [17]. The ability of RBM5 to reduce cell proliferation has been shown to be independent of p53, as p53 null H1299 human NSCLC transfected with RBM5 demonstrated a loss in cell growth [53]. Overexpression of RBM5 anti-sense RNAs in Jurkat cells suppressed apoptosis mediated by Fas ligand, TNF-α, and staurosporine, but not etoposide, while the RBM5 anti-sense RNAs upregulated expression of the apoptosis inhibitor BCL-2 [55]. In cisplatin-resistant A549 cells, RBM5 overexpression reduced resistance to cisplatin by increasing cisplatin-induced apoptosis through an increase in cytosolic cytochrome c, cleaved Caspase 9 and 3 and chromatin condensation [24].

RBM5 function has been deemed important in the nervous system. Decreased RBM5 expression in SHSY5Y human neuronal cells resulted in decreased caspase activation after staurosporine exposure [27]. The same study showed an increase in RBM5 protein expression following traumatic brain injury and hemorrhagic shock, suggesting that RBM5 is required post-injury [27].

RBM5 knockdown in the same cell line resulted in increased expression of cellular FLICE-like inhibitory protein (c-FLIP), LETm1 Domain-Containing Protein 1 (LETMD1) and amyloid precursor-like protein 2 (APLP2) but decreased Caspase 2 [27]. In a similar study, RBM5 mRNA and protein expression increased following spinal cord injury along with pro-apoptotic BAX protein, tumour suppressor gene p53 and cleaved Caspase 3 [28]. RBM5 knockdown in neuronal PC12 cells resulted in decreased p53 expression [28]. This result is identical to a previous study that demonstrated increased p53 expression when RBM5 was expressed, and decreased p53 expression when RBM5 was knocked down in various cell lines [54]. RBM5 expression also potentiated p53 inhibition of H1299 cell growth in the same study. These results, with the previous results from Oh et al [53], suggest that RBM5 acts upstream of p53 when suppressing cell growth and activating apoptosis. Taken as a whole, RBM5 is a potent modulator of apoptosis and regulator of the cell cycle.

As an RNA-binding protein, RBM5 has been implicated in the alternative splicing of pre-mRNA involved in cell proliferation, the regulation of apoptosis and cell signaling pathways [56]. RBM5 and its functional homologue, RBM10, are components of pre-spliceosomal complexes [57,58]. RBM5 binds to spliceosomal complex proteins DHX15 and PRP19, with RBM5 stimulating DHX15 helicase activity (a process required in splicing of pre-mRNA) [59]. RBM5 promotes the exclusion of exon 9 of Caspase 2, resulting in the expression of a proapoptotic variant of Caspase 2 [60]. Retention of exon 9 results in a Caspase 2 isoform that does not induce apoptosis. RBM5 also promotes the exclusion of exon 6 of Fas receptor, resulting in a form of Fas that does not promote apoptosis [61]. In the same study, RBM5 influenced the exclusion of exon 7 of c-FLIP, leading to a variant that regulates apoptosis [61,62]. Interestingly, an anti-sense sequence of Fas has the ability to bind RBM5 and regulate the alternative splicing of Fas at exon 6 [63]. These

findings suggest a role for RBM5 in promoting the alternative splicing regulation of key proteins involved in apoptosis regulation. Recently, the two RRM domains in RBM5 were found to be required for both its alternative splicing function and its ability to modulate apoptosis and cell proliferation in A549 cells [64]. Overall, it appears as though the ability of RBM5 to regulate alternative splicing may be key to its function in regulating cell cycle progression and apoptosis.

RBM5 has also been implicated in the alternative splicing of other targets. Increased RBM5 expression resulted in an increase in exon 4 skipping of AID (Activation-induced cytidine deaminase) pre-mRNA, establishing a putative oncogenic isoform [65]. RBM5 enhances exon 40 and 72 skipping of Dystrophin pre-mRNA [66]. Dysregulation of Dystrophin protein expression results in diseases such as Duchenne Muscular Dystrophy (DMD), resulting in a loss of muscle and possibly death [67]. Exon skipping has shown to restore some function of Dystrophin protein, resulting in a less severe disease in some cases [68]. Lastly, RBM5 has been implicated in mouse spermatid differentiation, as a single missense mutation in the second RRM domain resulted in spermatid differentiation arrest and apoptosis [69]. The missense mutation resulted in a splicing error in 11 spermatid differentiation specific pre-mRNAs, suggesting proper RBM5 expression is required for spermatid differentiation [69]. The role of RBM5 in spermatid differentiation and Dystrophin alternative splicing suggests that RBM5 may have a role in development.

1.2 RBM10

1.2.1 Splice variants

RBM10 or RNA Binding Protein Motif 10, was first cloned and identified in 1995 from bone marrow tissue [13]. The *RBM10* gene is located on the X chromosome at Xp11.23 and has one allele silenced in each somatic cell through X chromosome inactivation [70,71]. *RBM10* has three

identified variants termed RBM10 variant 1 (RBM10v1), RBM10 variant 2 (RBM10v2) and RBM10 variant 3 (RBM10v3) [2,72,73]. As noted in Figure 1, RBM10v1 is the full length variant consisting of 24 exons, while RBM10v2 lacks exon 4 and consists of 23 exons [2,72]. RBM10v3 is a much smaller variant due to an alternate transcriptional start site and a 23 bp deletion in exon 4 that results in a premature stop codon [72]. Both RBM10v1 and RBM10v2 have alternative isoforms with or without the addition of one valine residue [74]. This study will focus on RBM10v1 and v2 expression and function, irrespective of the additional valine isoforms.

The *RBM10* gene is comprised by approximately 42,000 base pairs, which is transcribed into two mRNA variants. RBM10v1 is a 3402 base transcript which codes for a 930 amino acid protein [2]. RBM10v2 is a 3171 base transcript with 23 exons that lacks the 231 base exon 4. RBM10v2 codes for a protein 853 amino acids in size [2,73,74]. As mentioned previously, both RBM10v1 and v2 share roughly 50% protein sequence homology with RBM5 (49% and 53%, respectively) RBM10v1 protein is a 103 kDa protein while RBM10v2 codes for a 94.5 kDa protein. Both variants have alternative isoforms that either have or do not have an additional valine located at amino acid 354 for RBM10v1 and 277 for RBM10v2 [74]. The presence of the valine appears to inhibit the formation of one of the two α-helices located in the RRM tertiary structure [74].

Although RBM5 and RBM10 share a high degree of homology, they do have three exons that differ in the amino acid sequence they encode. Exon 4 of RBM10v1 is non-existent in RBM5, while exons 9 and 15, which are identical in both RBM10 variants, share only 14% homology with RBM5 [2]. Due to the high degree of homology, it would appear that RBM5 and RBM10 share some similar functions.

1.2.2 Expression

RBM10 is ubiquitously expressed throughout human primary tissue and cell lines [70,71]. *RBM10* is mutated in 7% of lung adenocarcinomas with an increased mutational incidence in males over females [40,75]. Furthermore, it has been reported that some *RBM10* mutations in lung adenocarcinomas result in a truncated form of the protein being expressed [75]. *RBM10* mutations have also been observed in pancreatic intraductal papillary mucinous neoplasms [76], and appear to correlate with longer survival times with treatment, despite leading to a more aggressive cancer [77]. *RBM10* mutations have also been implicated in TARP syndrome (Talipes equinovarus, Atrial septal defect, Robin sequence, and Persistent left superior vena cava) [73,78,37]. TARP syndrome is a rare developmental abnormality that results in early death within infancy [73,78,79]. Lastly, RBM10v1 protein expression decreases towards the end of rat skeletal muscle differentiation, while RBM10v2 mRNA and protein expression decreased in rat skeletal muscle differentiation. RBM10v2 protein expression also decreases in rat cardiac muscle differentiation [29].

1.2.3 Function

Before 2005, there was no data on how RBM10 functioned [2]. It is now understood that RBM10 is involved in the alternative splicing of various transcripts. Supporting this view, RBM10 has been purified in pre-spliceosomal complexes [57,58]. RBM10 was found to promote the exclusion of exon 18 of DLG4 (Discs Large Homolog 4 of post-synaptic density protein 95), while RBM10 knockdown resulted in an increase in the inclusion of exon 18 [80]. In addition, RBM10 influenced the alternative splicing of FasR, c-FLIP, and BCL-x, but not of Caspases 2, 3 and 9 [61,81]. In these instances, RBM10 appeared to influence exon 6 exclusion of FasR, resulting in an increase in the soluble of FasR, an anti-apoptotic protein, whereas it also activated pro-apoptotic forms of c-FLIP and BCL-x (S) [81]. Furthermore, RBM10 affected the alternative splicing of exon 11 in

NUMB, a key NOTCH pathway regulator, amongst other genes [56]. The NOTCH pathway is involved in regulating cell proliferation [56]. A study from the Sutherland group expanded on this research, demonstrating that a two-fold increase in the RBM10v1 isoform without a valine in the second RRM domain resulted in preferential expression of NUMB with the inclusion of exon 11, which is lung cancer specific [74]. With the role of RBM10 in alternative splicing, a model was produced in 2013 that describes the splicing mechanism of RBM10. As described in this model, RBM10 binds preferentially to intronic sequences that surround exons, resulting in exon exclusion [37]. Various nuclear localization signals in RBM10 have been reported, regulating its localization to the nucleus, further implicating its role in alternative splicing regulation [82].

RBM10 is involved in regulating cell proliferation and apoptosis. In primary chondrocytes induced to hypertrophy, an increase in RBM10 expression correlated with a decrease in cell proliferation and an increase in apoptosis [83]. In breast cancer specimens, RBM10 mRNA was positively correlated with Caspase 3 protein, an important apoptosis protein [84]. In another study with breast cancer specimens, RBM10v1 expression correlated with the expression of proapoptotic BAX and the tumour suppressor gene p53 [85]. In the same study, both variants of RBM10 mRNA were positively correlated with VEGF mRNA, a promoter of new blood vessel growth [85]. In the study that demonstrated RBM10 regulation of NUMB alternative-splicing, RBM10 knockdown increased the proliferation of HeLa cells [56]. A recent study in 2015 using SHSY5Y human neuronal cells showed that RBM10 knockdown augmented proapoptotic caspase activity after staurosporine exposure [27]. The same study showed that RBM10 expression increased after hemorrhagic shock and traumatic brain injury [27]. They also demonstrated that RBM10 knockdown resulted in an increase in RBM5 protein expression [27]. In a study performed by the Sutherland group, a connection between RBM10 expression and TNFα (tumour necrosis

factor) expression was drawn [72]. When RBM10 expression was knocked down, both TNFα mRNA and soluble TNFα protein expression decreased, resulting in decreased apoptosis [72]. When RBM10 was overexpressed, TNFα mRNA and soluble protein expression increased, resulting in increased apoptosis [72]. Thus, RBM10 appears also to be a modulator of apoptosis.

Lastly, RBM10 appears to play a role in the etiology of different diseases. In patients with metastatic melanoma, high RBM10 expression was correlated with increased aggression of the disease, but patients responded positively to treatment with BRAF inhibitors [86]. Further research is needed to fully understand its role in cellular processes as well as in various diseases.

1.3 Lung cancer

1.3.1 Incidence and prevalence

In both Canada and worldwide, lung cancer is the leading cause of cancer-related deaths [87,88,89]. In 2011, there were more than 1.5 million new cases of lung cancer and 1.3 million lung cancer related deaths worldwide [88]. Approximately 13.5% of new cases of cancer in Canada are lung cancer for both men and women, ranking third behind prostate and colorectal cancer for men and second behind breast cancer for women [89]. Canadian Cancer Statistics estimates that lung cancer is the leading cause of cancer-related deaths in Canada, with an estimated 26.6% men and 27% of women dying from cancer due to lung cancer. With the increase in lung cancer morbidity and mortality, lung cancer is a serious disease that warrants further research and understanding.

The World Health Organization states that the leading cause of lung cancer is tobacco related [87]. Approximately 85% of lung cancers are reported to be due to smoking [90]. Worldwide, smoking is the cause of 80-90% of men's lung cancers and 50% of women's lung cancers [87,91,92]. Furthermore, many cases of lung cancer occur in people who have never smoked or those who

have ceased smoking for many years [93,94]. Other known causes of lung cancer include, but are not limited to, exposure to asbestos, arsenic, radon, and polycyclic aromatic hydrocarbons [95]. In addition, in many Asian countries, there is an increase in lung cancer incidence amongst women due to increased indoor air pollution from coal-fuelled stoves and cooking fumes [96]. Although the primary cause of lung cancer is tobacco smoke, further research is warranted on the additional factors contributing to lung cancer incidence.

1.3.2 Subtypes

Lung cancers can be classified into two main subtypes: NSCLC and SCLC [87]. NSCLC has three major subtypes called adenocarcinoma, squamous cell carcinoma and large cell carcinoma, whereas SCLC has no subtypes [87]. Approximately 80-90% of all lung cancers are diagnosed as NSCLC and approximately 10-20% of all lung cancers are diagnosed as SCLC [87,97,98].

Lung cancers, like all other cancers, have many molecular aberrations compared to normal lung tissue, including mutational changes, gene expression changes, and chromosomal alterations [87]. Table 1 highlights the major chromosomal alterations that have been documented for each lung cancer subtype. The most common NSCLC chromosome changes are found as deletions within 1q, 8p, and 10q, which appear specific to NSCLC [87]. Common changes amongst all NSCLC and SCLC include deletions within chromosomes 3p, 4, 5q, and 10q, additions within chromosome 8q, and changes within chromosome 17 [87]. Of particular interest are deletions within chromosome 3p, since these are the earliest chromosomal aberrations that may contribute to lung carcinogenesis.

Table 2 provides examples of some of the major genetic alterations in the form of common mutation and expression changes for each subtype. As with all cancers, lung cancer has many

Table 1. Common chromosomal alterations found in lung cancer subtypes.

Lung Cancer	Subtype	Chromosomal aberrations
NSCLC	Adenocarcinoma	- 2q[99], 3p[87,32], 4q[87], 5q[87], 6q [87,99], 8p[87], 9p[87], 10q[99] 13q[87], 17q[99], 18q[87], 22q[87] + 1q[87], 5p[87], 8q[87], 20q[87]
	Large cell	- 3p12-14[87], 3p21[32], 4p[87], 5q21[87], 8p22-23[87], 8q[87], 21q[87] + 1q21-22[87], 3q[87], 8q[87]
	Squamous	- 3p21[32,87,100] , 4q[87], 5q[87], 8p22[100], 9p21-22[100], 10q[87], 11q[87], 13q[87, 100], 17p12-13[100], 18q[87], 21q[87] + 1q31[100], 3q25-27[100], 5p13-14[87, 100], 8q23-24[87, 100], 8p12[87], 11q13[87], 12p[87]
SCLC	None	- 3p (3p12-13, 3p4, 3p21, 3p24-26) [32,87] , 4p[87], 5q[87], 10q[87], 13q[87], 17p[87] + 3q[87], 5p[87], 6p[87], 8q[87], 17q[87], 19[87], 20q[87]

- loss of heterozygosity/homozygosity
+ gain of chromosomal region

different genetic alterations. Although there are many differences between the subtypes, there are also similarities and oddities. For example, the most common genetic alteration is found in the tumour suppressor gene *p53*, which has a loss-of-function mutation in the majority of all subtypes of lung cancer [40,87,101,103]. *KRAS* gain-of-function mutations are common in 30% of adenocarcinoma and are also present in large cell carcinoma; however, these mutations occur infrequently in both squamous cell carcinoma and SCLC [40,87,101,103]. Although not common in lung cancer, loss of PTEN function through decreased expression and/or loss-of-function mutations appears common in all subtypes [87,100,103]. Most of the NSCLC subtypes share many mutations and expression changes in Her-2/Neu, EGFR, PI3K, and Cyclin D1 and E [40,99,100,101]. SCLC, one of the major subtypes of lung cancers, appears to share very few genetic alterations with the other subtypes, however, there are a few genes with common alterations such as those that lead to upregulation of the oncogene MYC, in both SCLC and adenocarcinoma, and the

Table 2. Common molecular alterations found in lung cancer subtypes.

Lung Cancer	Subtype	Mutations	Expression Changes
NSCLC	Adenocarcinoma	KRAS (+)[40,87] , EGFR (+)[40,99] , BRAF (+)[40,99] , PI3K (+)[40], p53 (-)[40,87,99,] , RBM10 (-)[40], RIT1 (+)[40], MGA (-)[40], P16INK4 (-)[87, 99], STK11(-)[40]	COX2 (+)[87], HER2/Neu (+)[99], MET (+)[40,99] , MYC (+)[40], PTEN (-)[99], Cyclin D1 +E (+)[87, 99]
	Large cell	MEN1 (-)[87], KRAS (+)[87], p53 (-)[87]	P16INK4 (-)[87], Cyclin D1 +E (+)[87,99], Bax (-)[87], Bcl-2 (+)[87], PTEN (-)[99]
	Squamous	PIK3CA (+)[87], p53 (-)[87, 99,117], EGFR (+)[87,99], Her2/Neu (+)[87,99], PTEN (-)[99], PI3K (+)[99,101], HLA-A (-)[101], CDKN2A (-)[101], P16INK4 (-)[101], PIK3CA (+)[87], RB1 (-)[87,101]	SOX2 (+)[102,101] , FGFR (+)[87, 99,101], PTEN (-)[114,100,117] , CDKN2A (-)[101], Cyclin D1 +E (+)[87,99], EGFR (+)[101], P16INK4 (-)[87,99], FGFR1 (+)[100,101]
SCLC	None	RB1 (-)[87,103,104], SOX2 (+) [102], p53 (-)[87,103], PTEN (-)[103], RASSF1 (-)[104], FHIT (-)[104], FUS1 (-)[104]	RB1 (-)[87,103], SOX2 (+) [102], MYC (+)[87,116,103], E2F1 (+)[87], FGFR (+)[103], BCL-2(+)[87]

- loss of function mutation/decrease in expression
+ gain of function mutation/increase in expression

overexpression of SOX2 and FGFR1, in both SCLC and squamous cell carcinoma [40,99,100,101,102]. Lastly, of particular interest, RBM10 was found to be mutated in 7% of lung adenocarcinomas, with an increased incidence of mutation in males over females [40,75].

1.4 Small cell lung cancer

1.4.1 Characteristics

As mentioned previously, approximately 10-20% of all lung cancers are diagnosed as small cell lung cancer (SCLC), a major subtype of lung cancer [87,97,98]. Historically, SCLC was also termed

oat cell carcinoma, small cell anaplastic carcinoma and intermediate cell type [87]. SCLC tumours are characterized as small white tumours that are difficult to image through radiographs (X-ray or CT-scan) [87]. Cytological specimens show SCLC cells as characterized by scant cytoplasm dominated nearly entirely by the nucleus. The cells form clusters/sheets or irregular linear patterns [87]. Cells borders commonly blend together, making it difficult to identify individual cells [87]. At the time of diagnosis, SCLC has generally metastasized to other localized regions of the body (lymph nodes, central nervous system, brain) [87,104]. SCLC is considered the most aggressive subtype of all the lung cancer subtypes, and, in addition to metastasis, commonly develops resistance to chemotherapy, generally after demonstrating a good response to treatment [87,104]. Most patients with SCLC will relapse after the initial treatment shows a reduction of the disease [104].

SCLC has many different chromosomal and molecular aberrations compared to the corresponding normal lung tissue, as noted in Table 1 and Table 2. As mentioned previously, nearly 100% of all SCLCs have a chromosome 3p deletion, with over 95% of cases having at least loss of heterozygosity at the 3p21.3 region, containing *RBM5* [15,32,87]. Many specific mutations with high incidence in SCLC occur in genes mapping to chromosome 3p, including *FHIT*, *RASSF1*, *RARB*, and *FUS1* [87,102,103,104]. All four of these genes, located within the 3p14-23 region, have demonstrated anti-tumorigenic properties relating to the cell cycle and/or apoptosis regulation [104,105,106,107,108]. Abnormalities in these four genes occur in over 70% of SCLC [104]. In addition, *RB1* and *p53* mutations occur in over 80% of all SCLCs [87,103,104], while *PTEN* is mutated in approximately 8% of SCLCs [87,102,104].

1.4.2 Staging and survival

SCLC is classified as two different stages by the Veteran's Administration Lung Study Group: limited stage (LS) and extensive stage (ES) [87,104,109]. Table 3 presents the two different stages, their associations with patient survival and staging diagnosis. LS is defined as occurring within a single field of radiation therapy (within one lung and localized lymph nodes) while ES is defined as not being within a single field of radiation therapy or as having metastasized to another location(s) [104,109]. A single field of radiation therapy is the region covered by one beam of external radiation. Approximately 60% of patients fall within ES [98,110], while the remaining are LS [98,104].

Table 3. SCLC stages and survival.

Stages	Survival	Description
Limited Stage (LS)	Median: ~17 months 5-year survival: 10-17%	Cancer is within a single field of radiation therapy **Eg:** in 1 lung, the mediastinum (lung cavity), and/or local lymph nodes
Extensive Stage (ES)	Median: ~7 months 5-year survival: 2% 2-year survival: 5%	Cancer has spread outside a single field of radiation therapy **Eg:** other lung, brain, liver, bone, or nonlocal lymph nodes

Note – information was pooled from references 98, 104, 109, 110, 111, and 115

Survival rates for SCLC are very poor, as it is estimated that 95% of diagnosed patients will eventually succumb to the disease [98,104,110]. Survival generally depends on the extent disease burden, the sex of the patient, and his or her overall health [98,104]. LS patients, with limited spread of the disease, have a greater chance of survival, as 80% of cases show a complete response to treatment [104]. LS patients have a 5-year survival rate of 10-17%, with a median survival of just over 17 months [98,104,111]. ES patients show 20% complete response to treatment, with a 2-year

survival rate of 5%, and a 5-year survival rate of approximately 2% [98,104,110]. The median survival for ES patients is 7 months [104,110]. Given the poor outcomes from SCLC, it appears as though more research is necessary to provide greater knowledge to prevent or treat the disease.

1.4.3 Treatment

SCLC is commonly treated based on the stage of the disease. Tumour resection is uncommon in North America, due to the cancer having metastasized at the time of presentation [87,104,112]. In recent years, surgery has been shown to be a viable treatment option for those few patients with early LS SCLC [112,113]. Studies in the United Kingdom have shown that in early LS SCLC cases, surgery results in an increase in the 5-year survival of patients from 5% to 52% [114]. Although there is evidence that tumour resection can be successful, the majority of SCLC treatments are based on the stage of the cancer, the presence of metastatic disease, and whether or not the cancer has relapsed after chemotherapy and radiation therapy.

Table 4 highlights the most common treatments for each stage of SCLC. Treatments in the table are based on what can be found in the literature as well as what is performed in Canada, taken from the Canadian Cancer Society [115]. The most common chemotherapy treatment for each stage of SCLC is a combination of platinum-based agents, such as cisplatin or carboplatin, and the topoisomerase inhibitor, etoposide [104,116]. Cisplatin is generally chosen over carboplatin due to its increase effectiveness, however, carboplatin demonstrates less toxicity [117]. In instances where a patient with LS disease is healthy, radiation therapy is coupled with the cisplatin and etoposide treatment [104,116]. In the past, and in rare cases, a combination of cyclophosphamide, doxorubicin, and vincristine was used to treat LS SCLC [104]. For ES patients, cisplatin and etoposide are still the preferred treatment [104]. In some instances, other topoisomerase inhibitors,

such as topotecan and irinotecan, are coupled with cisplatin [104], because they show a better response in comparison to cisplatin and etoposide [118]. For ES patients, radiation therapy is reserved for those with metastatic ES, typically for those in palliative care [104,116]. Lastly, as mentioned previously, most SCLC patients relapse sometime after the disease shows a complete response (defined as a complete reduction of the visual tumour via imaging) to the treatment, as the cancer develops a resistance to the original treatment [104]. In these cases, a combination of cyclophosphamide, doxorubicin and vincristine is used, or a topoisomerase inhibitor on its own [104]. Understanding how SCLC responds to and develops resistance to common treatments, such as cisplatin, is important in order to understanding how to maximize the efficiency of SCLC treatments, in order to increase SCLC survival rates.

Table 4. Common treatments of SCLC in North America.

Stages	Common Treatment
Limited stage (LS)	etoposide + cisplatin/carboplatin +/- radiation therapy
	cyclophosphamide + doxorubicin + vincristine
Extensive Stage (ES)	etoposide + cisplatin/carboplatin +/- irinotecan/ topotecan
	etoposide + cisplatin/carboplatin + cyclophosphamide +epirubicin
	etoposide + cisplatin/carboplatin +/- ifosfamide
	radiation therapy (palliative)
Recurrent disease	topotecan
	cyclophosphamide + doxorubicin + vincristine
	irinotecan +/- topotecan +/- paclitaxel

Note – information was pooled from references 104, 115, 116, and 118

1.4.3.1 Cisplatin

Cisplatin, or *cis*-diamminedichloroplatinum, was first discovered to have anti-tumour capabilities in the late 1960's [119]. As a result, cisplatin is now used in the treatment of a large number of cancers including lung, ovarian, head and neck, testicular, and gastric cancers [120,121]. Unfortunately, many cancers have an intrinsic resistance to cisplatin, while others, such as SCLC, develop a resistance to cisplatin upon treatment [121,122]. It is commonly understood that cisplatin's mode of action is through the formation of DNA adducts, which result in the activation of various pathways that lead to programmed cell death or apoptosis [121,123]. Nucleotide excision repair (NER) and mismatch repair (MMR) proteins, such as HMG1, recognize the DNA damage, resulting in activation of p53 and MAPK pathways (amongst others), leading to first cell cycle suppression, initiation of repair, and if not possible to repair/restore cell cycle progression, the activation of apoptosis, and in some cases necrosis or S/G_2 phase cell cycle arrest [121,122,124,125]. In addition, cisplatin binds to cytoplasmic proteins at cysteine residues [126]. This interaction also leads to p53 and MAPK apoptotic cell death, however, it may also lead cells to undergo necrosis [121,122]. It has been suggested that cells undergo cisplatin-induced necrosis if there are errors in the apoptotic mechanism [122].

Various concentrations of cisplatin have been reported in lung cancer cell-base treatment models. In A549 cells, a lung adenocarcinoma cell line, the IC_{50} values towards cisplatin (the concentration of drug that inhibits the growth of 50% of the cells) has been reported to be anywhere from 3.1 µM [127] after four hours of exposure to cisplatin to 2.3 µM [128] to 64-70 µM after 48 hours of exposure to cisplatin [129]. Furthermore, some SCLC cell lines, such as GLC20 and DMS114, have IC_{50} values towards cisplatin reported as 75.0 µM after 1 hour and 1.6 µM after 4 hours, respectively [127,130]. The variance in reported IC_{50}s, even for the same cell line, may

be due to differences in the preparation of the cisplatin solutions. As early as 2008, it was shown that cisplatin is deactivated in dimethylsulfoxide (DMSO) [131] and that the proper preparation of cisplatin is in an aqueous saline solution [132,133]. Many publications do not disclose their method of cisplatin preparation, making it difficult to interpret results [133].

1.5 GLC20 SCLC cell model

GLC20 is a SCLC cell line first reported in 1992 from the University Hospital Groningen in the Netherlands [130]. The cells were derived from a 67-year old male SCLC patient who was treated with a mixture of cyclophosphamide, doxorubicin and vincristine, with no reported tumour regression [130]. The male patient eventually passed away 28 weeks after diagnosis [130]. The GLC20 cell line has a homozygous 440 kb deletion on the short arm of chromosome 3, at the location 3p21.3 [3]. This cell line was instrumental in the discovery of the 3p21 deletion that is common in many lung cancers [1,5,15,32]. This deletion region overlaps with the smallest lung cancer specific deletion observed with two other SCLC cell lines, NCI-H740 and NCI-H1450 [1]. This deletion encompasses *RBM5*, resulting in a homozygous deletion of *RBM5*, providing a potential model to observe the effect of induced RBM5 expression [15] (Figure 2).

In addition to the wild type GLC20 cells, Dr. Leslie Sutherland previously developed three GLC20 stable sublines, two of which express RBM5 at differing levels. One subline contains an empty expression vector was termed Vector (V) or pcDNA3, while the cell lines containing RBM5 expression vectors were termed T2 (low-expression of RBM5) and C4 (high-expression of RBM5), as denoted in Figure 3. The pcDNA3 and T2 sublines were created from pooled populations of transfected cells selected in G418/geneticin. Soft agar cloning was performed to produce the clonal population C4, which was also selected in G418/geneticin.

Previously, GLC20 cells were shown to have an IC_{50} for cisplatin of roughly 75.0 µM after one hour of exposure to cisplatin [130] and a reduction in cell growth with 0.4 µM cisplatin after four days of exposure [134]. Very few experiments have been performed with the GLC20 cells, however the MTT (3-(4,5-dimethylthiazol-2-yl)-2,5-diphenyltetrazolium bromide) enzymatic activity assay has been used on a few occasions to measure drug sensitivity [130]. In Dr. Sutherland's laboratory, wild type GLC20 cells are most commonly used as a negative control

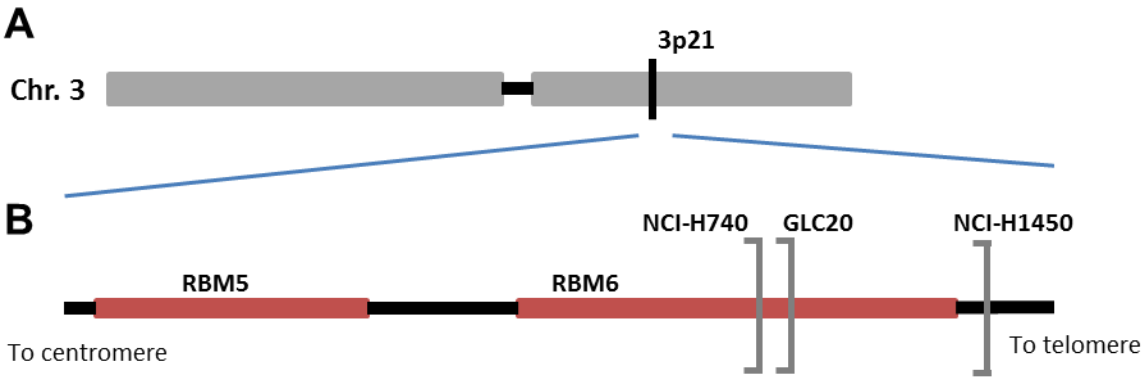

Figure 2. The location of *RBM5* on chromosome 3 and deletion in GLC20 cells. (A) A schematic representation of the location of *RBM5* on the small arm of chromosome 3, at 3p21.3. (B) The deletion region of the 3p21 deletions in 3 different SCLC cell lines. Lines presented are the end-point of deletions that encompass *RBM5*. Figure was obtained and edited from Dr. Sutherland, from a manuscript under preparation.

for RBM5 variant transcription analysis [10,135]. GLC20 cells have also been used to study RBM10 variants with two isoforms with or without a valine located in the second RRM domain [74]. GLC20 cells contain twice as much of the RBM10v1 valine-lacking isoform compared to the valine-containing isoform, meaning there is more exon 11-expressing than exon 11-excluding NUMB protein [74]. The exon 11 expressing NUMB variant is associated with lung cancer [56].

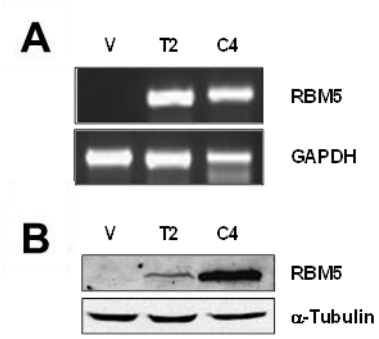

Figure 3. RBM5 expression in established GLC20 sublines. RBM5 (A) RNA and (B) protein expression analysis of previously established GLC20 sublines. 'V' is representative of the pcDNA3-transfected subline. Figure was obtained from Dr. Sutherland, from a manuscript under preparation.

1.6 Study Objectives

To date there has been a growing understanding of the expression and mutation status of *RBM5* in lung cancer [15,16,34]. Its location within the region 3p21.3 that suffers allelic loss in over 95% of SCLC and over 70% of NSCLC, suggests a function as a lung cancer tumour suppressor gene [1,30,31,32]. There are many studies that have attempted to understand the role of RBM5 in many different cell models, including its role as a tumour suppressor gene in NSCLC models. As a result, the main objective of this study was to further examine the function of RBM5 in lung cancer, using the GLC20 SCLC model. As described earlier, wild type GLC20 cells are RBM5-null. Using the two RBM5-expressing GLC20 sublines previously described, T2 and C4 (Figure 3), this study aimed to understand of the function of RBM5 by comparing various phenotypes in the RBM5-null and RBM5-expressing cell model. Specifically, our objective was to observe the effect of RBM5 expression on GLC20 cell proliferation, cell death and apoptosis. Our first aim was to monitor the effect of RBM5 expression on GCL20 cell proliferation using both the MTT and cell counting assays. Second, we observed the effect of RBM5 expression on GLC20 cell

death in the presence of cisplatin using the cell counting assay. Third, we examined cells undergoing cell death by observing changes in PARP cleavage by Western blotting, and chromatin condensation and membrane asymmetry by fluorescence microscopy, to determine the influence of RBM5 expression on apoptosis. With the understanding of the ability of RBM5 to modulate apoptosis and the cell cycle [46], we hypothesized that increased RBM5 expression would result in a decreased GLC20 cell proliferation and, in the presence of cisplatin, increases in apoptotic cell death. We also hypothesized that the effect of RBM5 would depend on its expression level.

During the course of our investigation we also noted that increased RBM5 expression was associated with a change in RBM10v1/v2 expression. Therefore, this study explored the function of RBM10 in the GLC20 cell model. Since RBM10 is a modulator of apoptosis and a regulator of cell proliferation [56,72], we hypothesized that RBM10 knockdown would result in an increase in GLC20 cell proliferation. GLC20 RBM10 knockdown sublines were produced from pooled populations using shRNA-targeting RBM10. The effect of RBM10 knockdown on cell proliferation was explored, using an MTT assay.

Chapter 2

2 Materials and Methods

2.1 GLC20 cells and sublines

SCLC GLC20 cells were a kind gift from the late Dr. Charles Buys from the University of Groningen (Groningen, Netherlands) and Dr. Leslie Sutherland previously generated the GLC20 RBM5-expressing sublines. GLC20 cells and sublines pcDNA3, T2 and C4 were maintained in RPMI 1640 (Gibco, Life Technologies, Burlington, Canada) supplemented with 10% fetal bovine serum (FBS, Gibco) (termed complete medium), with the addition of 0.1 mg/mL G418/Geneticin (Gibco) for pcDNA3, T2 and C4 sublines. Cells were maintained at 37°C with 5% CO_2 in a humidified chamber. Cells were scaled up and collected by centrifugation at 149 x g for 7 min at room temperature, the supernatant removed, then centrifuged again at 5,900 x g for 2 min at room temperature, the supernatant removed, and the pellet stored at -80°C. Cell stocks were prepared by transferring the cells into a freezing medium composed of 50% foetal bovine serum, 45% complete medium, and 5% dimethylsulfoxide (DMSO) (Sigma-Aldrich, St Louis, U.S.A) and stored in liquid nitrogen.

For all assays, cells were centrifuged at 149 x g for 7 min at room temperature and pretreated with 0.25% Trypsin-ethylenediaminetetraacetic acid (EDTA) (Gibco) for 10 min at 37°C with 5% CO_2 in a humidified chamber, to ensure a single cell population. Cells were washed three times in complete medium with centrifugation occurring between washes at 149 x g for 7 min at room temperature, suspended in complete medium and counted in a 1:1 solution of cells in complete medium and a 0.2% nigrosin (Sigma-Aldrich) solution, using a hemocytometer. Cells were then diluted to the cell density noted in each experiment. The remainder of the cells not

used for experiments were collected by centrifugation and the pellets were stored frozen until needed for later (RNA) analysis.

2.1.1 GLC20 RBM10 knockdown subline generation

SCLC GLC20 RBM10 stable KD sublines were generated from passage 7 GLC20 wild type cells. Several different visual dilutions of GLC20 cells were plated in 24 well flat-bottom plates (Sarstedt AG & Co., Nümbrecht, Germany) and incubated at 37°C with 5% CO_2 in a humidified chamber for 24 h. Half of the cells were then transfected with a control shRNA vector "Hush 300" (TR30003, Origene Technologies, Inc, Rockville, U.S.A) and the other half with a 50:50 shRNA mix of "Hush 29" (TI308329, Origene, 5'-GCCTTCGTCGAGTTTAGTCACTTGCAGGA) and "Hush 30" (TI308330, Origene, 5'-AGTCACTTGCAGGACGCTACACGATGGAT). These shRNA vectors were previously used by Dr. Sutherland [72]. Hush 29 and 30 both target exon 6 of RBM10 and are not variant specific (Figure 1). Cells were transfected using Lipofectamine 2000 (L2000) (Invitrogen, Life Technologies, Burlington, Canada) at a 1:3 shRNA:L2000 ratio. In summary, per one well, the transfection was first started by putting 50 µL Opti-MEM medium (Gibco) into two different 1.5 mL conical tubes, 1 mixed with 2 µL L2000 and the other with 0.7 µg shRNA (0.7 µg Hush 300 or 0.35 µg of Hush 29/30 each), and these solutions incubated for 5 min at room temperature. The contents of the two tubes were then combined, and the mixture incubated for 20 min at room temperature. The mixture (~100 µL) was then added dropwise onto the cells in one well. Cells were incubated for 48 h at 37°C with 5% CO_2 in a humidified chamber. After 48 h, transfected cells were selected for seven days using 0.1 µg/mL puromycin (Invitrogen) in complete medium at 37°C with 5% CO_2 in a humidified chamber.

After seven days of selection, cells were treated with a Histopaque solution (Sigma-Aldrich) to separate live from dead cells. Cells were taken from culture and carefully layered on top of the Histopaque solution. The Histopaque/cell solution was then subjected to centrifugation at 233 x g for 10 min at 10°C. The top layer of cells and medium was carefully collected with a plastic Pasteur pipette and subjected to centrifugation at 5,900 x g for 2 minutes at room temperature. Supernatant was discarded and cells were resuspended in complete medium supplemented with 0.1 μg/mL puromycin and incubated at 37°C with 5% CO_2 in a humidified chamber. The surviving cells were then scaled up. The stable negative control shRNA subline was named G300.3, and three surviving RBM10 KD sublines were named G29/30.1, G29/30.3 and G29/30.4, based on their location on the 24 well plate. Passage number was recorded post-transfection, with 0 designating the transfection pass.

2.2 RBM5 and RBM10 Western blot analysis

Proteins from GLC20 subline cell pellets were extracted by resuspension of cell pellets in lysis buffer, which consisted of 50 mM Tris pH 8.0, 150 mM NaCl, 0.5% NP-40, 100 mM NaF, 1 mM EDTA pH 8.0, 1 mM EGTA pH 7.5, and 1X protease inhibitor cocktail (Sigma-Aldrich) in deionized (d) H_2O. The suspension of cells was then subjected to centrifugation at 14,000 x g for 10 min at 4°C. The supernatant was kept after centrifugation. The lysates were then quantified using the Bio-Rad (Bio-Rad Laboratories, Hercules, U.S.A) DC Protein Assay Kit containing Reagents A, B and S, using bovine serum albumin as the standard (Life Technologies). Lysates were stored at -80°C.

Fifty μg of protein was diluted 1:2 (volume:volume) in sample loading buffer (0.06 M Tris-HCl pH 6.8, 25% glycerol, 2% SDS, 0.01% bromophenol blue, and 0.05% β-mercaptoethanol in dH_2O). The samples were separated by electrophoresis through a 4% acrylamide stacking gel

(0.125 M Tris pH 6.8, 0.1% SDS, and 4% acrylamide in dH_2O) and through a 7% acrylamide resolving gel (0.375 M Tris pH 8.8, 0.1% SDS, 7% acrylamide in dH_2O) at 40V for roughly 16 h in running buffer (0.025 M Tris, 0.2 M glycine, and 0.1% SDS in dH_2O). The proteins in the resolving gel were transferred to a 0.45 μm polyvinylidene fluoride membrane (PVDF) (Pall Life Sciences, GE-Health Science, Little Chalfont, U.K.) via a wet transfer in transfer buffer (25mM Tris, 192 mM glycine, 20% methanol in dH_2O) at 1 A for 1 h and 15 min at 4°C. After transfer, PVDF membranes were washed sequentially for 15 min, 5 min and 5 min in TBS-T (20 mM Tris, 0.5 M NaCl, 0.1% Tween (Bio-Rad) in dH_2O), with buffer changed after each wash. PVDF membranes were then blocked with 5% fat-free milk (Carnation® Evaporated Milk, Smuckers® Markham, Canada) in TBS-T for 1 h at room temperature. The PVDF membranes were again washed as noted above and probed for ~16 h at 4°C with a 1:2,500 or 1:5,000 dilution of rabbit anti-RBM5 LUCA-15-UK (non-commercially available [8]), a 1:10,000 or 1:2,000 dilution of rabbit anti-RBM10 (HPA034472, Sigma-Aldrich or A301-006A-1, Bethyl Laboratories, Inc, Montgomery, USA, respectively) or a 1:10,000 dilution of mouse anti-α-tubulin primary antibody (sc-8035, Santa Cruz Biotechnology, Inc., Dallas, U.S.A) in 3% milk in TBS-T (the position of the epitopes recognized by the RBM antibodies is shown in Figure 1). The PVDF membranes were washed in TBS-T after incubation as noted above and probed for 1 h at room temperature with 1:10,000 goat anti-rabbit IgG HRP-conjugated secondary antibody (sc-2004, Santa Cruz Biotechnology, Inc.) or 1:10,000 goat anti-mouse IgG HRP-conjugated secondary antibody (sc-2005, Santa Cruz Biotechnology, Inc.) in 3% milk in TBS-T. The PVDF membranes were washed again with TBS-T and detection was done by chemiluminescence using Amersham ECL Western blotting detection reagents (GE-Healthcare, Little Chalfont, U.K.) and capturing the signal by exposure to Amersham Hyperfilm (GE-Healthcare). Longer exposures

were used when RBM10v2 expression was captured. Film was then developed using a SRX-101A medical film processor (Konica Minolta Medical and Graphic Inc., Tokyo, Japan)

2.3 PCR validation of GLC20 RBM5-expressing sublines

RNA was isolated from cell pellets using Tri-Reagent (Molecular Research Center, Inc., Cedarlane, Burlington, Canada). Cells were resuspended in Tri-Reagent solution until pellets were visibly dissolved. After a 5 min incubation at room temperature, 1-bromo-3-chloro-propane (BCP) (Sigma-Aldrich) was added to the suspension, and incubated for 10 minutes at room temperature. The suspension was then subjected to centrifugation at 16,100 x g for 15 min at 4°C. The top (aqueous) layer was collected and the remainder discarded. RNA was precipitated from the solution using 100% isopropanol and then collected after centrifugation at 16,800 x g for 8 min at room temperature. The RNA was washed with 75% ethanol in dH_2O and subjected to centrifugation at 5,900 x g for 5 min at room temperature. The supernatant was discarded and the RNA pellets were air-dried for roughly 10 min, on ice. RNA was then suspended in TE buffer (10 mM Tris-HCl pH 8.0 and 0.1 mM EDTA pH 8.0) and incubated at 55°C for 10 minutes. RNase OUT (Life Technologies) was added to the RNA, which was then stored at -80°C.

RNA was quantified using a NanoDrop 2000 UV-Vis Spectrophotometer (Thermo Scientific, Waltham, U.S.A) and only RNA with a 260nm/280nm ratio above 1.8 was used in assays. Reverse transcription (RT) was performed using 1 µg of RNA in an RT-buffer (0.526 mM dNTPs (New England Biolabs, Inc., Ipswich, U.S.A), 0.01 mM DTT (Invitrogen), 26.3 ng/µL Oligo (dT) (AlphaDNA, Montreal, Canada)) in 1X First Strand Buffer (Invitrogen) and dH_2O. Moloney Murine Leukemia Virus (M-MLV)-Reverse Transcriptase (Life Technologies) was added at 10.5 U/µL and the solution was incubated at 42°C for 50 minutes and then at 70°C for

15 minutes in a T100 Thermal Cycler (Bio-Rad Laboratories). The cDNA produced was stored at -20°C.

End-point PCR was performed on cDNA using RBM5 and GAPDH gene-specific primers (AlphaDNA), detailed in Table 5. End-point PCR reactions were performed in the following reaction mixture: 1X PCR buffer (10 mM Tris-HCl, 50 mM KCl, 1.5 mM $MgCl_2$ pH 8.3) (New England Biolabs), 0.2 mM dNTPs (New England Biolabs), 0.4 μM of each primer (AlphaDNA), and 50 U/mL Taq polymerase (New England Biolabs). Reactions were performed in a T100 Thermal Cycler using the following conditions: 1. 95°C for 5 minutes, 2. gene-specific cycle number (25 cycles for GAPDH and 32 or 40 cycle for RBM5) of 95°C for 30 seconds, 59°C for GAPDH or 58°C for RBM5 for 30 seconds, and 72°C for 45 seconds for GAPDH and 30 seconds for RBM5, followed by 3. 72°C for 10 minutes. PCR products were then diluted with 6X loading buffer (0.25% bromophenol blue and 30% glycerol in dH_2O) and visualized following electrophoresis through a 2% agarose gel (Amresco, Inc., VWR International, Radnor,

Table 5. List of PCR primers and parameters used for GLC20 subline validation

Gene	Primers		Exon	Ann.[1] temp	Amp.[2] size
GAPDH	hmr[3]-GAPDH-F	5' AACACAGTCCATGCCATCAC	6	59 °C	471 nt
	hmr-GAPDH-R	5' TCCACCACCCTGTTGCTGTA	7		
RBM5	LU15(2)	5' GCACGACTATAGGCATGACAT	4	58 °C	380 nt
	LU15(3)	5' AGTCAAACTTGTCTGCTCCA	8/9		
	Oligo(dT)	5' TTTTTTTTTTTTTTTTTTTT			

[1] – Annealing, [2] – Amplicon, [3] – Human, mouse and rat homology

U.S.A) in 1X TAE (40 mM Tris-acetate, 10 mM EDTA pH 8.0) buffer containing SYBR Safe DNA gel stain (Life Technologies) at 100 V for 50 minutes then imaged using Fluorchem FC3 (Protein Simple, San Jose, U.S.A).

2.4 MTT cell growth assay

GLC20 cells and sublines were plated at 10,000 cells per well in 96-well flat-bottom plates (Sarstedt) at a cell density of 50 cells/μL in eight technical replicates, in complete medium. Cells were incubated for 24 h at 37°C with 5% CO_2 in a humidified chamber, and then monitored every day for 10 days (RBM5 sublines) or five days (RBM10 KD sublines) by MTT assay. At the indicated time intervals, cells were treated with 10 μL of 5 mg/mL MTT (3-(4,5-dimethylthiazol-2-yl)-2,5-diphenyltetrazolium bromide) Reagent (Life Technologies) in PBS (Gibco) for 2 h and 45 min at 37°C with 5% CO_2 in a humidified container, as previously described [130]. After incubation time, cells were transferred to a 96-well Vee-bottom plate (Sarstedt) and subjected to centrifugation at 500 x g for 5 min at room temperature. Supernatant was discarded and the blue formazan precipitate was dissolved in DMSO (BDH Chemicals, VWR International, Radnor, U.S.A). Dissolved crystals were then transferred to a 96-well flat-bottom plate and incubated at 37°C with 5% CO_2 for 10 min in a humidified chamber. After incubation, absorbances were taken from the 96-well plates at 540 nm using a BioTek Synergy S4 Spectrophotometer (BioTek Instruments, Inc., Winooski, U.S.A). Experiments were repeated in four biological replicates (RBM5 sublines) or three biological replicates (RBM10 KD sublines) represented by different passage numbers.

Absorbances of each biological replicate were normalized to their respective day 0 absorbance value, and the averages of three or four biological replicates for each day are presented. A Two-way ANOVA statistical analysis was performed with Bonferroni post-hoc test comparing all growth to the pcDNA3 subline for the RBM5 sublines or G300.3 for the RBM10 KD sublines, using Graphpad Prism 5 (Graphpad Software, Inc., San Diego, U.S.A).

2.5 Cell counting cell growth and cell death assays

GLC20 cells and RBM5 sublines were monitored every other day for 10 days for cell growth and death, using 0.2% nigrosin and a hemocytometer. Cells were plated at 10,000 cells per well in 96-well flat-bottom plates at a cell density of 50 cells/μL, in triplicate wells per treatment. Cells were then left for 24 h at 37°C with 5% CO_2 in a humidified chamber. After 24 h, the cells were treated with the following conditions: left untreated, saline (0.9% NaCl in H_2O) control, 1.0 μM cisplatin in saline for 0, 2, 4, 6, 8 and 10 days, or 0.1, 0.5, 10.0 and 100.0 μM cisplatin for 4 and 8 days (see Table 6 for summary of treatments). Cisplatin (Sigma) was prepared, as previously described, in saline at a concentration of 1.0 mg/mL [131-133]. The cells were then counted every other day by transferring cells to a 96-well Vee-bottom plate and subjecting them to centrifugation at 500 x g for 5 min at room temperature. The supernatant was then discarded and cells were treated with 0.25% Trypsin-EDTA for 10 min at 37°C with 5% CO_2 in a humidified chamber. Complete medium was then added to cells and they were subjected to centrifugation at 500 x g for 5 min room temperature. Cells were then resuspended into complete medium and counted in a 1:1 ratio of cells in complete medium and 0.2% nigrosin, using a hemocytometer.

Live cells were counted as cells with intact membranes, characterized by a lack of blue/purple nigrosin within the cells, and dead cells were counted as cells without intact membranes, characterized by the presence of blue/purple nigrosin within the cell. Live cell counts were used to monitor cell growth, relative to day 0 counts, and the average of biological triplicates was plotted. A Two-way ANOVA was performed with Bonferroni post-hoc analysis, comparing all subline cell growth to the pcDNA3 subline, calculated using Graphpad Prism 5. Cell viability or percent intact membrane by nigrosin was calculated using the following equation:

$$Cell\ viability\ or\ \text{percent intact membrane by nigrosin} = \#\ live\ cells/(\#\ live + \#\ dead\ cells)$$

Cell viability or percent intact membrane by nigrosin for the 1.0 μM cisplatin values were also expressed relative to saline controls, and the average of biological triplicates was plotted. A Two-way ANOVA was performed with Bonferroni post-hoc analysis, comparing all subline cell viabilities to the pcDNA3 subline, calculated using Graphpad Prism 5. Day four and eight cisplatin cell viabilities were made relative to the saline control viability for the calculation of EC_{50} values. EC_{50} values were calculated using 'log(inhibitor) vs. response (three parameters)' on Graphpad Prism 5, and the average of biological triplicates was plotted with the saline control represented at 10^{-10} M on the graphs. A One-way ANOVA was performed with Tukey post-hoc analysis, comparing all sublines to the pcDNA3 subline.

2.6 Confirmation of a 5.0 μM cisplatin EC_{50} using PARP cleavage

GLC20, pcDNA3, T2 and C4 cells were counted and 1.5 $x10^6$ cells were plated into T75 flasks (Sarstedt) at a cell density of 50 cells/μL. After a 24 h incubation at 37°C with 5% CO_2 in a humidified chamber, cells were exposed to 5.0 μM cisplatin for 4 days. Cells were collected by centrifugation at 149 x g for 7 min at room temperature followed by 5,900 x g for 2 min at room temperature and stored at -80°C.

Protein lysates were prepared by resuspension of cell pellets in lysis buffer, as noted in Section 2.2. Fifty μg of protein was electrophoresed and transferred to a PVDF membrane, as noted in Section 2.2. PVDF membranes were probed with a 1:2,000 dilution of mouse anti-PARP primary

antibody (C2-10, BD Pharmingen, BD Biosciences, San Jose, U.S.A) or a 1:10,000 dilution of mouse anti-α-tubulin primary antibody (sc-8035, Santa Cruz Biotechnology, Inc.) in 3% milk in TBS-T. PVDF membranes were washed after incubation and probed for 1 h at room temperature with a 1:10,000 dilution of goat anti-mouse IgG HRP-conjugated secondary antibody (sc-2005, Santa Cruz Biotechnology, Inc.) in 3% milk in TBS-T.

Selected protein bands appearing on the autoradiograph were quantified by densitometry. The intensity of the 89 kDa cleaved PARP product levels for each subline were expressed relative to the α-tubulin control and compared to the pcDNA3 subline. An average of three biological replicates was represented and a One-way ANOVA was performed with Tukey post-hoc analysis using GraphPad Prism 5, comparing all sublines to the pcDNA3 subline.

2.7 Apoptosis Assays

2.7.1 5.0 μM cisplatin exposure

GLC20 cells and sublines were counted and 2.0 $x10^6$ cells were plated in T75 flasks at a cell density of 50 cells/μL. After a 24 h incubation at 37°C with 5% CO_2 in a humidified chamber, cells were either exposed to 5.0 μM cisplatin or left untreated for 4 days (see Table 6 for summary of treatments). A fraction of cells was collected by centrifugation at 149 x g for 7 min at room temperature and supernatant was discarded, followed by centrifugation at 5,900 x g for 2 min at room temperature, the supernatant was discarded, and the pellet stored at -80°C. Another fraction of cells was subjected to centrifugation at 149 x g for 7 min at room temperature, supernatant was discarded, and the cells were treated with 0.25% Trypsin-EDTA for 10 min at 37°C with 5% CO_2 in a humidified chamber.

Table 6. Concentrations of cisplatin tested at different time points

Experiment	Trial	Time Points	[cisplatin] (μM)
Cisplatin cell growth	2	2, 4, 6, 8, 10 days	1 saline
EC_{50} calculations		4, 8 days	0.1 0.5 1 10 100 saline
5 μM cisplatin, PARP cleavage	3	4 days	5
5 μM cisplatin, PARP cleavage and fluorescence microscopy	4	4 days	5

Cells were then washed twice in complete medium and centrifuged at 500 x g for 5 min at room temperature, with changes in medium between each centrifugation, then counted in a 1:1 ratio of cells in complete medium and 0.2% nigrosin, using a hemocytometer. 0.5 $x10^6$ cells were resuspended at a 1000 cell/μL density in cold PBS for fluorescence analysis. If fewer than 0.5 $x10^6$ cells were counted, cells were adjusted to a smaller volume at a 1000 cell/μL density in cold PBS.

2.7.2 PARP Western blot analysis

Protein extracts from cell pellets collected in experiments highlighted in Section 2.7.1 were prepared by resuspension of cell pellets in lysis buffer, as noted in Section 2.2. Twenty-five μg of protein processed for electrophoresis and transferred to a PVDF membrane as noted in Section 2.2. PVDF membranes were probed, as noted above in Section 2.6.

Film was then scanned and densitometry was performed by using the '1D multi – AUTOGRID' analysis tool on the AlphaEaseFC gel documentation system (Alpha Innotech). Comparisons were made between the 116 kDa uncleaved PARP product and 89 kDa cleaved PARP product, to show percent 89 kDa cleavage product, as follows:

$$\%\ 89\ kDa\ PARP\ cleavage = \left(\frac{89\ kDa\ PARP}{Total\ PARP\ (116\ kDa\ +\ 89\ kDa\ PARP)}\right) * 100\%$$

An average of three biological replicates was presented and a One-way ANOVA was performed with Tukey post-hoc analysis, comparing all the sublines to the pcDNA3 subline.

2.7.3 Fluorescence microscopy

Cells previously collected at a density of 1000 cells/µL, as described in Section 2.7.1, were washed three times in cold PBS at 5,900 x g for 2 min at room temperature, with changes in cold PBS between centrifugations, then resuspended in Annexin-V binding buffer (10 mM HEPES, 140 mM NaCl, and 2.5 mM $CaCl_2$) at a density of 1000 cells/µL. Cells were triple stained with 7-aminoactinomycin D (7AAD) in DMSO, Annexin-V-AlexaFluor® 488 conjugated, and Hoechst 33342 Nucblue® Live Cell Stain ReadyProbe Reagent (all Life Technologies) at 0.02 mg/mL, 5 µL/100µL, and 1 drop/500µL concentrations, respectively, at room temperature for 15 min in the dark. Cells were then washed three times in cold Annexin-V binding buffer at 5,900 x g for 10 minutes at room temperature, with changes in cold Annexin-V between centrifugations, then resuspended in 100 µL of cold PBS. Samples were loaded into Cytospin™ columns (Symport, VWR International, Radnor, U.S.A) pre-loaded with a microscope slide (VistaVision, VWR International, Radnor, U.S.A). Cells were then centrifuged onto the microscope slides at 500 rpm for 2 min at room temperature in a Shandon Cytospin™ 4 cytocentrifuge (Thermo Scientific), rotor # 4127 0806 59930093.

Samples on slides were air-dried, then fixed with 4% paraformaldehyde (Sigma-Aldrich) in PBS at room temperature in the dark for 10 min. Slides were washed sequentially in three changes of PBS, and then air-dried. 90% glycerol (Sigma-Aldrich) in PBS was added to the samples and a No. 1 cover slip (VWR) was placed on top of the sample. The cover slip was sealed with nail polish and the slides stored at 4°C in the dark until visualized (~24 h later).

Cells were visualized using the Olympus 1x73 Microscope (Olympus Life Sciences, Tokyo, Japan). Fluorophores were excited using Lumen Dynamics Xcite 120 LED (Lumen Dynamics, Mississauga, Canada), Olympus LED PS and LBM laser systems (Olympus Life Sciences). Fluorescence emission spectra were captured for Hoechst 33342 (Ex: 250 nm/Em: 461 nm), for AlexaFluor® 488 (Ex: 495 nm/Em: 519 nm), and for 7-AAD (Ex: 546 nm/Em: 647 nm). In addition to fluorophores, cell morphology was observed using phase contrast (images not included). Images of the stained cells were captured using the Olympus DP80 camera (Olympus Life Sciences) and cellSens Dimensions imaging software (Olympus Life Sciences). Images obtained that were later counted underwent no post-production adjustments. Images presented in figures in this study underwent post-production adjustments using the 'Adjust Display' function in the cellSens Dimensions imaging software. In brief, background colour intensities were excluded from the images using the histogram tool. Colour threshold intensity was then increased. These changes were applied to all the images and at the same intensities.

Exposure times and gain were made constant during the imaging of each biological replicate. Although exposure times varied between biological replicates, the Hoechst 33342 stain was exposed for roughly 250 ms, the Annexin-V-Alex-Fluor 488 stain was exposed for roughly 2 s with a gain of 2X, and the 7-AAD stain was exposed for roughly 800 ms. All images were taken using a 40X objective lens. Ten different fields of view were captured as images for all sublines

at each time point and a minimum of 300 total events was counted per biological replicate. Figure 4 illustrates how each event was defined, 'Live', 'Early Apoptosis', or 'Late Apoptosis/Necrosis'. In summary, Figure 4A demonstrates examples of 'Live' events, defined by cells with visually uncondensed nuclei, stained with Hoechst 33342, and a lack of green Annexin-V stain or red 7-AAD stain. 'Early Apoptosis' events were defined as cells that had either or both green Annexin-V stain (indicative of phosphatidylserine flipping) and condensed nuclei (condensed blue Hoechst 33342 staining). Figure 4Bi and ii provide examples of high and low levels of only the green Annexin-V stain, respectively. Figure 4Biii and iv provide examples of high and low levels of chromatin condensation, respectively. Figure 4Bv provides an example of the presence of both the green Annexin-V stain and the chromatin condensation. Lastly, 'Late Apoptosis/Necrosis' was defined by the loss of membrane integrity, which is indicated by the presence of the red stain of 7-AAD (made purple/pink in images), as noted in Figure 4C.

Three biological replicates were performed. For each biological replicate, the events were totaled between the ten fields of view counted. A minimum of 300 events was counted per biological replicate. Values were then transformed to a percentage of the total number of events that were counted, for each biological replicate. The average of the three biological was presented and One-way ANOVA was performed between the sublines for each defined event. Tukey post-hoc analysis was done, comparing all the sublines to the pcDNA3 subline.

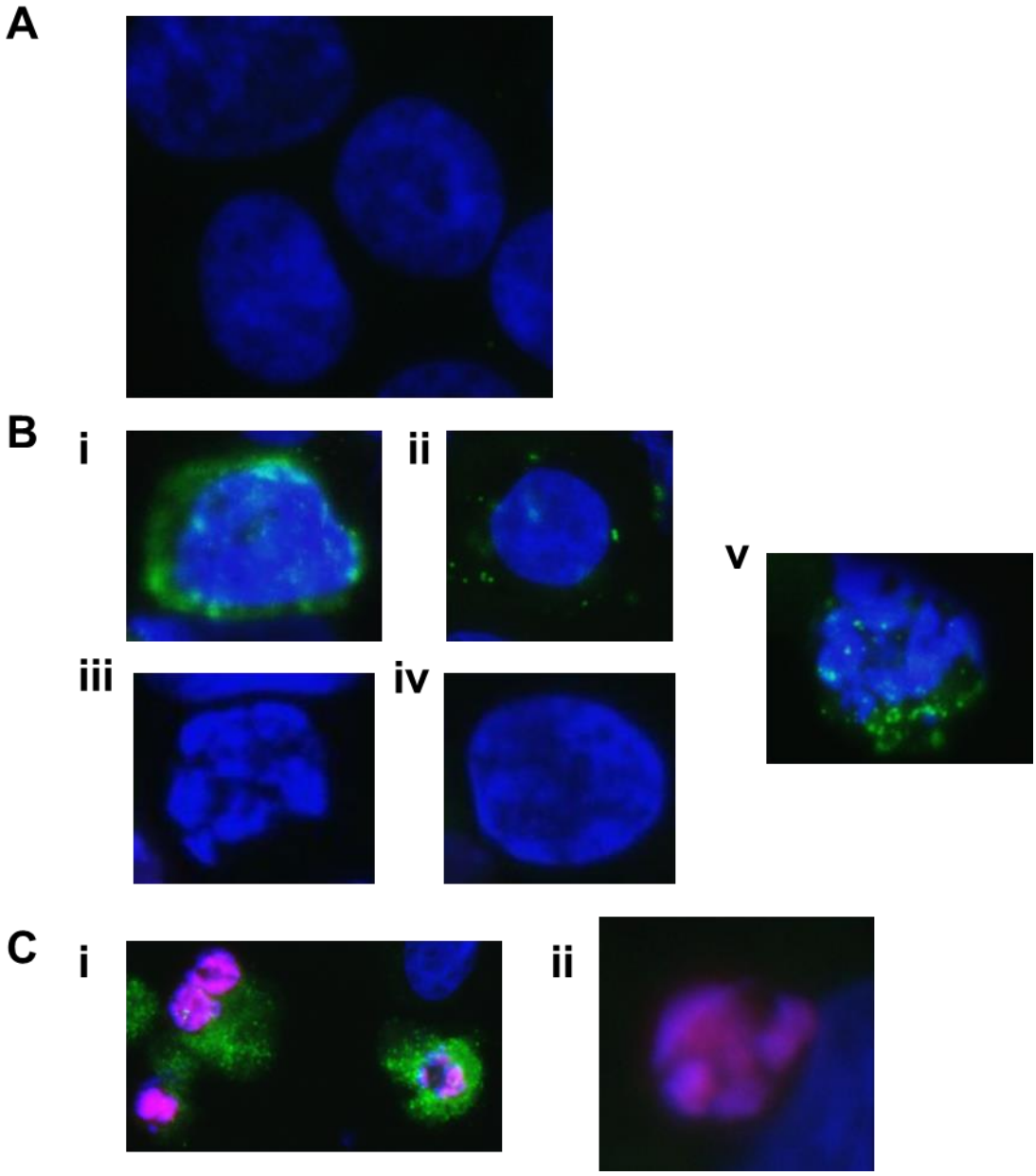

Figure 4. Sample images to denote the classification of different events refered to in the fluorescence microscopy results section. 10 different fields of view were counted for all sublines in each treatment and events were counted. Events were classified into (A) Live, (B) Early Apoptosis, and (C) Late Apoptosis/Necrosis. (A) Live cells were characterized by blue nuclei with no other stains that demonstrated no visual condensation of chromatin. (B) Early Apoptosis cells were defined as those with green stain (Annexin-V/PS flipping) at high (B i) or low (B ii) levels or chromatin condensation (darkening of blue Hoechst stain nucleus) at high (B iii) or low (B iv) levels. A combination of Annexin-V binding and chromatin condensation was also labeled as Early Apoptosis (B v). Lastly, (C) Late Apoptosis/Necrosis was defined as any cell with the presence of the red 7-AAD stain whether with (C i) or without (C ii) Annexin-V stain. All images are samples of those counted. Images were taken using a 40X objective lens.

Chapter 3

3 Results

3.1 Confirmation of RBM5 expression

To understand the role of RBM5 in SCLC, the GLC20 cell line was used. As noted previously in Figures 2 and 3, GLC20 cells do not have RBM5 expression [15] and, therefore, provide a useful model to monitor how differing levels of RBM5 may affect SCLC cells. With the use of the GLC20 sublines, pcDNA3, T2 and C4, some insight into the functions of RBM5 in SCLC can be obtained. Prior to starting experimental studies, RBM5 and RBM10 expression was confirmed and examined in the three sublines and wild type GLC20 cells. RBM5 expression was expected to be identical to what was determined by others in the laboratory (Figure 3). Figure 5 shows the levels of RBM5 and RBM10 expression within each subline at the protein level, and RBM5 at the mRNA level. It can be noted that RBM5 expression within each subline was at levels similar to those reported by others (Figure 3). RBM5 expression was absent in the wild type GLC20 cells. The stable empty vector-transfected subline (pcDNA3) had no RBM5 expression, while the stabled pooled population of RBM5-transfected cells (T2), had some RBM5 expression. The stable clonal population of RBM5-transfected cells, C4, had more expression than the T2 subline. Furthermore, RBM10v2 in the high RBM5-expressing C4 subline appeared to be increased when compared to the other sublines. This observation was further addressed in Section 3.5. Figure 5C provides an example of wild type (untransfected) GLC20 cells. The image taken in Figure 5C denotes GLC20 cells roughly at a density that would require subculturing.

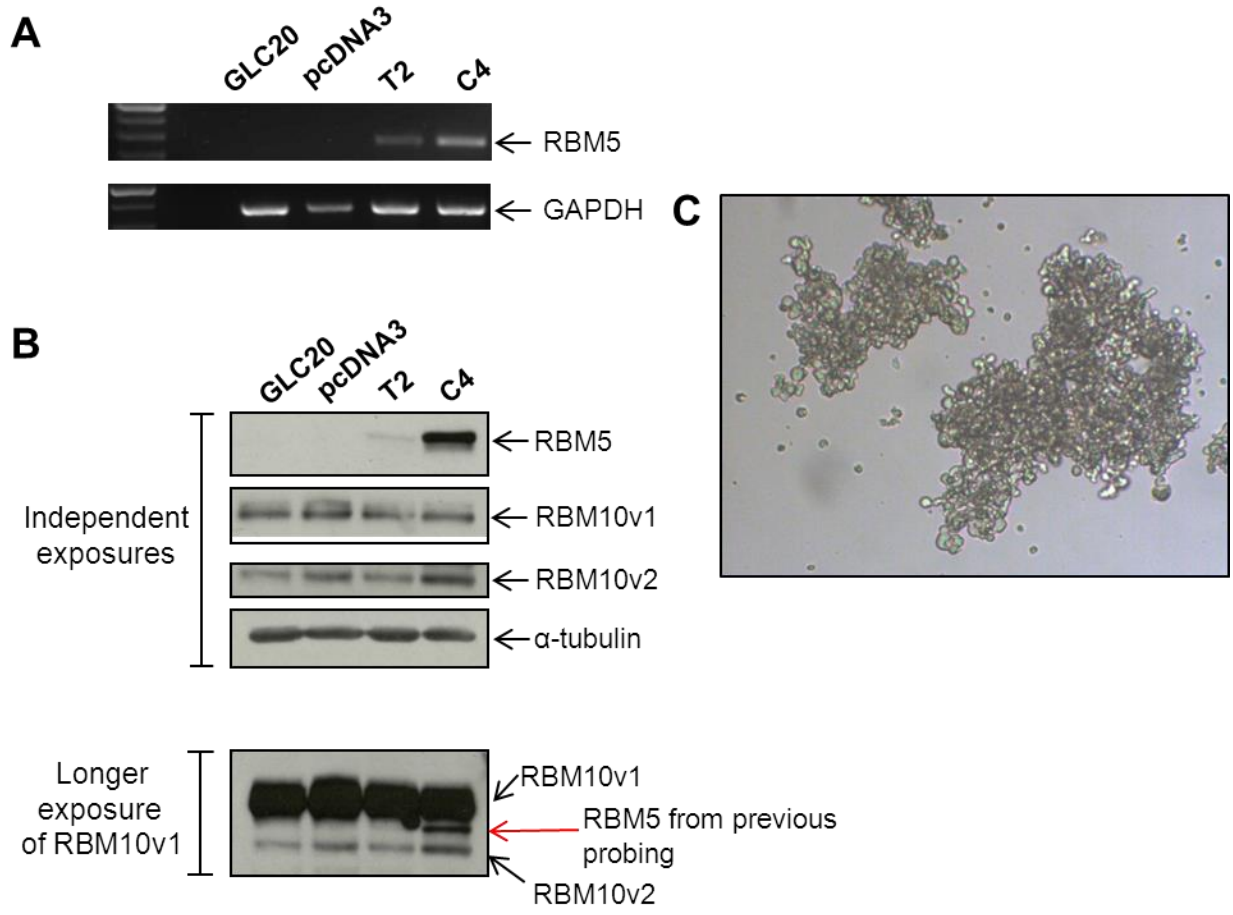

Figure 5. Confirmation of RBM5 and RBM10 expression in GLC20 sublines. (A) RT-PCR analysis of RBM5 expression in GLC20, pcDNA3, T2 and C4 sublines with GAPDH control. (B) Protein analysis of RBM5 and RBM10 expression (Sigma Antibody) in GLC20, pcDNA3, T2 and C4 populations with tubulin control for protein. A longer exposure shows the relative abundance of RBM10v1 and RBM10v2 in GLC20 cells. mRNA from Trial #5 was not analyzed, as RBM5 protein expression was observed instead, found in Figure 13 **(C)** Sample image of GLC20 cells in culture using a 4X objective lens.

Table 7 highlights the details of each trial that is described in this study. A 'trial' is defined as a new subset of previously frozen cells, used for a particular subset of experiments, represented by figure. This information was relevant to understanding whether any variances between trials could be explained by the number of times that the cells had been subcultured (represented by passage number) prior to the beginning of the experiment. It was important to ensure that all

Table 7. Summary of experimental trials and biological replicates

Trial #	Sublines	Passage #	BR* #	Figures - Experiment	Thesis Page
1	GLC20	7-12	1-4	Figure 7 – MTT cell growth assay	48
	pcDNA3	43-47	1-4		
	T2	29-32	1-4		
	C4	14-17	1-4		
2	GLC20	10-12	1-3	Figure 7 – Cell counting cell growth	48
	pcDNA3	48-50	1-3	assay	
	T2	31-33	1-3	Figure 8 – Cisplatin cell growth assay	50
	C4	13-15	1-3	Figure 9 – Membrane integrity assay	54
				Figure 10 – EC_{50} assay	57
3	GLC20	8-12	1-3	Figure 11– 5.0 μM cisplatin PARP	60
	pcDNA3	46-50	1-3	cleavage	
	T2	30-34	1-3		
	C4	11-13	1-3		
4	GLC20	10-12	1-3	Figure 12 – 5.0 μM cisplatin PARP	62
	pcDNA3	47-49	1-3	cleavage and 5.0 μM fluorescence	
	T2	30-32	1-3	microscopy	
	C4	13-15	1-3		
5	GLC20	6-12	1-5	Figure 13 – RBM5 effects on RBM10	68
	pcDNA3	42-48	1-5		
	T2	27-32	1-5		
	C4	9-13	1-5		
6	G300.3	1-6	1-3	Figure 14 – RBM10 KD analysis	71
	G29/30.1	1-6	1-3		
	G29/30.3	1-5	1-3		
	G29/30.4	1-4	1-3		
7	G300.3	5-8	1-3	Figure 15– RBM10 KD effects on cell	73
	G29/30.1	5-7	1-3	proliferation	
	G29/30.3	4-7	1-3		
	G29/30.4	3-5	1-3		

* denotes 'Biological replicate'

experiments were performed with similar passage number in order to control for differences in time of propagation or passage number amongst experiments and cell lines.

In order to ensure that the expression of RBM5 remained constant between the cell stocks used in our experiments, mRNA from nearly all the biological replicates was isolated from the cells from each trial as described in Table 7. The mRNA was then transformed into cDNA by reverse-transcription, and PCR was carried out. Forty PCR cycles were done to ensure that any residual expression of RBM5 in the GLC20 and pcDNA3 control sublines would be detected as this could indicate cross-contamination between the sublines. As noted in Figure 6, RBM5 expression was found only in the T2 and C4 sublines throughout all the trials. In all biological replicates within each trial, RBM5 expression was present in each RBM5-expressing subline. There was no visual presence of RBM5 mRNA expression in the GLC20 and pcDNA3 in any trials of the experiments that were performed.

These RT-PCR experiments ensured that RBM5 expression was monitored within each trial of experiments. The observation of a lack of RBM5 expression within the GLC20 and pcDNA3 sublines in addition to the expected expression of RBM5 within the T2 and C4 sublines increases confidence that the following experiments and results are indicative of the effect RBM5 expression on cell physiology. This suggests that any differences observed between the sublines could be due to the differences in RBM5 expression.

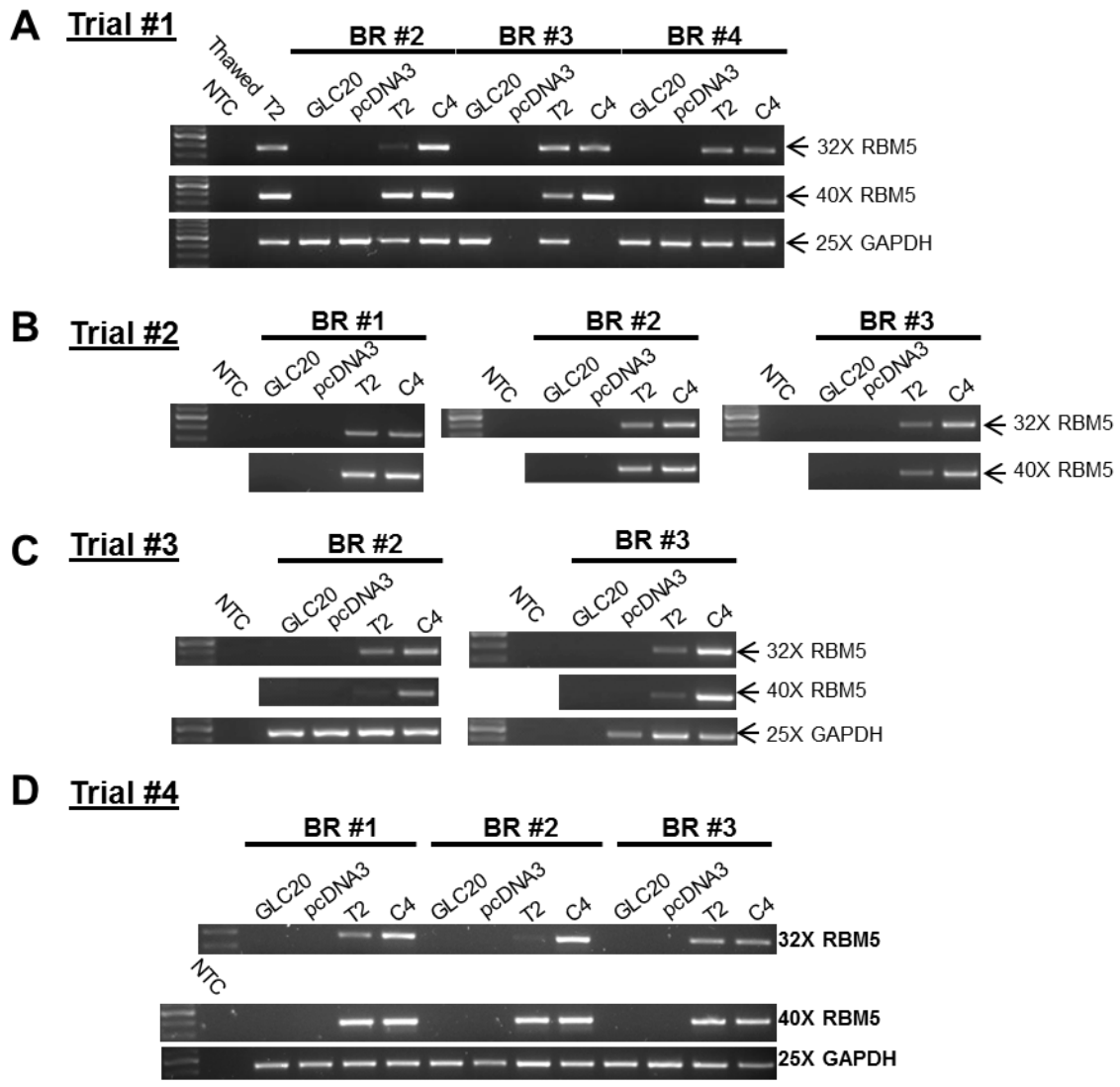

Figure 6. RBM5 mRNA expression in each subline for several trials. End-Point PCR analysis was carried out on mRNA extracted from GLC20, pcDNA3, T2 and C4 cell pellets collected at the same time as the plating of experiments. Each trial denotes a set of biological replicates. 32 and 40 cycle RBM5 PCR and 25 cycle GAPDH PCR reactions were carried out, as shown, for each BR. One technical replicate was performed for each biological replicate. NTC stands for 'no template control'. 'Thawed T2' represents an mRNA sample extracted from the first passage of T2 cells there were used in the experiments.

3.2 Increased RBM5 expression resulted in decreased GLC20 cell proliferation

To observe the effect of differing levels of RBM5 expression on GLC20 cell proliferation, two assays were employed, MTT and cell counting. RBM5 is a known regulator of the cell cycle, and RBM5 overexpression has previously been associated with G_1 phase arrest [53]. RBM5 overexpression has also been shown interfere with the proliferation of various cell lines, including A549 cells (lung adenocarcinoma) [6,16,17,20,54]. As a result, it was expected that the proliferation of the SCLC cell lines would decrease as RBM5 expression would increase.

Cell proliferation was first examined using the MTT assay (Figure 7A). The MTT assay uses the addition of MTT reagent (Section 2.4), which is metabolized in functional mitochondria into a formazan dye, to provide a colorimetric tool to quantify at 540 nm [136]. Cell proliferation was also determined using a hemocytometer (Figure 7B). In this case, the number of live cells excluding nigrosin was used as a measure of proliferation. The MTT assay was previously used to examine the response of GLC20 cells following their exposure to different reagents [130,134]. Cell proliferation was monitored every day using the MTT assay (Figure 7A) and every other day by cell counting (Figure 7B) for a ten-day period. In both assays, average values from each day in which a measurement was taken was made relative to the values obtained on the first day of the experiment (day zero) to demonstrate relative cell growth.

Figure 7 presents the results obtained from the MTT (trial #1) and cell counting (trial #2) assays. The results from the MTT assay (Figure 7A) show that the growth of the high RBM5-expressing C4 subline was significantly less than the pcDNA3-transfected RBM5-null subline from day five to day ten (day five $p<0.01$, day six-ten $p<0.0001$). The non-transfected wild type GLC20 subline also showed a significant decrease in cell growth from day eight to day ten of the assay

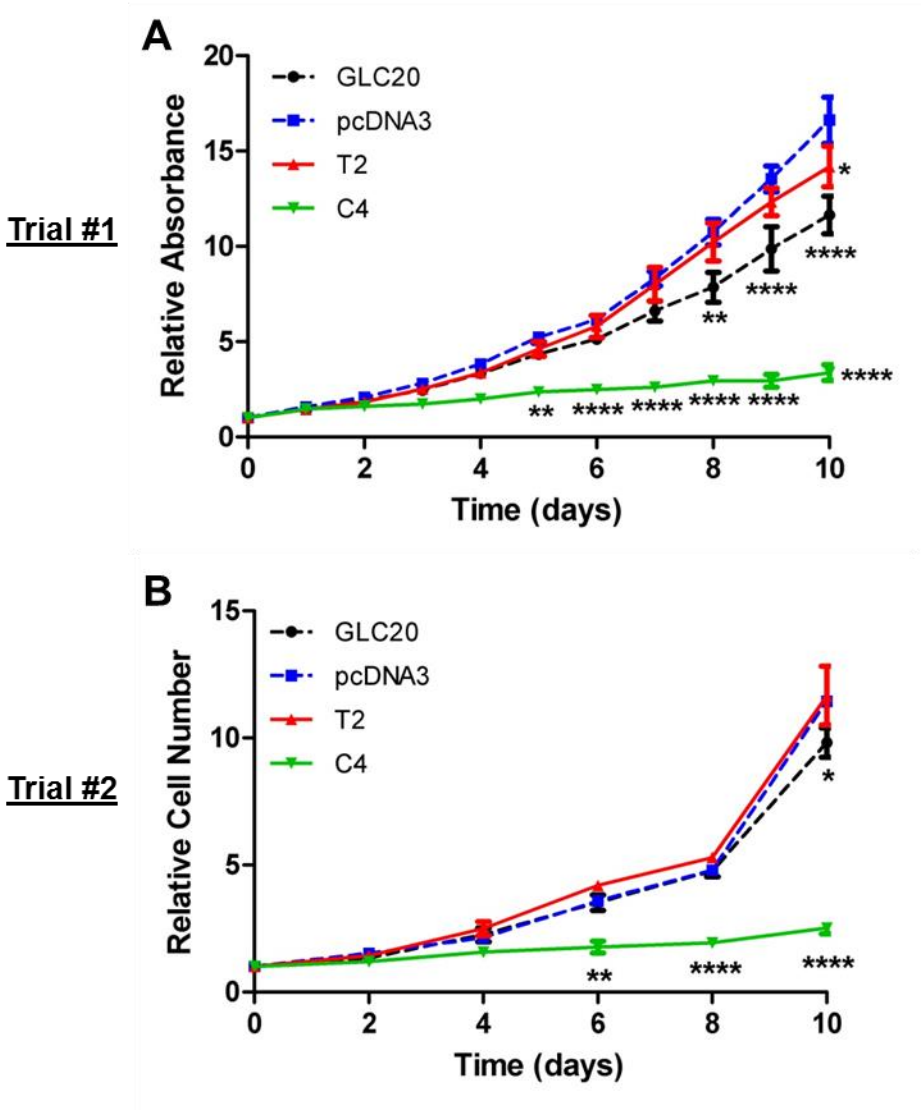

Figure 7. Increased RBM5 expression resulted in decreased GLC20 cell proliferation. GLC20, pcDNA3, T2 and C4 GLC20 sublines were grown for 10 days and their growth monitored (A) daily by a MTT assay, and (B) every other day by cell counting using a hemocytometer. (A) Average of four biological replicates performed in eight technical replicates with standard error. (B) Average of three biological replicates carried out in technical triplicate with standard error is displayed. A Two-way ANOVA was performed between pcDNA3 and the other sublines, with Bonferroni post-hoc analysis, for (A) and (B). *p<0.05, **p<0.01, ***p<0.001 and ****p<0.0001.

(day eight p<0.01, day nine, day ten p<0.0001), compared to the pcDNA3 subline. Lastly, the low RBM5-expressing T2 subline demonstrated no significant difference in cell growth from the pcDNA3 control subline until day ten (p>0.05) in Figure 7A.

The results from the cell counting assay (Figure 7B) show that the C4 subline had significantly less cell growth when compared to the pcDNA3 subline, from day six to day ten (day six $p<0.01$, day eight, day 10 $p<0.0001$). As in the MTT assay, the GLC20 wild type cell line showed a significant decrease in cell growth, compared to the pcDNA3 subline but by the later time point of day ten ($p<0.05$) rather than day eight (Figure 7A). The low RBM5-expressing T2 subline showed no growth difference compared to the pcDNA3 subline, in contrast to what was noted by MTT. Using both assays, the results demonstrate that highly increased RBM5 expression appears to induce a decrease in GLC20 cell proliferation.

Following the observation of the effect of RBM5 on GLC20 cell proliferation, the additive effect of cisplatin exposure on the role of RBM5 in cell proliferation was investigated. RBM5 is a known modulator of both the cell cycle and apoptosis [53], and so this experiment was performed to understand whether cisplatin would increase the effect of RBM5 expression on cell proliferation. Cisplatin was chosen as it is commonly used in chemotherapy for SCLC [104]. Live cell counting, as noted above, was used to monitor each subline's proliferation in the presence of a saline control or 1.0 μM cisplatin (in saline).

As shown in Figure 8A, we noticed that the proliferation of each subline after exposure to saline was similar to that of untreated cells found in Figure 7B. Both the GLC20 and T2 sublines did not show a significant difference in cell growth when treated with saline, relative to the pcDNA3 subline. Similar to the unexposed cells in Figure 7B, the C4 subline had a significant difference in cell proliferation when compared to the pcDNA3 subline, from day six to day ten (day six $p<0.001$, day eight, day ten $p<0.0001$). Figure 8B shows that all sublines exhibited a cisplatin-induced reduction in proliferation over the ten-day period. Both the wild type GLC20

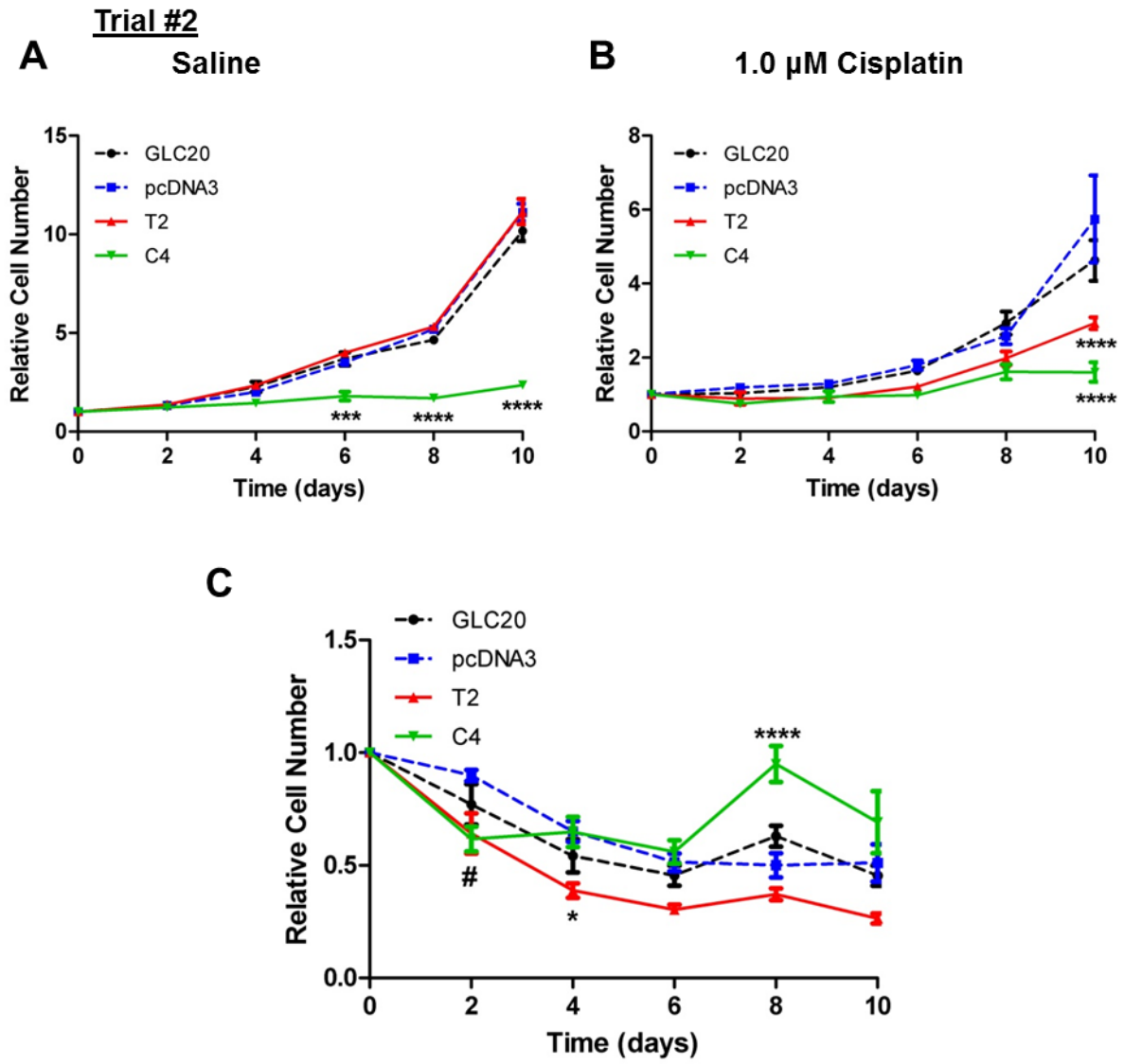

Figure 8. RBM5 expression did not induce an additional effect on GLC20 cell proliferation decrease in presence of cisplatin. Trial #2 GLC20, pcDNA3, T2 and C4 cell growth was monitored by hemocytometer every other day for 10 days after treatment with either (A) a saline control, or (B) 1.0 µM cisplatin. (A) and (B) Average of the three biological replicates performed in technical triplicate with standard error. (C) Average of all three biological replicates of 1.0 µM cisplatin made relative to the saline control of its biological replicate with standard error. A Two-way ANOVA was performed between pcDNA3 and the other sublines, with Bonferroni post-hoc analysis for (A), (B) and (C). */# (where two sublines are significant) $p<0.05$, *** $p<0.001$ and **** $p<0.0001$.

and pcDNA3 control sublines had similar results for cell proliferation. The T2 and C4 sublines showed a greater decrease in relative live cell number in the presence of cisplatin that was significant on day ten (both $p<0.0001$), when compared to pcDNA3-transfected cells.

To determine if the exposure to cisplatin resulted in an increase of the effect of RBM5 on cell proliferation, the results obtained in the presence of 1.0 μM cisplatin (Figure 8B) were normalized to those exposed to saline (Figure 8A) and are presented in Figure 8C. This was performed to understand if the reduction in cell proliferation, observed as a loss in relative live cell counts, was due to RBM5 expression. Over the ten-day experiment, a trend appears in which the relative cell proliferation of each subline decreased uniformly with no differences. However, on day two of the experiment, both the T2 and C4 sublines showed a significant decrease in relative cell growth (day two both $p<0.05$), suggesting an additive effect of cisplatin on the RBM5-expressing sublines' cell proliferation. The T2 subline also showed a significant decrease in relative cell growth on day four ($p<0.05$), compared to the pcDNA3 subline. The C4 subline demonstrated a significant increase in cell growth on day eight ($p<0.001$), compared to the pcDNA3 subline, which differs from the downward trend in each subline. By day ten, the proliferation of the C4 subline was again decreased. This result may suggest that, in the presence of cisplatin, there is a reduction in cell proliferation in the RBM5-expressing sublines early after exposure that occurs before RBM5 expression is observed to reduce cell proliferation in the untreated cells (Figure 7). The effect does not occur over a longer period of time, as each subline reverts to the observed trend after day six. Most likely, this is could be simply variation in the data over time.

These results demonstrated that the cell lines with high RBM5 expression exhibit reduced cell proliferation, as made evident by the significant decrease in cell growth noted in the C4

population (Figure 7). Clonal variation can also account for these observations in the C4 subline, and will be discussed further in the discussion section. In addition, exposure to saline has no effect on the proliferation of the sublines (Figure 8A). In contrast, exposure to cisplatin resulted in a reduction of cell proliferation in each subline (Figure 8C), which was observed to be significant in the T2 and C4 sublines by day ten, when compared to the pcDNA3 subline. Upon comparing the cell proliferation of cells exposed to 1.0 μM cisplatin relative to the saline exposed cells, RBM5 expression induced a significant decrease in cell proliferation early after exposure, although there was an observed downward trend common in each subline (Figure 8C).

3.3 RBM5 expression was associated with increased GLC20 cell death in the presence of cisplatin

Having noted a significant decrease in cell proliferation in the high RBM5-expressing C4 subline, but no overall difference in cell proliferation in cisplatin exposed cells, relative to the pcDNA3-transfected subline, the effect of RBM5 expression on GLC20 cell death was examined. RBM5 is a modulator of cell death through apoptosis [46,53]. Therefore, RBM5 expression may be influencing GLC20 cell death in the presence of cisplatin. It was anticipated that there would be an increase in GLC20 cell death in the RBM5-expressing sublines, relative to the expression of RBM5.

To ascertain whether or not RBM5 increased GLC20 cell death, live and dead cell counts were performed every other day for ten days and percent membrane integrity was determined, as noted in Section 2.5, using a nigrosin exclusion assay. The percentage of cells with intact membrane is surrogate for cell viability. It was observed that roughly 80% of unexposed GLC20 cells and sublines retained plasma membrane integrity throughout the ten days of the experiment, as shown in Figure 9A. The control saline exposed cells in Figure 9B were also observed to have

maintained roughly 80% of cell membrane integrity through the experiments. In each of the unexposed and saline exposed cells, no subline demonstrated a significant difference in intact membrane when compared to the pcDNA3 subline. The lack of significant differences provides evidence that RBM5 expression on its own did not result in a decrease in cell membrane integrity, suggesting there was no increase in cell death.

In the cisplatin-treated cells, a significant decrease was observed in the percentage of cells with membrane intergity, suggesting that cell viability was reduced (Figure 9C). The GLC20 and pcDNA3 sublines reached a minimum of approximately 70% of cells with membrane intergrity on day four, that was maintained for the remainder of the experiment. Both RBM5-expressing sublines demonstrated a greater decrease in the percentage of cells with membrane integrity. The T2 subline reached a minimum of approximately 50% of cells with intact plasma membranes by day eight, increasing slightly thereafter. The percentage of C4 subline cells with membrane integrity continued to decrease throughout the ten-day experiment, reaching a minimum of approximately 40% of cells with membrane integrity by day ten. Both the T2 and C4 sublines demonstrated a significant decrease in the percentage of cells with membrane integrity, relative to the pcDNA3 subline, starting on day four, and continuing throughout the experiment (Figure 9C) (T2: day four $p<0.05$, day six $p<0.001$, day eight $p<0.0001$, day ten $p<0.01$, C4: day four $p<0.001$, days six-ten $p<0.0001$). This significant decrease in T2 and C4 subline membrane integrity when the cells were exposed to 1.0 μM cisplatin suggests that RBM5 expression sensitized cells to death-inducing stresses.

As shown in Figure 9D, when the percentage of cells with membrane integrity of the cisplatin-exposed sublines was compared to those exposed to saline, the GLC20 and pcDNA3 sublines

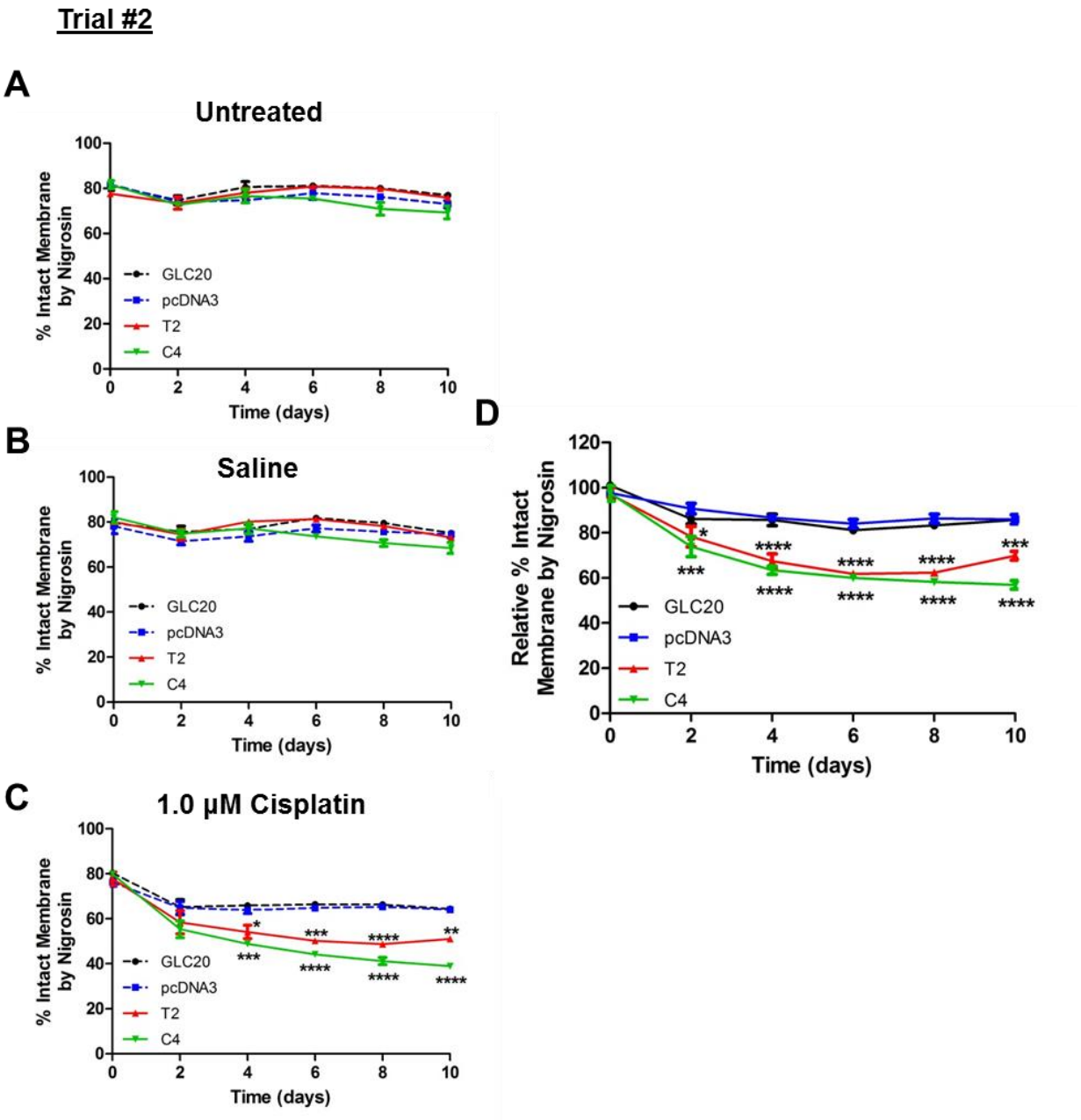

Figure 9. GLC20 cell membrane integrity decreased with RBM5 expression in the presence of cisplatin. Trial #2 GLC20, pcDNA3, T2 and C4 membrane integrity was monitored by hemocytometer every other day for 10 days and were (A) left untreated, or exposed to either (B) a saline control or (C) 1.0 µM cisplatin. Average of the three biological replicates performed in technical triplicate with standard error is displayed for each treatment. (D) GLC20, pcDNA3, T2 and C4 1.0 µM cisplatin was made relative to the saline control for each time point. Average of all three biological replicates of 1.0 µM cisplatin were normalized to the saline control of its biological replicate with standard error is displayed. A Two-way ANOVA was performed between pcDNA3 and the other sublines, with Bonferroni post-hoc analysis for (A), (B), (C) and (D). * $p<0.05$, ** $p<0.01$, *** $p<0.001$ and **** $p<0.0001$.

showed similar decreases in the percentage of cells with membrane integrity, with a minimum of roughly 85% of cells having intact membranes by day two, a level maintained throughout the experiment. In contrast, the T2 and C4 sublines had a greater decrease, with a minimum of roughly 60% of cells having intact membranes by day eight. The decrease in the percentage of T2 and C4 cells with membrane integrity was significant when compared to the pcDNA3 subline from day two to ten (T2: day two $p<0.05$, days four-eight $p<0.0001$, day ten $p<0.001$, C4: day two $p<0.001$, days four-ten $p<0.0001$). There were no significant differences between the GLC20 wild type and pcDNA3 control sublines. This indicates transfection of cells with the empty vector did not affect the cells' response to 1.0 μM cisplatin exposure. In summary, the experimental results presented in Figure 9 demonstrated that in the presence of 1.0 μM cisplatin the percentage of cells with membrane integrity decreased for all sublines, with those expressing RBM5 resulting in a greater significant decrease.

To further explore the significant decrease in membrane integrity observed in the RBM5-expressing sublines, the EC_{50} or the concentration of cisplatin required to reach 50% relative intact membrane was calculated for each subline on day four and day eight. The GLC20 cells have previously been documented to have an IC_{50} of approximately 75.0 μM cisplatin after one hour through the use of the MTT assay [130]. In addition to a saline control, cells were exposed to increasing concentrations of cisplatin for either four or eight days and cell membrane integrity was determined. Percent intact membrane values were then calculated and expressed relative to the saline control for each time point (as previously presented in Figure 9D) and plotted on a 'non-linear fit-log(inhibitor) vs response model (3parameters)' plot in Graphpad Prism 5, to obtain the EC_{50} values. The saline control was given a concentration of 10^{-10} μM cisplatin, since the log of zero is undefined. Figure 10 shows the calculated EC_{50} values for each four-day

exposure (Figure 10A) and eight-day exposure (Figure 10B). Figure 10Ai and Bi show the calculated EC_{50} curves for each subline, with comparisons to the pcDNA3 control subline. The GLC20 and pcDNA3 sublines showed no significant viability differences at any concentration of cisplatin at either time point. At cisplatin concentrations of 0.5, 1.0 and 10.0 μM cisplatin, both the T2 and C4 sublines had significant differences in relative cell membrane integrity, when compared to the pcDNA3 subline, after four days (Figure 10Ai) and eight days (Figure 10Bi) exposure (day four T2: 0.5 μM $p<0.001$, 1.0 and 10.0 μM $p<0.0001$, C4: 0.5 μM - 10.0 μM $p<0.0001$; day eight T2: 0.5 μM $p<0.05$, 1.0 μM $p<0.0001$, 10.0 μM $p<0.05$, C4: 0.5 μM - 10.0 μM $p<0.0001$). At cisplatin concentrations of 0.1 and 100.0 μM, no significant differences, on either day, were observed, when compared to the pcDNA3 subline.

The EC_{50} value for each subline was then calculated from the curves in Figure 10Ai, Bi, and presented as a bar graph in Figure 10Aii, Bii. GLC20 and pcDNA3 sublines were calculated to have an EC_{50} of 17.97 μM and 17.16 μM on day four and 3.58 μM and 3.59 μM on day eight, respectively, with no significant differences on either day. In comparison, T2 and C4 sublines were calculated to have EC_{50} values of 4.86 μM and 2.52 μM on day four and 1.74 μM and 1.29 μM on day eight, respectively. When compared to the pcDNA3 subline, the EC_{50} of both the T2 and C4 sublines showed a significant difference on both day four (T2 $p<0.05$, C4 $p<0.01$) and day eight (T2 $p<0.001$, C4 $p<0.001$). These results support the earlier observation of decreased membrane integrity in the RBM5-expressing sublines, at 1.0 μM cisplatin, as shown in Figure 9, suggesting that the observed decrease in cisplatin EC_{50} is attributable to RBM5 expression. Furthermore, neither the T2 nor the C4 sublines showed a significant difference in its EC_{50} for cisplatin on day four and day eight. However, there was a decrease in cisplatin EC_{50} in all sublines between day four and day eight, suggesting the longer the exposure to cisplatin, the less

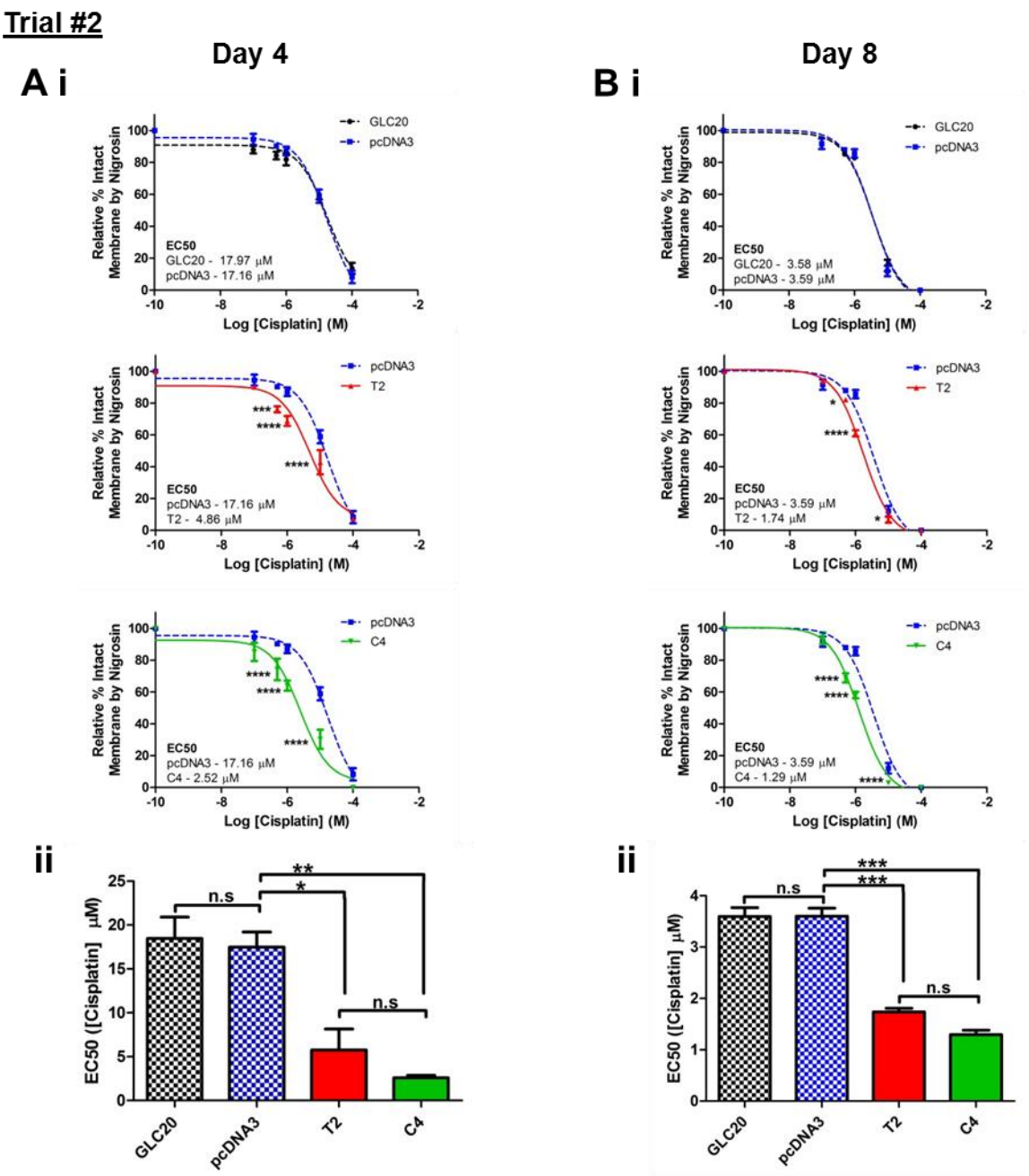

Figure 10. GLC20 cisplatin EC_{50} decreased with RBM5 expression. Trial #2 GLC20, pcDNA3, T2 and C4 membrane integrity was monitored by hemocytometer after (A) 4 and (B) 8 days of exposure to a saline control (10^{-10} M cisplatin), and 0.1, 0.5, 1, 10, and 100 µM cisplatin. Membrane integrity of each concentration was made relative to the saline control and displayed as relative intact membrane by nigrosin (%) over log concentration of cisplatin. (i) Average relative intact membrane of three biological replicates performed in technical triplicate with standard error and the calculated average EC_{50} (calculated from Graphpad Prism 5, 'non-linear fit–log(inhibitor) vs response (3 parameters)'). (ii) Average EC_{50} of three biological replicates is plotted for each subline. One-way ANOVA was performed, with Tukey post-hoc analysis where noted between the sublines. * p<0.05, ** p<0.01, *** p<0.001 and **** p<0.0001.

cisplatin is required to result in a loss of 50% of the cells. This result suggests that RBM5 expression, no matter the level, is associated with an expression-level dependent reduction in cisplatin EC_{50}.

In summary, these results demonstrate a significant decrease in intact cell membranes in the RBM5-expressing T2 and C4 sublines, relative to the pcDNA3 subline in the presence of 1.0 μM cisplatin. Also, there was a significant decrease in the EC_{50} values of the T2 and C4 sublines, compared to the pcDNA3 control, and no change between the pcDNA3 and GLC20 sublines, after four and eight days of exposure cisplatin. When taken as a whole, these observations demonstrate that high RBM5 expression induces increased cell death in the presence of cisplatin.

3.4 Increased RBM5 expression resulted in increased apoptotic cell death in GLC20 cells in the presence of cisplatin

Following the discovery that RBM5 expression in the T2 and C4 sublines resulted in (a) significantly increased cell death (measured as decrease in the percentage of cells with membrane integrity) (Figure 9) and (b) a significantly decreased cisplatin EC_{50} (Figure 10), further experimentation was carried out to determine whether or not this decrease in membrane integrity was due to increased apoptosis. Since cisplatin commonly kills cells by triggering apoptosis [121,123], and RBM5 is a modulator of this type of cell death [46], it was anticipated that the presence of RBM5 in the T2 and C4 sublines was influencing the effect of cisplatin on death signalling pathways.

To first explore whether or not the decreased membrane integrity of the RBM5-expressing sublines in the presence of cisplatin was a result of apoptosis activation, cells were exposed to 5.0 μM cisplatin for four days and PARP cleavage was monitored. The first preliminary

experiment was performed to determine if 5.0 μM cisplatin exposure was sufficient to induce apoptosis, and to confirm the T2 subline's EC_{50} at day four. Figure 11 highlights the results from this experiment. As shown in Figure 11A, it was observed that there was an increase in the 89 kDa PARP cleavage product, but no visual decrease in intact PARP (116 kDa). This observation could be due to saturation of the upper PARP band, or due to the capturing of very early apoptosis. Regardless, this was an initial test to confirm previous results, and therefore, 89 kDa band intensity measurements by densitometry were expressed relative to α-tubulin for each subline, and then normalized to that obtained for the pcDNA3-transfected subline (Figure 11B). Although the error bars show a high level of variance (Figure 11B), the densitometry results demonstrated an approximately 1.8-fold increase in the 89 kDa PARP cleavage product in the T2 subline (p=0.0457) and a 5.5-fold increase in the 89 kDa PARP cleavage product in the C4 subline (p=0.0068), when compared to the pcDNA3-transfected cell line (Figure 11B). Furthermore, the level of the 89 kDa PARP cleavage product in the GLC20 and pcDNA3-transfected cell lines was not significantly different from each other (p=0.4255). These results demonstrated that there was a significant increase in the generation of the 89 kDa product after four days of cisplatin exposure in the RBM5-expressing sublines T2 and C4. This was the first indication that the increase in cell death, or decrease in cell membrane integrity, that was observed in the RBM5-expressing sublines exposed to cisplatin may be due to apoptosis.

To confirm that the increase in cell death and the increase in the 89 kDa PARP cleavage product in the T2 and C4 sublines was through the promotion of apoptosis, further experiments looking into other apoptotic markers were performed. RBM5, as a modulator of apoptosis, has been shown to influence many markers of apoptosis such as chromatin condensation and phosphatidylserine exposure on the external plasma membrane surface (phosphatidylserine

Trial #3

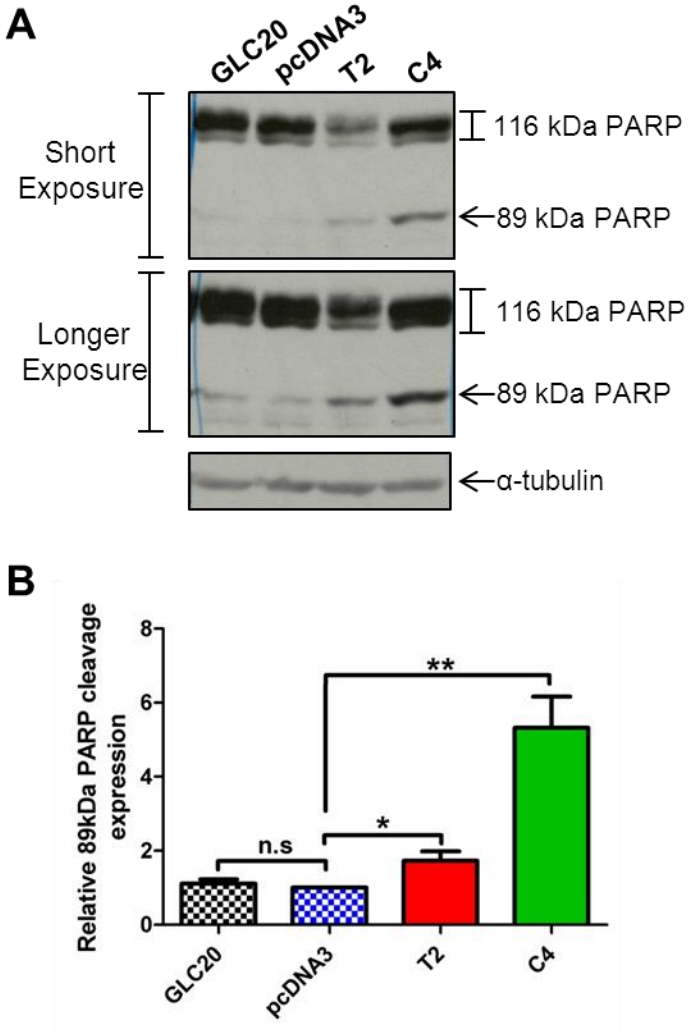

Figure 11. RBM5-related cell death in presence of 5 μM cisplatin corresponded with an increase in PARP cleavage. PARP cleavage was monitored in Trial #3 GLC20, pcDNA3, T2 and C4 cells after treatment with 5.0 μM cisplatin for four days. (A) One representative biological replicate Western blot result is presented at two different exposures. (B) Densitometry of the scanned Western blot autoradiographs of each biological replicate was performed using the AlphaEaseFC, '1D-Multi' analysis tool. Values of 89 kDa PARP cleavage product were normalized to the α-tubulin of the biological replicate, and then normalized to the pcDNA3 control. Average 89 kDa cleavage product of three biological replicates with standard error is presented. One-way ANOVA was performed with Tukey post-hoc analysis, between sublines. * $p<0.05$, ** $p<0.01$, *** $p<0.001$ and **** $p<0.0001$.

flipping or membrane asymmetry) [24,53], and cisplatin is known to kill cells through apoptosis [121,123]. It was anticipated that the RBM5-expressing sublines (T2 and C4) would show evidence of other apoptotic markers in the presence of cisplatin. Therefore, fluorescence microscopy was performed to investigate chromatin condensation and phosphatidylserine flipping (via Annexin-V binding), both hallmarks of apoptotic cells [45,48]. In addition, PARP cleavage was again monitored, in the same trials (#4) used for fluorescence microscopy. Cells were exposed to 5.0 μM cisplatin over a period of four days, after which fluorescence microscopy and PARP cleavage assays were conducted. As noted in Section 2.7.3 and Figure 4, several different stains were used to distinguish different cellular phenotypes. A summary of the classifications of events was presented in Section 2.7.3.

Figure 12 highlights the results that were obtained from the fluorescence microscopy experiments and Western blot analysis of PARP cleavage. Cells from trial #4 were used in these studies, as noted in Table 7. Figure 12A presents sample images of untreated cells incubated for four days while Figure 12B presents sample images of cells that were exposed to 5.0 μM cisplatin for four days. Figure 12C shows PARP cleavage by Western blot analysis of the same cells for fluorescence microscopy. In the untreated cells, there was no visible chromatin condensation (Figure 12A, left most panel), Annexin-V binding (an indication of potential phosphatidylserine flipping) (Figure 12A, middle-left panel) or changes in membrane integrity (Figure 12A, middle-right panel) for the four sublines. The merge images provided in the far-right panels in Figure 12A combine the three stains in one image.

Cells exposed to 5.0 μM cisplatin for four days (Figure 12B) exhibited differences in phenotypes compared to untreated cells (Figure 12A). In the cisplatin-exposed cells, there were visual increases in chromatin condensation, Annexin-V binding (potential phosphatidylserine flipping)

Trial #4

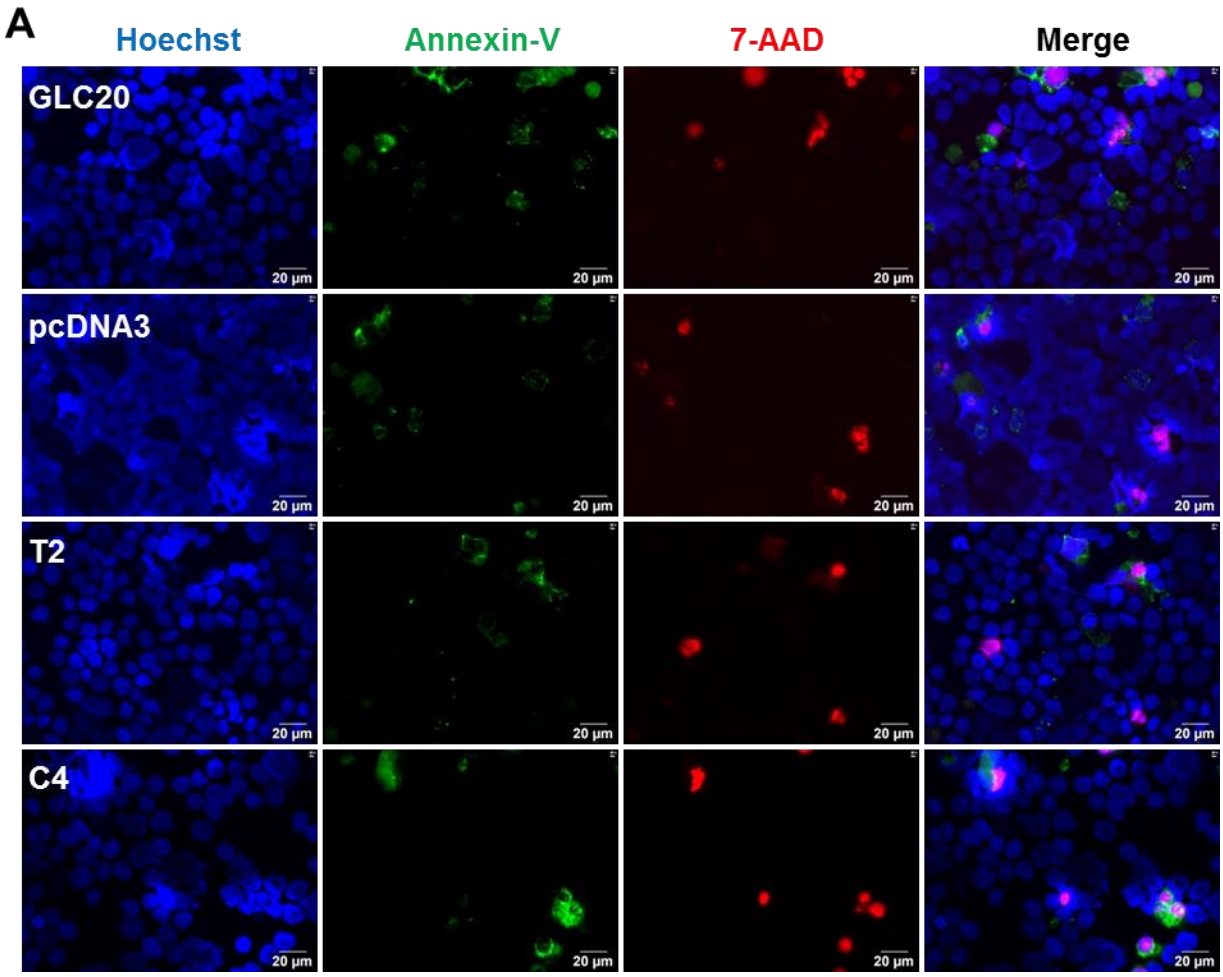

Figure 12. Increased RBM5 expression resulted in increased apoptosis in the presence of 5 µM cisplatin. Trial #4 GLC20, pcDNA3, T2 and C4 cells were left (A) untreated or (B) treated with 5 µM cisplatin and collected after four days for fluorescence microscopy using a 40X objective lens (A/B) or PARP cleavage analysis (C i/ii). One representative image of each cell line (A) left untreated or (B) exposed to 5 µM cisplatin for four days is presented. Apoptotic markers chromatin condensation (Hoechst/blue) and Annexin-V binding (phosphatidylserine flipping) (Annexin-V/green) as well as late apoptosis/necrosis marker of presence of red 7-AAD stain were analyzed by fluorescence microscopy. (C i) One representative biological replicate Western blot result is presented. (C ii) Densitometric analysis of each biological replicate was done using AlphaEaseFC, '1D-Multi' analysis tool. Percent 89kDa PARP cleavage product [(89kDa cleaved PARP/total PARP)*100] analysis of three biological replicates with standard error of the 5 µM cisplatin treated and untreated cells is presented. (C iii) Average number of fluorescence microscopy events pooled into Live (only blue), Early Apoptosis (condensed blue and/or green) and Late Apoptosis/Necrosis (Red) performed in three biological replicates, each with 10 different fields of view, with standard error of the 5 µM cisplatin and untreated cells. One-way ANOVA was performed with Tukey post-hoc analysis, between sublines. * $p<0.05$ and *** $p<0.001$.

Trial #4

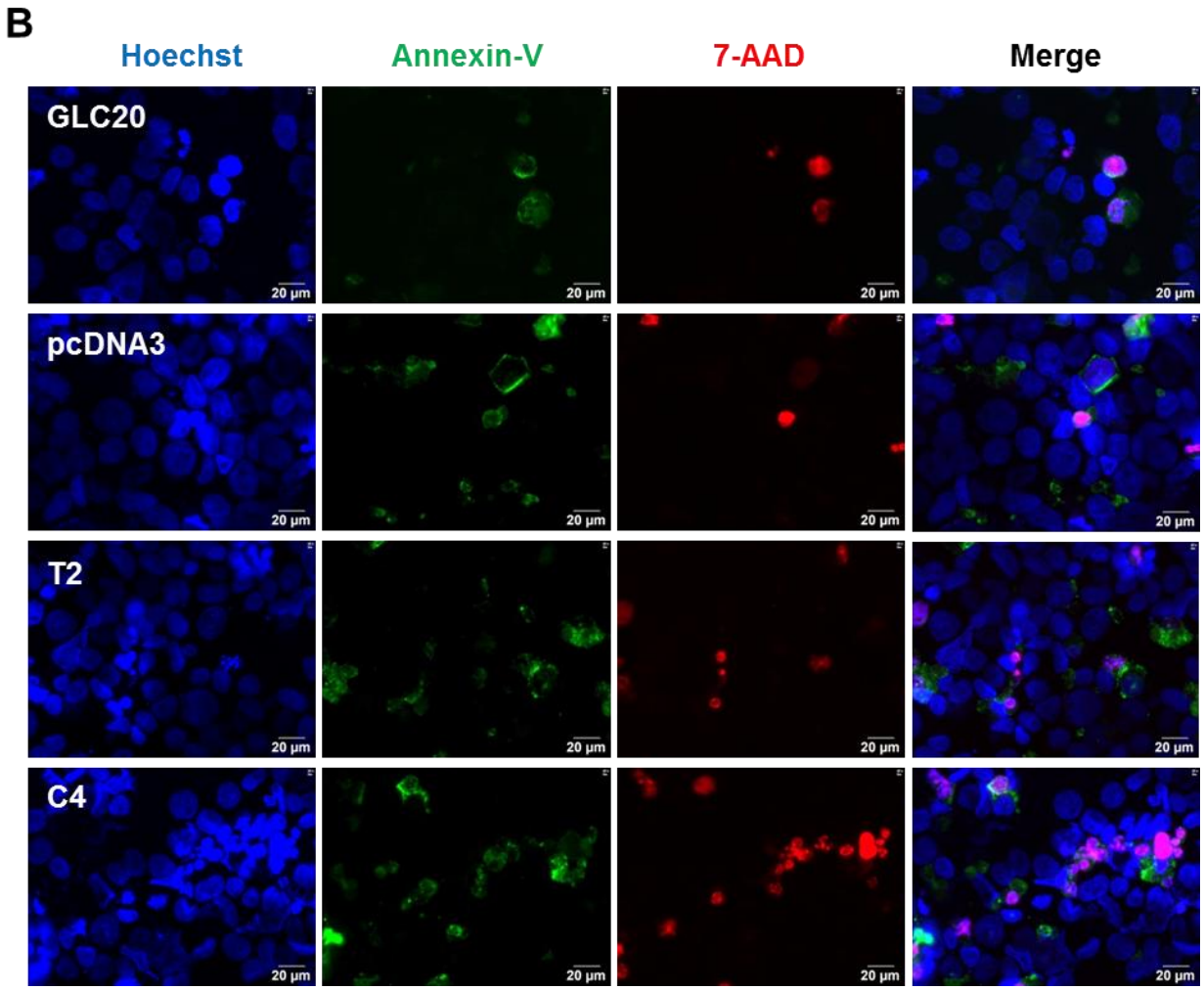

Figure 12. Increased RBM5 expression resulted in increased apoptosis in the presence of 5 µM cisplatin.

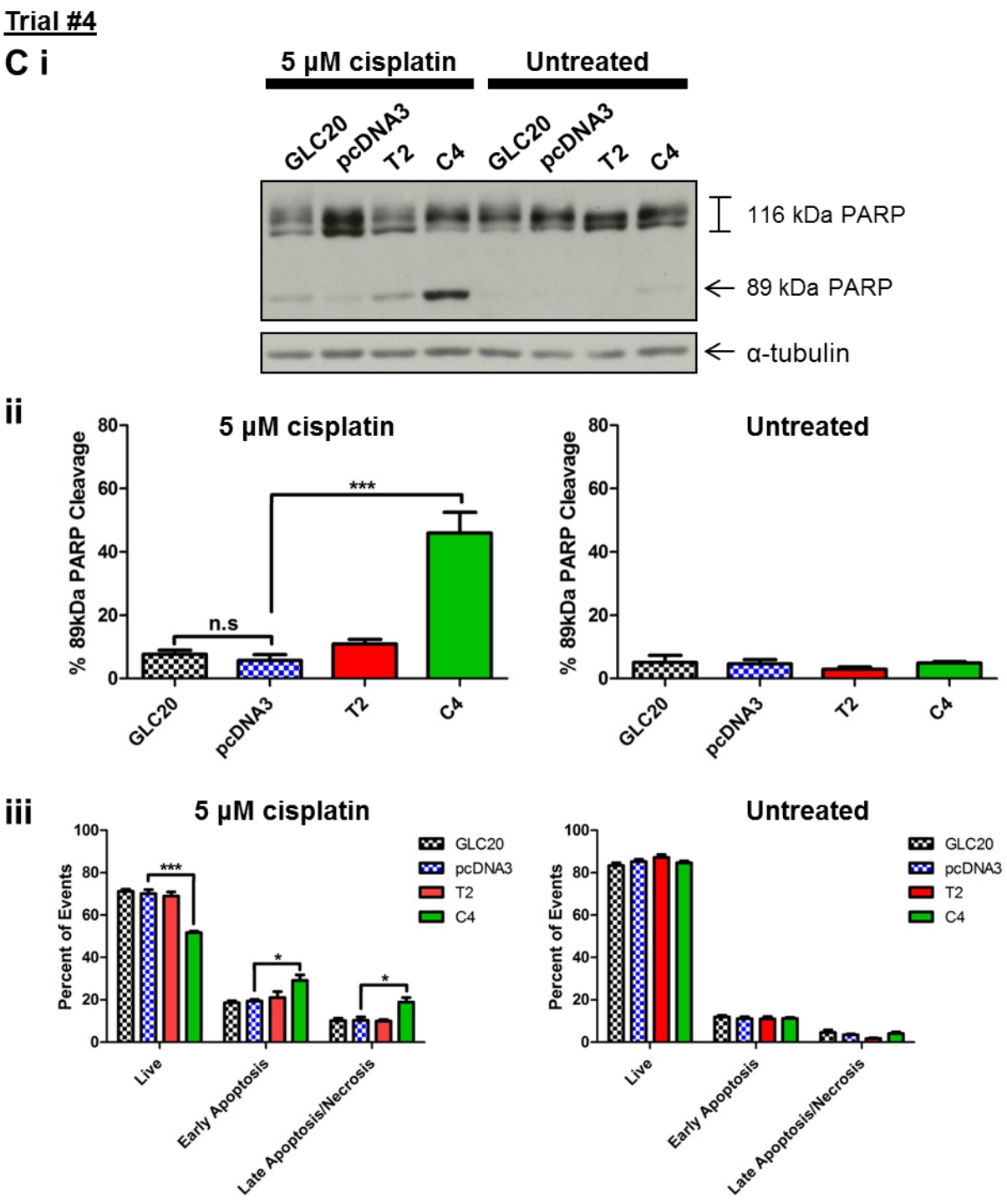

Figure 12. Increased RBM5 expression resulted in increased apoptosis in the presence of 5 μM cisplatin.

and loss of membrane integrity that was even greater in the C4 subline. These markers suggest that in the high RBM5-expressing subline exhibited an even greater decrease in 'Live' cells and an increase in the number of cells exhibiting 'Early Apoptosis' or 'Late Apoptosis/Necrosis'. In addition, it was noted that the two RBM5-null sublines (GLC20 and pcDNA3) had larger nuclei than the two RBM5-expressing sublines (T2 and C4) when exposed to cisplatin. This observation was not quantified, however may possibly suggest that there is less chromatin condensation or apoptosis in the absence of RBM5 expression.

The PARP cleavage results are presented in Figure 12C. In this trial, expression of the 89 kDa PARP cleavage product was quantified as a percentage of the uncleaved product, rather than expression due to the visual decrease in the 116 kDa full-length PARP noted in the C4 sublines. This differed from what was noted and quantified in Figure 11, which was also performed with 5.0 μM cisplatin exposure after four days.

Overall, cells that were left unexposed for four days maintained low levels of PARP cleavage (4% 89 kDa PARP cleavage) (Figure 12Cii), high levels of 'Live' cells (85% of events), and low levels of 'Early Apoptotic' and 'Late Apoptotic/Necrotic' cells at roughly 11% and 4% of events, respectively (Figure 12Ciii). There were no significant differences between the sublines, signifying no effect of RBM5 in the absence of cisplatin. However, when exposed to 5.0 μM cisplatin for four days, differences between the sublines arose. Both the GLC20 and pcDNA3-transfected sublines demonstrated roughly 7% PARP cleavage, with no significant difference between the sublines. The T2 subline had 1.6-fold higher PARP cleavage relative to the pcDNA3-transfected subline (11% vs 7%, respectively), although this difference was not significant. The high RBM5-expressing subline, C4, demonstrated roughly 45% PARP cleavage, which was significantly higher than that of the pcDNA3-transfected cells ($p<0.001$). This

observation was further supported by the fluorescence microscopy results in Figure 12Ciii, as the percentage of 'Live' C4 cells was significantly reduced to roughly 50% compared to the pcDNA3-transfected control cell line value of 70% ($p<0.001$). In addition, there was a significantly higher percentage of 'Early Apoptotic' and 'Late Apoptotic/Necrotic' C4 cells compared to the pcDNA3-transfected subline [30% versus 19% cells ($p<0.05$) and 19% versus 10% cells ($p<0.05$), respectively]. The GLC20 and T2 sublines showed no significant differences relative to the pcDNA3-transfected subline in terms of PARP cleavage or any of the three fluorescence microscopy categories. Each of the GLC20, pcDNA3 and T2 sublines had 70% 'Live' cells, 20% 'Early Apoptotic' cells, and 10% 'Late Apoptotic/Necrotic' cells. In comparison, the T2 subline had a significant increase in PARP cleavage relative to the pcDNA3-transfected cells, as shown in Figure 11. This difference was not further investigated.

In summary, the results presented in Figure 11 and Figure 12 indicate that the increase in cell death (Figure 9 and 10) observed in the RBM-expressing sublines (T2 and C4) was due to increased apoptosis. The high RBM5-expressing C4 subline had considerably higher PARP cleavage (Figure 11 and Figure 12Ci/ii), chromatin condensation, and phosphatidylserine flipping (Figure 12A/B) compared to the pcDNA3-transfected subline. These observations are consistent with the activation of apoptosis. The T2 subline demonstrated a significant increase in the 89 kDa PARP cleavage product relative to the pcDNA3-tranfected subline (Figure 11) but no significant increase in PARP cleavage or other apoptotic events in Figure 12. The low level of RBM5 expression in the T2 subline may explain the discrepancy in these results. However, when taken as a whole, there appeared to be a positive relationship between RBM5 expression and an increase in apoptosis in the presence of cisplatin.

3.5 RBM5 expression affected RBM10v1/v2 expression levels in GLC20 cells

In the course of our studies aiming at elucidating the function of RBM5 in GLC20 cells, we observed that the expression of RBM5 was accompanied by a change in the protein levels of different RBM10 variants. As noted earlier, RBM10 is a functional homologue of RBM5 that modulates apoptosis [72]. RBM5 is also known to be involved in the regulation of the expression of various genes via alternative splicing [60,61]. It was observed that in the high RBM5-expressing C4 subline, there was an increase in RBM10v2 protein expression and a decrease in RBM10v1 protein expression (Figure 5B). As this may be indicative of alternative splicing of the *RBM10* transcript by RBM5, this was further analyzed by a set of Western blot analysis of five biologically independent extracts of the above cell lines, using duplicate determinations.

Figure 13 highlights the work completed to investigate the association between increased RBM5 expression and a change in RBM10v1/v2 expression. Trial #5 cells were used for the analysis, as outlined in Table 7. In Figure 13A, representative Western blot results are presented. It should be noted that the exposure time to capture RBM10v2 as much longer than that of RBM10v1, as there was a much greater amount of RBM10v1 within the GLC20 cell system (Figure 5). Due to RBM10v1 saturation in RBM10v2 exposures, true RBM10v1/v2 ratios could not be presented. Therefore, while relative values of RBM10v1 and v2 expression were presented, these results should be taken as hypothetical to what may be truly occurring. In the C4 subline there appears to be a relative increase in RBM10v2 protein expression and a decrease in RBM10v1 protein expression. Densitometry was performed on each set of technical duplicates for each biological replicate and the average of these five biological replicates was quantified (Figure 13B). When comparing RBM10v1/v2 expression in the C4 subline to that in the pcDNA3 subline, there was a

Trial # 5

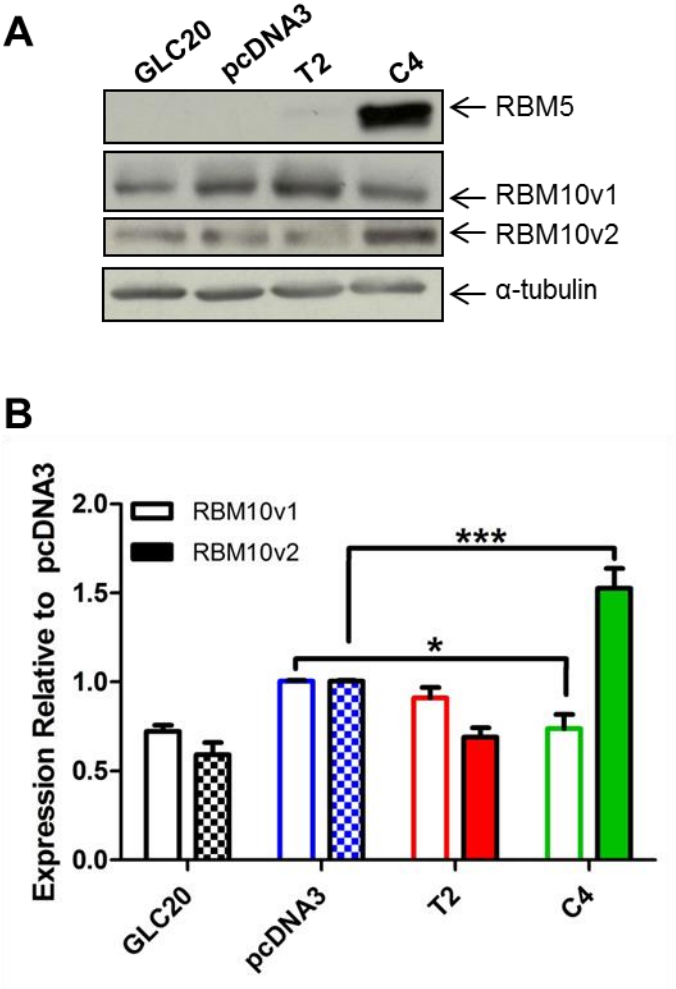

Figure 13. Increased RBM5 expression influenced an increase in RBM10v2 and a decrease in RBM10v1 protein expression. RBM10v1/v2 protein expression was monitored in GLC20, pcDNA3, T2 and C4 cells using the Sigma RBM10 antibody. (A) One representative Western blot result is presented for RBM10v1/v2, RBM5 and α-tubulin. RBM10v2 was captured using a longer exposure as mentioned previous in Figure 6. (B) Densitometric results of the average RBM10v1/v2 expression of three biological replicates each performed in technical duplicate was performed using AlphaEaseFC, '1D-Multi' analysis tool. Values of RBM10v1 and RBM10v2 were normalized to the α-tubulin of each biological technical duplicate, and then made relative to the pcDNA3 controls. Standard error is presented. One-way ANOVA was performed with Tukey post-hoc analysis, between sublines. * $p<0.05$ and *** $p<0.001$.

significant 1.5-fold high expression (52%) of RBM10v2 in C4 cells than pcDNA3-transfect cells ($p<0.001$). RBM10v1 protein expression in the C4 subline decreased by roughly 27% relative to

pcDNA3-transfected cells, which was also significant ($p<0.05$). Although the increase in RBM10v2 expression was not equivalent to the decrease in RBM10v1 expression, there was a significant change in RBM10v1/v2 protein expression induced with increased RBM5 expression (C4 subline). Due to the reciprocal nature of the changes in expression between RBM10v1 and RBM10v2, it was postulated that increased RBM5 expression influenced changes in RBM10 alternative splicing. These results suggest that RBM5, above a certain threshold level, could regulate RBM10 alternative splicing, promoting increased RBM10v2 expression and decreased RBM10v1 expression. Alternatively, RBM5 could also potentially differentially modulate the stability of the mRNA encoding these RBM10 isoforms.

3.6 RBM10v1 knockdown induced a decrease in GLC20 cell proliferation

Following the observation that the increased RBM5 expression found in the C4 subline influenced RBM10v1/v2 expression, further studies were carried out to observe the effect of changed RBM10 expression on the GLC20 cells. RBM10 is a modulator of apoptosis, and has been documented to influence cell proliferation [56,72]. As it was observed that there was a decrease in RBM10v1 expression in the RBM5-expressing C4 subline, RBM10 knockdowns (KDs) were performed. RBM10v1 was not specifically targeted in this study as the shRNA used targeted exon 6 of RBM10 [72]. Although this would target both RBM10v1/v2, due to the almost exclusive expression of RBM10v1 in the GLC20 cells (Figure 5), all decreases in RBM10 protein were reported as RBM10v1, and any effect that was observed was assumed to be due to decreased RBM10v1 expression. It should be noted that the presence of RBM10v2 expression presented in Figure 13 was due to a longer exposure. Further analysis of the effect of RBM10 KDs on cell proliferation was performed using the MTT assay. Effects of RBM10 KDs were compared to

previously described effects of high RBM5 expression (C4 cells), to see if increased RBM5 expression and decreased RBM10v1 expression had similar effects.

Stable RBM10 KDs were produced as noted in Section 2.1.1. As previously described, GLC20 cells were subject to transfection with two RBM10 knockdown shRNA plasmids, which together were termed 29/30, and targeted exon 6 of RBM10. GLC20 sublines were then selected with puromycin and the surviving sublines characterized for RBM10v1 protein expression by Western blot analysis. Three RBM10 KD sublines were produced, termed G29/30.1, G29/30.3 and G29/30.4. A control subline was also produced, termed G300.3, using the shRNA scramble control plasmid.

Figure 14 highlights RBM10v1 protein expression in each of the sublines produced. Trial #6 cells were used for these experiments, as noted in Table 7. Figure 14A shows a decrease in RBM10v1 expression in G29/30.3 subline and an even greater decrease in G29/30.4 subline. Densitometry was performed on three biological replicates, performed in technical duplicate, and presented in Figure 14B as expression relative to G300.3 scrambled control subline RBM10v1 protein expression. Both G29/30.3 and G29/30.4 cells had significantly lower RBM10v1 protein expression relative to G300.3 subline, with 55% (p=0.0026) and 16% (p=0.0033) of control cells, respectively. The G29/30.1 subline demonstrated a great variance in protein expression, and had no significant decrease in RBM10v1 expression relative to G300.3 (99% expression, p=0.9836).

The effect of the RBM10 KD on cell proliferation was analyzed by MTT assay, which was previously used to observe the effect of RBM5 expression on cell proliferation (Figure 7A). All four sublines produced (G300.3, G29/30.1, G29/30.3 and G29/30.4) were used in the MTT

Trial # 6

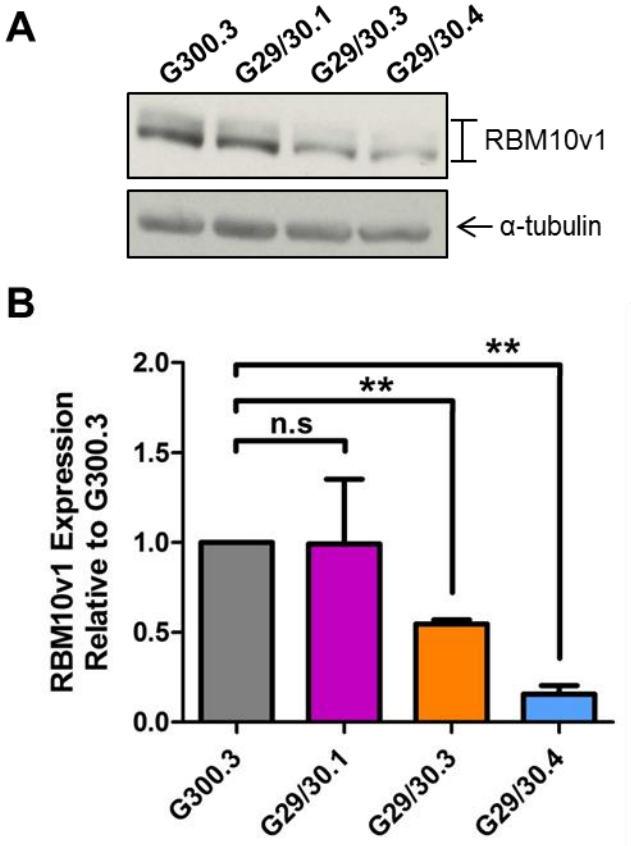

Figure 14. RBM10v1 expression in GLC20 RBM10 KD sublines. RBM10v1 expression was monitored in the G300.3, G29/30.1, G29/30.3 and G29/30.4 sublines using the Bethyl RBM10 antibody. (A) One representative Western blot result is presented for RBM10v1 and α-tubulin protein expression. (B) Densitometric results of the average RBM10v1 expression of three biological replicates performed in duplicate was performed using the AlphaEaseFC, '1D-Multi' analysis tool. Values of RBM10v1 were normalized to the α-tubulin of each biological replicate, and then made relative to the G300.3 control subline. Standard error is presented. Subline expression levels were compared using the Student's unpaired *t*-test, between sublines. ** $p<0.01$.

assays. Cell growth was monitored daily for five days, with absorbance readings taken each day.

These absorbances were then made relative to the day zero value of the respective subline and

presented as relative absorbances. The experiment was performed three times, each performed with eight technical replicates.

Figure 15 presents the results from the MTT experiments. Trial #7 cells were used for these experiments, as noted in Table 7. The G300.3 control and G29/30.1 sublines both had similar cell growth rates. This result was anticipated as both sublines had nearly identical levels of RBM10v1 protein expression (100% versus 99%). However, the G29/30.3 and G29/30.4 sublines both displayed significant differences in cell growth relative to the G300.3 control subline. G29/30.3 cells displayed reduced growth compared to G300.3 cells throughout the five days; however, G29/30.3 cells also had a greater degree of variance relative to the other sublines. As a result, G29/30.3 only demonstrated a significant difference in cell proliferation on day five of the experiment ($p<0.05$), when compared to the G300.3 control. G29/30.4 demonstrated the greatest difference in cell growth, with significant differences on day four and day five ($p<0.01$ and $p<0.0001$, respectively), when compared to the G300.3 control. These results suggest that a RBM10 KD results in a decrease in GLC20 cell proliferation and were not anticipated. Furthermore, this decrease in cell proliferation was related to the level of RBM10 KD, as the G29/30.3, with 55% RBM10v1 protein expression, displayed a significant difference in cell proliferation later than G29/30.4, which had only 16% RBM10v1 protein expression. In summary, these results indicate that a decrease in RBM10v1 protein expression resulted in a decrease in GLC20 cell proliferation and, therefore, RBM10 may be directly or indirectly involved in the regulation of cell proliferation.

Trial # 7

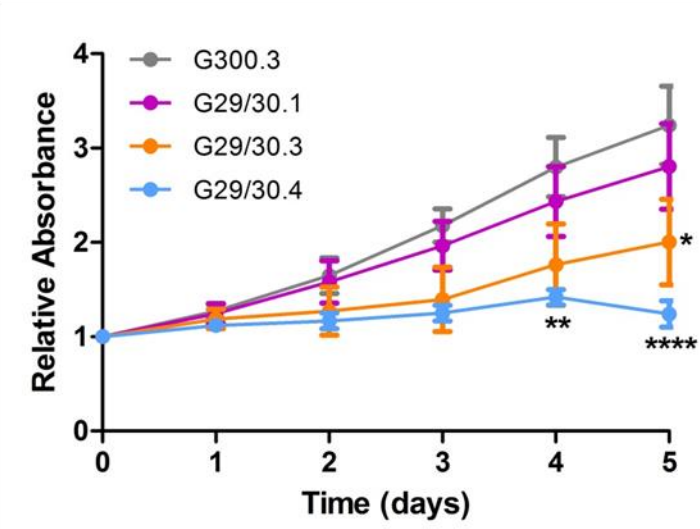

Figure 15. Decreased RBM10 expression was associated with decreased GLC20 cell proliferation. G300.3, G29/30.1, G29/30.3 and G29/30.4 were grown for 5 days and cell growth was monitored daily using an MTT assay. Proliferation was plotted relative to day 0. The average of three biological replicates performed in eight technical replicates with standard error is presented. A Two-way ANOVA was performed between the G300.3 and other sublines, with Bonferroni post-hoc analysis. * $p<0.05$, ** $p<0.01$, and **** $p<0.0001$.

Chapter 4

4 Discussion

Due to the fact that lung cancer is the leading cause of cancer deaths in Canada, there is a growing need to investigate the underlying mechanisms of lung cancer development and response to chemotherapy. Understanding the roles of various lung cancer tumour suppressor genes would provide insight into lung cancer incidence and progression and highlight potential biomarkers. In this study, we set out to further understand the function of RBM5 within the SCLC model. RBM5 has been identified as a modulator of apoptosis, a regulator of the cell cycle, and is involved in the alternative splicing of various pre-mRNAs [7,61,53,46,60]. *RBM5* has also been characterized as a putative lung cancer tumour suppressor gene as its location on the short arm of chromosome 3 often undergoes allelic loss in many cancers, resulting in decreased expression [25]. The downregulation of RBM5 is considered a common marker of malignancies, including lung cancers [22,38,39]. Decreased RBM5 expression has also been demonstrated as a characteristic of a cell line displaying cisplatin resistance [17]. Understanding the function of RBM5 in a lung cancer model system may provide further insight into its role in general and an explanation as to why the gene is commonly downregulated in lung cancers. Using a SCLC cell line that is RBM5-null, GLC20, we aimed to understand the effect of RBM5 expression, at two levels: on cell death (specifically apoptosis) in the presence of cisplatin, and on cell proliferation. It was anticipated that we would observe a positive relationship between RBM5 expression and apoptosis induction and a negative relationship between RBM5 expression and cell proliferation.

As anticipated, RBM5 expression resulted in changes in GLC20 cell proliferation and cell death. High RBM5 expression (C4 subline) resulted in a significant decrease in proliferation (Figure 7)

and, in the presence of cisplatin, a further decrease in cell proliferation (Figure 8) and increased cell death (Figures 9 and 10) relative to the control pcDNA3-transfected subline. The increase in cell death was determined to be apoptotic in nature (Figures 11 and 12). High RBM5 expression also resulted in a decrease in RBM10v1 and an increase in RBM10v2 expression (Figure 13), which was not anticipated. This warranted further investigation into the function of RBM10 (Figures 14 and 15). In addition, although it was hypothesized that the effects of RBM5 would be directly proportionate to its expression, this was not the case in all experiments; however, as high RBM5 expression was always associated with increased cisplatin-mediated apoptosis and decreased cell proliferation.

4.1 Physiological relevance

The GLC20 sublines were used as an *in vitro* model to compare the functional consequences of differing RBM5 expression levels and was not intended to reflect an *in vivo* model. An argument could be made that the expression levels of RBM5 in the C4 population may be beyond what is physiologically relevant. *In vivo,* RBM5 expression exists at varying levels in different tissues [9,15], meaning that it is of substantial importance to understand the effects of differing RBM5 expression levels. Therefore, it is unnecessary to argue the physiological relevance in the context of this *in vitro* study.

All of the experiments in this study were performed *in vitro*. Therefore, the results that were observed may not apply *in vivo* where a multitude of other factors such as tumour size, neighboring cells, and the tumour microenvironment may affect the outcomes. For instance, there was a significant increase in 'Late Apoptotic/Necrotic' cells in the C4 subline relative to the pcDNA3-transfected subline (Figure 12C). In culture, there are no macrophages to uptake the cells undergoing apoptosis, resulting in the cells going through secondary necrosis. We

cannot ascertain whether the effects observed in this study *in vitro*, such as increases in apoptotic and necrotic cells, would result in similar outcomes *in vivo*. However, it should be noted that RBM5 expression decreases in many primary cancer tissue samples [16,19,21,22,23]. In fact, *RBM5* is one of nine genes that are downregulated as part of a 17-gene metastatic signature in solid tumours [38,] and decreases in RBM5 expression in lung tumours was associated with an increase in expression of pro-metastatic protein [40]. Considering the loss of heterozygosity at 3p21.3 (to which *RBM5* maps) occurs in the majority of lung cancers [15], it could be speculated that *RBM5* is potentially one of many genes in which decreased expression is vital for lung cancer tumour incidence, progression, aggression, and metastasis. This speculation concurs with the results obtained in this study, demonstrating that cell death and cell proliferation were influenced by changes in RBM5 expression. In order to fully understand the role of RBM5 expression *in vivo*, experiments utilizing mouse models should be performed. An example of an appropriate study would be the one performed by Shao et al in 2012, in which RBM5-transfected A549 cells resulted in decreased tumour growth when compared to non-transfected A549 cells in mice [17].

4.2 RBM5 expression level and clonal effects

We anticipated that alterations in cell proliferation, membrane integrity, and apoptosis would be dependent on RBM5 expression levels. We initially thought that any changes observed would manifest in proportion to gradual changes in RBM5 expression levels, but we were also aware that these changes may have required an absolute or threshold RBM5 expression level (C4 subline) before they became observable. Decreases in cell proliferation in the presence of cisplatin (Figure 8), membrane integrity/cell death (Figure 9), cisplatin EC_{50} (Figure 10), and increases in PARP cleavage (Figure 11) demonstrated a positive relationship with increased RBM5 expression levels. There were some instances where the low-RBM5 expressing T2

subline did not demonstrate any effects. In those instances, only the high RBM5-expressing C4 subline demonstrated changes in cell proliferation (Figure 7), apoptosis (Figure 12), and RBM10v1/v2 expression (Figure 13), suggesting that in these cases, a specific threshold of RBM5 may be necessary. Our results suggest that high levels of RBM5 expression are required to affect cell proliferation and alternative splicing, but in some instances, minor changes in RBM5 expression can influence cisplatin-mediated cell death. The effect of RBM5 expression on increasing the number of cells undergoing apoptosis appeared to either relate to RBM5 expression level (Figure 11) or to a threshold of RBM5 expression (Figure 12). This anomaly could be explained by the use of two different cell populations for the separate experiments. However, the experiment performed in Figure 12 demonstrated more apoptotic characteristics (chromatin condensation, membrane asymmetry, and PARP cleavage), which could be a more representative test of apoptosis in the GLC20 cells in comparison to the experiment performed in Figure 11 (PARP cleavage). Furthermore, the 116 kDa PARP band was not taken into account in Figure 11 due to a lack of an observed decrease. This may hint at a potential experimental error such as film saturation, further suggesting Figure 11 may not be the best representation of what is occurring within this system. Due to these observations, it may be suggested that apoptosis in the GLC20 cell system requires a specific RBM5 expression level to manifest itself. To identify if and when a threshold of RBM5 expression is required for apoptosis, we could repeat our experiments using a larger number of stable GLC20 sublines with incrementally varying levels of RBM5 expression. Nonetheless, all of the significant effects observed in this study were related to the high RBM5 expression in the C4 subline.

Throughout this study, clonal effects must be taken into consideration when attributing specific changes in the C4 phenotype to RBM5 expression. Clonal effects can be described as the

propagation of cellular changes that are not due to overexpression of a gene but rather the random integration of the plasmid DNA into the genome of a single cell [137,138]. The integration of the plasmid DNA within the genome could have changed the expression of other growth regulatory genes (oncogenic or tumour suppressor genes), leading to a unique phenotype only observed in the C4 subline. In addition, the plasmid DNA could have changed repressor or promoter functions of similar genes. Therefore, it was possible that the single clone used to produce the C4 subline may have had a strongly reduce growth rate (Figure 7) independent of RBM5 expression levels. To minimize the confounding effect of clonal variation, described as the propagation of a rare variant in the population, which is not reflective of the entire population [137], similar passage numbers were used throughout the experiments (Table 7). However, all of the results observed using the C4 subline are consistent with other studies that examined RBM5 overexpression, such as decreased cell proliferation, increased sensitivity to chemotherapy and increased apoptosis in the presence of a stressor [7,8,11,17,20,24,51,53,55]. This suggests that the changes observed in this study were, in fact, due to high RBM5 expression in the C4 subline and not necessarily clonal effects. Further studies in this area should attempt to use more than one clonal population from both the RBM5-expressing and non-expressing sublines. The use of an inducible expression system, where the level of RBM5 expression can be controlled, would also help to rule out any clonal effects.

4.3 Role of *RBM5* as a putative lung cancer tumour suppressor gene

As mentioned in Dr. Sutherland's review in 2010, *RBM5* is considered to be a putative lung cancer tumour suppressor gene [25]. Using a SCLC cell line, we supported the role of *RBM5* as a potential lung cancer tumour suppressor gene since high RBM5 expression reduced cell

proliferation (Figure 7) and increased cell death (Figures 9 and 10), which was determined to be apoptosis (Figures 11 and 12). This was further confirmed in similar studies using other lung cancer cell lines such as A549 (adenocarcinoma), and H1299 (NSCLC) cells [53,54]. In addition, many RBM5 overexpression studies have been performed in other cancer cell lines such as those performed in HT188 (human fibrosarcoma), A9 (mouse non-malignant fibrosarcoma), PC-3 (prostate cancer), Jurkat (T-lymphocyte) and CEM-C7 (human leukemia) cells, demonstrating that RBM5 may function as a tumour suppressor gene via the reduction of cell proliferation or an increase in apoptosis [6,7,16,17,52,53,55]. Although the downregulation of RBM5 occurs in lung cancer most often, *RBM5* could be considered a putative general tumour suppressor gene. The reduction of RBM5 expression has been established in various carcinomas other than lung cancer [16] including vestibular schwannomas [19], cancerous prostatic tissue [20], biliary tract cancers [21], pancreatic ductal adenocarcinomas [22], and stage III ovarian carcinomas [23], when compared to adjacent normal tissues. Furthermore, the overexpression of RBM5 in A549 xenografts in BALB/c mice resulted in decreased tumour growth [17], further supporting the role of *RBM5* as a putative tumour suppressor gene. However, to conclusively demonstrate the role of *RBM5* as a tumour suppressor gene, RBM5 knockdown studies in tumour xenografts should be performed, such as those performed in 2016 that demonstrated the role of RBM10 as a tumour suppressor gene [139]. If the knockdown of RBM5 expression resulted in an increase in tumour growth, in addition to other studies such as this one, one could conclusively state that RBM5 is a tumour suppressor gene.

In this study, the changes in cell proliferation, membrane integrity, apoptosis and RBM10 expression were proportionate to RBM5 expression levels, suggesting that the potential role of RBM5 as a tumour suppressor is dependent on its expression. 3p21.3, the region which *RBM5*

maps to, is known to undergo a loss of heterozygosity (the loss of one functional allele out of two) in 95% of SCLC and 70% of NSCLC relative to normal tissue [15,30,32]. In NSCLC, relative to neighbouring tissue, RBM5 expression was reduced by 82% and 73% at the mRNA and protein levels, respectively [16]. It has been suggested that genes within this region, including *RBM5*, exhibit haploinsufficiency [15,31,33]. Haploinsufficiency is defined as the incapability of one functional allele to produce the protein required to maintain normal function. Therefore, in the case of *RBM5*, the loss of heterozygosity at 3p21.3 results in the loss of one functional allele, which does not produce enough RBM5 to maintain tumour suppressor function. Consequently, similar to what was observed in this study, low RBM5 expression (such as the T2 subline in this study, or lost in tissues that underwent loss of 3p21.3 heterozygosity) results in a decrease in RBM5 tumour suppressor function. This would suggest that *RBM5* does not follow Knudson's two-hit hypothesis for classic tumour suppressors, requiring both alleles to be non-functional in order for the onset or progression of cancer, such as *RB1*, and instead is similar to *FHIT* or *CDKN1B* which also demonstrate haploinsufficiency [140,141]. We can postulate that loss of heterozygosity at 3p21.3 results in decreased RBM5 expression, impairing its function as a tumour suppressor gene in lung cancer, specifically in regulating cell proliferation and the activation of apoptosis.

4.4 RBM5 regulation of cell proliferation

We discovered that increased RBM5 expression resulted in decreased GLC20 cell proliferation (Figure 7). In A549 cells, the increase in RBM5 expression was demonstrated to induce G_1 cell cycle arrest, thereby providing a possible mechanism to explain the decrease in cell proliferation [53]. Based on previous research, RBM5 may have the ability to alter cell proliferation though the alternative splicing of genes related to cell proliferation pathways [57,60,61]. RBM5 has been shown

to influence specific pathways such as EGFR/KRAS and Wnt/β-catenin in other systems and, therefore, RBM5 may also play a direct or indirect role in these pathways in the GLC20 model [6,18,22,39,42]. However, the role of RBM5 in the EGFR/KRAS pathway is debatable. Interestingly, in H1975 lung adenocarcinoma cells, changes in EGFR expression had no effect on RBM5 expression [36]. In contrast, changes in RBM5 expression in A549 cells were associated with decreases in EGFR expression, suggesting RBM5 may affect EGFR expression upstream by affecting the processing of the transcript [41]. RNA-seq results from Dr. Sutherland's lab show a significant decrease in KRAS expression between the pcDNA3-transfected and C4 sublines (unpublished), supporting the notion that RBM5 influences KRAS expression. Further studies to elucidate that pathway(s) by which RBM5 may influence cell proliferation in the C4 subline should examine changes in EGFR/KRAS or Wnt/β-catenin expression and pathway-related protein expression. Analysis of RBM5 specific alternative splice targets within these pathways would also aid in determining whether these changes are directly or indirectly influenced by RBM5 expression.

Interestingly, the pcDNA3-transfected and T2 sublines demonstrated greater cell proliferation than the wild type GLC20 cells (Figure 7). This increase could be attributed to the transfection process, resulting in an increase in stress within the cells. Increased stress could have caused an increase in mitochondrial activity, which the MTT assay measures [136], resulting in a greater increase in cell proliferation (Figure 7A). However, the cell counting experiments that were performed (Figure 7B) suggest that the differences between the sublines are true.

4.5 The role of RBM5 in cell death

In this study, we demonstrated the importance of RBM5 expression within cell death and, more specifically, apoptotic cell death in the GLC20 cell model. These results suggest that RBM5

expression is enough to influence the survival of the cells, but a higher expression level increases the likelihood of apoptosis activation in this model. This difference could indicate a relationsip between changes in RBM5 expression and cells undergoing cell death, where cell death is proportionate to RBM5 expression level, but the activation of apoptotic cell death requires a specific threshold. A potential test for this could be through the use of an inducible promoter that ables one to have varying levels of RBM5 expression in the same cell line.

While only cisplatin was used to induce cell death in this study, it can be suggested that the RBM5-related cell death observed in this study was not cisplatin-specific. Activation of apoptosis has previously been observed in other cancer cell lines with other stressors such as TNF-α, Fas ligand, TRAIL death receptor, and staurosporine as well as cisplatin when RBM5 was overexpressed [11,17,51,55]. It would then be expected that similar results would be obtained with other stressors. However, one should note that RBM5 may not increase the effects of a stressor at various concentrations, as high concentrations (100 μM) of cisplatin was a strong inducer of cell death, and did not require RBM5 expression to potentiate its effects (Figure 10). RBM5 enchances apoptosis through numerous apoptogenic stimuli, in many different cell lines, and it is, therefore, not unexpected that high RBM5 expression resulted in cisplatin-mediated apoptosis in GLC20 cells.

Interestingly, RBM5 expression alone was not enough to induce cell death (Figures 9, 11 and 12). The lack of apoptosis in the RBM5-expressing cells that were not exposed to cisplatin suggests that an external stimulus is required to initiate the cell death/apoptotic process and that RBM5 may potentiate it. Possible mechanisms by which RBM5 could potentiate apoptosis could be through the upregulation of pro-apoptotic proteins such as p53 and BAX or increases in cytochrome c levels that are not high enough to initiate apoptosis, but high enough to promote

apoptotic signaling with stimulus. RBM5 expression also correlates with a decrease in anti-apoptotic Bcl-2 protein [55], which may increase activation of apoptosis in the presence of a stressor. Lastly, another possibility is that cisplatin initiates cell death via its ability to bind to DNA, which initiates apoptosis through p53 or MAPK [121,122,123,124,125]. RBM5 expression correlates with an increase in p53 [54] that, on its own, may not be able to initiate apoptosis. It is possible that upon cisplatin binding to the DNA, the increase in p53 or the decrease in pathways such as KRAS, that regulate MAPK, increases the apoptotic response to cisplatin.

Further analysis of the mechanism by which RBM5 expression influences apoptosis is required within the GLC20 cell model. Studies examining the expression levels of potential RBM5 targets such as BAX, Bcl-2 and p53 should be performed to detect any changes in expression levels. Additional experiments using the GLC20 sublines with other initiators of cell death would indicate whether or not this observed apoptosis is a cisplatin-specific event, which would aid in understanding how RBM5 may influence apoptosis.

4.6 Effect of RBM5 on RBM10 alternative splicing

The fact that the high RBM5-expressing subline, C4, had a significant increase in RBM10v2 and a measurable decrease in RBM10v1 proteins expression levels (Figure 13) suggests that RBM5 may influence the exclusion of exon 4 within RBM10. Increases in RBM5 expression have been implicated in the exclusion of exons within various targets such as exon 4 of AID [65], exon 7 of c-Flip [61,64], exon 9 of Caspase 2 [60], exons 40 and 72 of Dystrophin [66] and exon 6 of FasR [61]. Whether RBM5 is directly or indirectly responsible for the exclusion of exon 4 (alternative splicing) in RBM10 was not addressed in this study.

The changes in RBM10v1 and v2 expression levels in the C4 subline suggest potential differences in the roles of each RBM10 variant in the GLC20 cell model. A recent study using GLC20 cells showed that there was a two-fold increase in an isoform of RBM10v1 that lacks a valine, promoting increased expression of lung cancer-specific isoforms of NUMB, a component of the Notch pathway that regulates cell proliferation [74]. RBM10v1 is more highly expressed than v2 in many cancer cell lines, such as Jurkat cells [72], but has lower expression than v2 in non-cancerous cells such as H9C2 cardiomyocytes [29], C2C12 myoblasts [142], and bronchial epithelial BEAS-2B cells (unpublished). It could then be suggested that high RBM5 expression influences the observed decrease in RBM10v1 expression and increase in RBM10v2 expression. The changes in RBM10v1 and v2 expression may also be one of many alterations that occur in cancer, with high RBM10v1 levels indicating a cancerous phenotype and high RBM10v2 levels indicating a non-cancerous phenotype. Further expression level research in different cell lines and tissue specimens would need to be completed to confirm these suggestions.

4.7 RBM10 function in the GLC20 SCLC cell model

Having observed a change in the expression of RBM10 in relation to RBM5 expression, we investigated RBM10 function in the GLC20 cells. Using three stable RBM10 knockdown pooled sublines created from non-variant specific shRNA, the decrease in cell proliferation related with the level of knockdown (Figure 15). These results indicate that RBM10 expression influences GLC20 cell proliferation. RBM10 was previously implicated in cell proliferation through regulating proteins that regulate proliferation, further validating our findings [56,85].

Although the shRNA used in this study was not variant specific, one could assume that the RBM10 knockdown resulted in decreased levels of RBM10v1, as there is much more RBM10v1 protein than v2 (Figure 5). This result agrees with the decrease in RBM10v1 protein (Figure 13)

that was observed in the slow-growing (Figure 7) high RBM5-expressing C4 subline. The dominant RBM10v1 isoform found in GLC20 cells promotes a lung cancer specific NUMB variant, which promotes cell proliferation [74]. Decreased cell proliferation in the RBM10v1 knockdown sublines would then suggest a downregulation of the pathway of the lung cancer specific NUMB variant. However, repeating the studies performed using variant specific shRNA and monitoring the expression of the specific NUMB variant would have to be completed in order to confirm this assumption.

4.8 Further Directions

A further understanding of the role of RBM5 in this SCLC model would be an ideal direction for future studies. In order to understand the mechanism of cisplatin-mediated apoptosis and whether or not RBM5 is directly involved in cisplatin-specific pathways, studies exploring the apoptotic pathways activated in GLC20 cells in the presence of cisplatin and how RBM5 influences an increase in apoptosis should be conducted. Studies observing how RBM5 decreases GLC20 cell proliferation by cell cycle analysis or EGFR/RAS and Wnt/β-catenin pathway inactivation would aid in understanding the role of RBM5 in SCLC. Further analysis of the function of RBM5 in primary tissue samples or mouse models would aid in confirming assumptions proposed in this study. Using the GLC20 model to explore the effect of RBM5 on cell death induced by other common SCLC chemotherapies, highlighted in Table 4, would provide insight into whether RBM5 potentiates the cytotoxicity of multiple chemotherapy agents or whether RBM5 generally increases apoptosis in conjunction with any apoptogenic agent.

To elucidate the role of RBM10 in the GLC20 model, further research understanding the relationship between RBM5 expression and cellular RBM10v1 and RBM10v2 levels would provide insight into the function of these RBM proteins and their impact on cell growth and cell

death pathways. The relationship between RBM5 and RBM10 should also be explored further, to understand if and how they regulate each other's expression. Lastly, investigations into RBM10v1 specific knockdown or RBM10v2 specific overexpression should be performed to better elucidate the function of each RBM10 variant within the GLC20 model.

4.9 Significance

This study's aim was to further elucidate the role of RBM5 in cell proliferation and apoptosis through a SCLC model. In demonstrating that high RBM5 expression was associated with decreased cell proliferation and increased apoptosis in a SCLC cell line, some insight has been gained as to the potential role of RBM5 and RBM10 in lung cancer. This study also demonstrated the importance of RBM5 expression level in its ability to affect different cellular processes. Based on the function of RBM5 presented in this study, and others, and understanding that the expression of RBM5 is lost or down regulated in most lung cancers, RBM5 expression may be a potential prognostic tool for lung cancers.

References

1. Wei MH, Latif F, Bader S, et al. Construction of a 600-kilobase cosmid clone contig and generation of a transcriptional map surrounding the lung cancer tumor suppressor gene (TSG) locus on human chromosome 3p21.3: progress toward the isolation of a lung cancer TSG. Cancer Res 1996;56:1487-92.

2. Sutherland LC, Rintala-Maki ND, White RD, Morin CD. RNA binding motif (RBM) proteins: a novel family of apoptosis modulators? J Cell Biochem 2005;94:5-24.

3. Kok K, van den Berg A, Veldhuis PM, et al. A homozygous deletion in a small cell lung cancer cell line involving a 3p21 region with a marked instability in yeast artificial chromosomes. Cancer Res 1994;54:4183-7.

4. Oh JJ, Grosshans DR, Wong SG, Slamon DJ. Identification of differentially expressed genes associated with HER- 2/neu overexpression in human breast cancer cells. Nucleic Acids Res 1999;27:4008-17.

5. Timmer T, Terpstra P, van den Berg A, et al. A comparison of genomic structures and expression patterns of two closely related flanking genes in a critical lung cancer region at 3p21.3. Eur J Hum Genet 1999;7:478-86.

6. Edamatsu H, Kaziro Y, Itoh H. LUCA15, a putative tumour suppressor gene encoding an RNA-binding nuclear protein, is down-regulated in ras-transformed Rat-1 cells. Genes Cells 2000;5:849-58.

7. Mourtada-Maarabouni M, Sutherland LC, Meredith JM, Williams GT. Simultaneous acceleration of the cell cycle and suppression of apoptosis by splice variant delta-6 of the candidate tumour suppressor LUCA-15/RBM5. Genes Cells 2003;8:109-19.

8. Sutherland LC, Edwards SE, Cable HC, et al. LUCA-15-encoded sequence variants regulate CD95-mediated apoptosis. Oncogene 2000;19:3774-81.

9. Drabkin HA, West JD, Hotfilder M, et al. DEF-3(g16/NY-LU-12), an RNA binding protein from the 3p21.3 homozygous deletion region in SCLC. Oncogene 1999;18:2589-97.

10. Rintala-Maki ND, Sutherland LC. Identification and characterisation of a novel antisense non-coding RNA from the RBM5 gene locus. Gene 2009;445:7-16.

11. Rintala-Maki ND, Sutherland LC. LUCA-15/RBM5, a putative tumour suppressor, enhances multiple receptor-initiated death signals. Apoptosis 2004;9:475-84.

12. Shu Y, Rintala-Maki ND, Wall VE, et al. The apoptosis modulator and tumour suppressor protein RBM5 is a phosphoprotein. Cell Biochem Funct 2007;25:643-53.

13. Nagase T, Seki N, Tanaka A, Ishikawa K, Nomura N. Prediction of the coding sequences of unidentified human genes. IV. The coding sequences of 40 new genes (KIAA0121-KIAA0160) deduced by analysis of cDNA clones from human cell line KG-1. DNA Res 1995;2:167-210.

14. Timmer T, Terpstra P, van den Berg A, et al. An evolutionary rearrangement of the Xp11.3-11.23 region in 3p21.3, a region frequently deleted in a variety of cancers. Genomics 1999;60:238-40.

15. Lerman MI, Minna JD. The 630-kb lung cancer homozygous deletion region on human chromosome 3p21.3: identification and evaluation of the resident candidate tumor suppressor genes. The International Lung Cancer Chromosome 3p21.3 Tumor Suppressor Gene Consortium. Cancer Res 2000;60:6116-33.

16. Oh JJ, West AR, Fishbein MC, Slamon DJ. A candidate tumor suppressor gene, H37, from the human lung cancer tumor suppressor locus 3p21.3. Cancer Res 2002;62:3207-13.

17. Shao C, Zhao L, Wang K, Xu W, Zhang J, Yang B. The tumor suppressor gene RBM5 inhibits lung adenocarcinoma cell growth and induces apoptosis. World J Surg Oncol 2012;10:160.

18. Liang H, Zhang J, Shao C, et al. Differential expression of RBM5, EGFR and KRAS mRNA and protein in non-small cell lung cancer tissues. J Exp Clin Cancer Res 2012;31:36.

19. Welling DB, Lasak JM, Akhmametyeva E, Ghaheri B, Chang LS. cDNA microarray analysis of vestibular schwannomas. Otol Neurotol 2002;23:736-48.

20. Zhao L, Li R, Shao C, Li P, Liu J, Wang K. 3p21.3 tumor suppressor gene RBM5 inhibits growth of human prostate cancer PC-3 cells through apoptosis. World J Surg Oncol 2012;10:247.

21. Miller G, Socci ND, Dhall D, et al. Genome wide analysis and clinical correlation of chromosomal and transcriptional mutations in cancers of the biliary tract. J Exp Clin Cancer Res 2009;28:62.

22. Peng J, Valeshabad AK, Li Q, Wang Y. Differential expression of RBM5 and KRAS in pancreatic ductal adenocarcinoma and their association with clinicopathological features. Oncol Lett 2013;5:1000-4.

23. Kim YS, Hwan JD, Bae S, Bae DH, Shick WA. Identification of differentially expressed genes using an annealing control primer system in stage III serous ovarian carcinoma. BMC Cancer 2010;10:576.

24. Li P, Wang K, Zhang J, et al. The 3p21.3 tumor suppressor RBM5 resensitizes cisplatin-resistant human non-small cell lung cancer cells to cisplatin. Cancer Epidemiol 2012;36:481-9.

25. Sutherland LC, Wang K, Robinson AG. RBM5 as a putative tumor suppressor gene for lung cancer. J Thorac Oncol 2010;5:294-8.

26. Rintala-Maki ND, Goard CA, Langdon CE, et al. Expression of RBM5-related factors in primary breast tissue. J Cell Biochem 2007;100:1440-58.

27. Jackson TC, Du L, Janesko-Feldman K, et al. The nuclear splicing factor RNA binding motif 5 promotes caspase activation in human neuronal cells, and increases after traumatic brain injury in mice. J Cereb Blood Flow Metab 2015;35:655-66.

28. Zhang J, Cui Z, Feng G, et al. RBM5 and p53 expression after rat spinal cord injury: implications for neuronal apoptosis. Int J Biochem Cell Biol 2015;60:43-52.

29. Loiselle JJ, Sutherland LC. Differential downregulation of Rbm5 and Rbm10 during skeletal and cardiac differentiation. In Vitro Cell Dev Biol Anim 2014;50:331-9.

30. Wistuba II, Behrens C, Virmani AK, et al. High resolution chromosome 3p allelotyping of human lung cancer and preneoplastic/preinvasive bronchial epithelium reveals multiple, discontinuous sites of 3p allele loss and three regions of frequent breakpoints. Cancer Res 2000;60:1949-60.

31. Ji L, Minna JD, Roth JA. 3p21.3 tumor suppressor cluster: prospects for translational applications. Future Oncol 2005;1:79-92.

32. Kok K, Naylor SL, Buys CH. Deletions of the short arm of chromosome 3 in solid tumors and the search for suppressor genes. Adv Cancer Res 1997;71:27-92.

33. Oh JJ, Koegel AK, Phan DT, Razfar A, Slamon DJ. The two single nucleotide polymorphisms in the H37/RBM5 tumour suppressor gene at 3p21.3 correlated with different subtypes of non-small cell lung cancers. Lung Cancer 2007;58:7-14.

34. Oh JJ, Boctor BN, Jimenez CA, et al. Promoter methylation study of the H37/RBM5 tumor suppressor gene from the 3p21.3 human lung cancer tumor suppressor locus. Hum Genet 2008;123:55-64.

35. Smith KS, Yadav VK, Pedersen BS, et al. Signatures of accelerated somatic evolution in gene promoters in multiple cancer types. Nucleic Acids Res 2015;43:5307-17.

36. Masilamani TJ, Rintala-Maki ND, Wang K, Sutherland LC. Downregulating activated epidermal growth factor receptor has no effect on RBM5 expression. Chin Med J (Engl) 2012;125:2378-81.

37. Wang Y, Gogol-Doring A, Hu H, et al. Integrative analysis revealed the molecular mechanism underlying RBM10-mediated splicing regulation. EMBO Mol Med 2013;5:1431-42.

38. Ramaswamy S, Ross KN, Lander ES, Golub TR. A molecular signature of metastasis in primary solid tumors. Nat Genet 2003;33:49-54.

39. Oh JJ, Taschereau EO, Koegel AK, et al. RBM5/H37 tumor suppressor, located at the lung cancer hot spot 3p21.3, alters expression of genes involved in metastasis. Lung Cancer 2010;70:253-62.

40. Comprehensive molecular profiling of lung adenocarcinoma. Nature 2014;511:543-50.

41. Su Z, Yin J, Zhao L, et al. Lentiviral vector-mediated RBM5 overexpression downregulates EGFR expression in human non-small cell lung cancer cells. World J Surg Oncol 2014;12:367.

42. Hao YQ, Su ZZ, Lv XJ, et al. RNA-binding motif protein 5 negatively regulates the activity of Wnt/beta-catenin signaling in cigarette smoke-induced alveolar epithelial injury. Oncol Rep 2015;33:2438-44.

43. Solaimani P, Damoiseaux R, Hankinson O. Genome-wide RNAi high-throughput screen identifies proteins necessary for the AHR-dependent induction of CYP1A1 by 2,3,7,8-tetrachlorodibenzo-p-dioxin. Toxicol Sci 2013;136:107-19.

44. Kerr JF, Wyllie AH, Currie AR. Apoptosis: a basic biological phenomenon with wide-ranging implications in tissue kinetics. Br J Cancer 1972;26:239-57.

45. Giansanti V, Tillhon M, Mazzini G, Prosperi E, Lombardi P, Scovassi AI. Killing of tumor cells: a drama in two acts. Biochem Pharmacol 2011;82:1304-10.

46. Mourtada-Maarabouni M, Sutherland LC, Williams GT. Candidate tumour suppressor LUCA-15 can regulate multiple apoptotic pathways. Apoptosis 2002;7:421-32.

47. Elmore S. Apoptosis: a review of programmed cell death. Toxicol Pathol 2007;35:495-516.

48. Giansanti V, Torriglia A, Scovassi AI. Conversation between apoptosis and autophagy: "Is it your turn or mine?". Apoptosis 2011;16:321-33.

49. Saraste A, Pulkki K. Morphologic and biochemical hallmarks of apoptosis. Cardiovasc Res 2000;45:528-37.

50. Eum HA, Billiar TR. TNF/TNF receptor 1-mediated apoptosis in hepatocytes. Adv Exp Med Biol 2011;691:617-24.

51. Rintala-Maki ND, Abrasonis V, Burd M, Sutherland LC. Genetic instability of RBM5/LUCA-15/H37 in MCF-7 breast carcinoma sublines may affect susceptibility to apoptosis. Cell Biochem Funct 2004;22:307-13.

52. Mourtada-Maarabouni M, Keen J, Clark J, Cooper CS, Williams GT. Candidate tumor suppressor LUCA-15/RBM5/H37 modulates expression of apoptosis and cell cycle genes. Exp Cell Res 2006;312:1745-52.

53. Oh JJ, Razfar A, Delgado I, et al. 3p21.3 tumor suppressor gene H37/Luca15/RBM5 inhibits growth of human lung cancer cells through cell cycle arrest and apoptosis. Cancer Res 2006;66:3419-27.

54. Kobayashi T, Ishida J, Musashi M, et al. p53 transactivation is involved in the antiproliferative activity of the putative tumor suppressor RBM5. Int J Cancer 2011;128:304-18.

55. Sutherland LC, Lerman M, Williams GT, Miller BA. LUCA-15 suppresses CD95-mediated apoptosis in Jurkat T cells. Oncogene 2001;20:2713-9.

56. Bechara EG, Sebestyen E, Bernardis I, Eyras E, Valcarcel J. RBM5, 6, and 10 Differentially Regulate NUMB Alternative Splicing to Control Cancer Cell Proliferation. Mol Cell 2013;52:720-33.

57. Behzadnia N, Golas MM, Hartmuth K, et al. Composition and three-dimensional EM structure of double affinity-purified, human prespliceosomal A complexes. EMBO J 2007;26:1737-48.

58. Deckert J, Hartmuth K, Boehringer D, et al. Protein composition and electron microscopy structure of affinity-purified human spliceosomal B complexes isolated under physiological conditions. Mol Cell Biol 2006;26:5528-43.

59. Niu Z, Jin W, Zhang L, Li X. Tumor suppressor RBM5 directly interacts with the DExD/H-box protein DHX15 and stimulates its helicase activity. FEBS Lett 2012;586:977-83.

60. Fushimi K, Ray P, Kar A, Wang L, Sutherland LC, Wu JY. Up-regulation of the proapoptotic caspase 2 splicing isoform by a candidate tumor suppressor, RBM5. Proc Natl Acad Sci U S A 2008;105:15708-13.

61. Bonnal S, Martinez C, Forch P, Bachi A, Wilm M, Valcarcel J. RBM5/Luca-15/H37 regulates Fas alternative splice site pairing after exon definition. Mol Cell 2008;32:81-95.

62. Chang DW, Xing Z, Pan Y, et al. c-FLIP(L) is a dual function regulator for caspase-8 activation and CD95-mediated apoptosis. EMBO J 2002;21:3704-14.

63. Sehgal L, Mathur R, Braun FK, et al. FAS-antisense 1 lncRNA and production of soluble versus membrane Fas in B-cell lymphoma. Leukemia 2014;28:2376-87.

64. Zhang L, Zhang Q, Yang Y, Wu C. The RNA recognition motif domains of RBM5 are required for RNA binding and cancer cell proliferation inhibition. Biochem Biophys Res Commun 2014;444:445-50.

65. Jin W, Niu Z, Xu D, Li X. RBM5 promotes exon 4 skipping of AID pre-mRNA by competing with the binding of U2AF65 to the polypyrimidine tract. FEBS Lett 2012;586:3852-7.

66. O'Leary DA, Sharif O, Anderson P, et al. Identification of small molecule and genetic modulators of AON-induced dystrophin exon skipping by high-throughput screening. PLoS One 2009;4:e8348.

67. Koenig M, Hoffman EP, Bertelson CJ, Monaco AP, Feener C, Kunkel LM. Complete cloning of the Duchenne muscular dystrophy (DMD) cDNA and preliminary genomic organization of the DMD gene in normal and affected individuals. Cell 1987;50:509-17.

68. van Deutekom JC, Janson AA, Ginjaar IB, et al. Local dystrophin restoration with antisense oligonucleotide PRO051. N Engl J Med 2007;357:2677-86.

69. O'Bryan MK, Clark BJ, McLaughlin EA, et al. RBM5 Is a Male Germ Cell Splicing Factor and Is Required for Spermatid Differentiation and Male Fertility. PLoS Genet 2013;9:e1003628.

70. Coleman MP, Ambrose HJ, Carrel L, Nemeth AH, Willard HF, Davies KE. A novel gene, DXS8237E, lies within 20 kb upstream of UBE1 in Xp11.23 and has a different X inactivation status. Genomics 1996;31:135-8.

71. Thiselton DL, McDowall J, Brandau O, et al. An integrated, functionally annotated gene map of the DXS8026-ELK1 interval on human Xp11.3-Xp11.23: potential hotspot for neurogenetic disorders. Genomics 2002;79:560-72.

72. Wang K, Bacon ML, Tessier JJ, Rintala-Maki ND, Tang V, Sutherland LC. RBM10 Modulates Apoptosis and Influences TNA-α Gene Expression. Journal of Cell Death 2012;5:1-19.

73. Johnston JJ, Teer JK, Cherukuri PF, et al. Massively parallel sequencing of exons on the X chromosome identifies RBM10 as the gene that causes a syndromic form of cleft palate. Am J Hum Genet 2010;86:743-8.

74. Tessier SJ, Loiselle JJ, McBain A, et al. Insight into the role of alternative splicing within the RBM10v1 exon 10 tandem donor site. BMC Res Notes 2015;8:46.

75. Imielinski M, Berger AH, Hammerman PS, et al. Mapping the hallmarks of lung adenocarcinoma with massively parallel sequencing. Cell 2012;150:1107-20.

76. Furukawa T, Kuboki Y, Tanji E, et al. Whole-exome sequencing uncovers frequent GNAS mutations in intraductal papillary mucinous neoplasms of the pancreas. Sci Rep 2011;1:161.

77. Witkiewicz AK, McMillan EA, Balaji U, et al. Whole-exome sequencing of pancreatic cancer defines genetic diversity and therapeutic targets. Nat Commun 2015;6:6744.

78. Gripp KW, Hopkins E, Johnston JJ, Krause C, Dobyns WB, Biesecker LG. Long-term survival in TARP syndrome and confirmation of RBM10 as the disease-causing gene. Am J Med Genet A 2011;155A:2516-20.

79. Johnston JJ, Sapp JC, Curry C, et al. Expansion of the TARP syndrome phenotype associated with de novo mutations and mosaicism. Am J Med Genet A 2014;164A:120-8.

80. Zheng S, Damoiseaux R, Chen L, Black DL. A broadly applicable high-throughput screening strategy identifies new regulators of Dlg4 (Psd-95) alternative splicing. Genome Res 2013;23:998-1007.

81. Inoue A, Yamamoto N, Kimura M, Nishio K, Yamane H, Nakajima K. RBM10 regulates alternative splicing. FEBS Lett 2014;588:942-7.

82. Xiao SJ, Wang LY, Kimura M, et al. S1-1/RBM10: multiplicity and cooperativity of nuclear localisation domains. Biol Cell 2013;105:162-74.

83. James CG, Ulici V, Tuckermann J, Underhill TM, Beier F. Expression profiling of Dexamethasone-treated primary chondrocytes identifies targets of glucocorticoid signalling in endochondral bone development. BMC Genomics 2007;8:205.

84. Martin-Garabato E, Martinez-Arribas F, Pollan M, Lucas AR, Sanchez J, Schneider J. The small variant of the apoptosis-associated X-chromosome RBM10 gene is co-expressed with caspase-3 in breast cancer. Cancer Genomics Proteomics 2008;5:169-73.

85. Martinez-Arribas F, Agudo D, Pollan M, et al. Positive correlation between the expression of X-chromosome RBM genes (RBMX, RBM3, RBM10) and the proapoptotic Bax gene in human breast cancer. J Cell Biochem 2006;97:1275-82.

86. Garrisi VM, Strippoli S, De SS, et al. Proteomic profile and in silico analysis in metastatic melanoma with and without BRAF mutation. PLoS One 2014;9:e112025.

87. Travis W.D. BE, Muller-Hermelink H.K., Harris C.C. World Health Organization Classification of Tumours. Pathology and Genetics of Tumours of the Lung, Pleura, Thymus and Heart. Lyon, France: IARC Press; 2004.

88. Jemal A, Bray F, Center MM, Ferlay J, Ward E, Forman D. Global cancer statistics. CA Cancer J Clin 2011;61:69-90.

89. Canadian Cancer Society's Advisory Committee on Cancer Statistics. *Canadian Cancer Statistics 2015.* Toronto, ON: Canadian Cancer Society; 2015.

90. Canada LC. The Faces of Lung Cancer: Fighting Disease, Fighting Disparity 2014. Toronto, Ontario2014 2014.

91. Ezzati M, Lopez AD. Estimates of global mortality attributable to smoking in 2000. Lancet 2003;362:847-52.

92. Ezzati M, Henley SJ, Lopez AD, Thun MJ. Role of smoking in global and regional cancer epidemiology: current patterns and data needs. Int J Cancer 2005;116:963-71.

93. Shields PG. Molecular epidemiology of smoking and lung cancer. Oncogene 2002;21:6870-6.

94. Khuder SA, Mutgi AB. Effect of smoking cessation on major histologic types of lung cancer. Chest 2001;120:1577-83.

95. Spitz M, Wu X, Wilkinson A, Wei Q. Cancer of the Lung. Oxford, United Kingdom: Oxford University Press; 2006.

96. Lam WK, White NW, Chan-Yeung MM. Lung cancer epidemiology and risk factors in Asia and Africa. Int J Tuberc Lung Dis 2004;8:1045-57.

97. Molina JR YP, Cassivi SD, Schild SE, Adjei AA. Non-small cell lung cancer: epidemiology, risk factors, treatment, and survivorship. Mayo Clinic Proceedings 2008;83:584-94.

98. Govindan R, Page N, Morgensztern D, et al. Changing epidemiology of small-cell lung cancer in the United States over the last 30 years: analysis of the surveillance, epidemiologic, and end results database. J Clin Oncol 2006;24:4539-44.

99. Cooper WA, Lam DC, O'Toole SA, Minna JD. Molecular biology of lung cancer. J Thorac Dis 2013;5 Suppl 5:S479-S90.

100. Heist RS, Sequist LV, Engelman JA. Genetic changes in squamous cell lung cancer: a review. J Thorac Oncol 2012;7:924-33.

101. Comprehensive genomic characterization of squamous cell lung cancers. Nature 2012;489:519-25.

102. Rudin CM, Durinck S, Stawiski EW, et al. Comprehensive genomic analysis identifies SOX2 as a frequently amplified gene in small-cell lung cancer. Nat Genet 2012;44:1111-6.

103. Peifer M, Fernandez-Cuesta L, Sos ML, et al. Integrative genome analyses identify key somatic driver mutations of small-cell lung cancer. Nat Genet 2012;44:1104-10.

104. Jackman DM, Johnson BE. Small-cell lung cancer. Lancet 2005;366:1385-96.

105. Zabarovsky ER, Lerman MI, Minna JD. Tumor suppressor genes on chromosome 3p involved in the pathogenesis of lung and other cancers. Oncogene 2002;21:6915-35.

106. Ter Elst A, Hiemstra BE, van der Vlies P, et al. Functional analysis of lung tumor suppressor activity at 3p21.3. Genes Chromosomes Cancer 2006;45:1077-93.

107. Ji L, Roth JA. Tumor suppressor FUS1 signaling pathway. J Thorac Oncol 2008;3:327-30.

108. Agathanggelou A, Bieche I, hmed-Choudhury J, et al. Identification of novel gene expression targets for the Ras association domain family 1 (RASSF1A) tumor suppressor gene in non-small cell lung cancer and neuroblastoma. Cancer Res 2003;63:5344-51.

109. Simon GR, Wagner H. Small cell lung cancer. Chest 2003;123:259S-71S.

110. Chute JP, Chen T, Feigal E, Simon R, Johnson BE. Twenty years of phase III trials for patients with extensive-stage small-cell lung cancer: perceptible progress. J Clin Oncol 1999;17:1794-801.

111. Janne PA, Freidlin B, Saxman S, et al. Twenty-five years of clinical research for patients with limited-stage small cell lung carcinoma in North America. Cancer 2002;95:1528-38.

112. Johnson DH, Schiller JH, Bunn PA, Jr. Recent clinical advances in lung cancer management. J Clin Oncol 2014;32:973-82.

113. Koletsis EN, Prokakis C, Karanikolas M, Apostolakis E, Dougenis D. Current role of surgery in small cell lung carcinoma. J Cardiothorac Surg 2009;4:30.

114. Lim E, Belcher E, Yap YK, Nicholson AG, Goldstraw P. The role of surgery in the treatment of limited disease small cell lung cancer: time to reevaluate. J Thorac Oncol 2008;3:1267-71.

115. Small Cell Lung Cancer. 2015. (Accessed May 15, 2015, at http://www.cancer.ca/en/cancer-information/cancer-type/lung/lung-cancer/small-cell-lung-cancer/?region=on.)

116. Gaspar LE, McNamara EJ, Gay EG, et al. Small-cell lung cancer: prognostic factors and changing treatment over 15 years. Clin Lung Cancer 2012;13:115-22.

117. Ardizzoni A, Boni L, Tiseo M, et al. Cisplatin- versus carboplatin-based chemotherapy in first-line treatment of advanced non-small-cell lung cancer: an individual patient data meta-analysis. J Natl Cancer Inst 2007;99:847-57.

118. Noda K, Nishiwaki Y, Kawahara M, et al. Irinotecan plus cisplatin compared with etoposide plus cisplatin for extensive small-cell lung cancer. N Engl J Med 2002;346:85-91.

119. Rosenberg B, VanCamp L, Trosko JE, Mansour VH. Platinum compounds: a new class of potent antitumour agents. Nature 1969;222:385-6.

120. Galanski M. Recent developments in the field of anticancer platinum complexes. Recent Pat Anticancer Drug Discov 2006;1:285-95.

121. Galluzzi L, Senovilla L, Vitale I, et al. Molecular mechanisms of cisplatin resistance. Oncogene 2012;31:1869-83.

122. Cepeda V, Fuertes MA, Castilla J, Alonso C, Quevedo C, Perez JM. Biochemical mechanisms of cisplatin cytotoxicity. Anticancer Agents Med Chem 2007;7:3-18.

123. Gonzalez VM, Fuertes MA, Alonso C, Perez JM. Is cisplatin-induced cell death always produced by apoptosis? Mol Pharmacol 2001;59:657-63.

124. Furuta T, Ueda T, Aune G, Sarasin A, Kraemer KH, Pommier Y. Transcription-coupled nucleotide excision repair as a determinant of cisplatin sensitivity of human cells. Cancer Res 2002;62:4899-902.

125. Kunkel TA, Erie DA. DNA mismatch repair. Annu Rev Biochem 2005;74:681-710.

126. Timerbaev AR, Hartinger CG, Aleksenko SS, Keppler BK. Interactions of antitumor metallodrugs with serum proteins: advances in characterization using modern analytical methodology. Chem Rev 2006;106:2224-48.

127. Chen J, Emara N, Solomides C, Parekh H, Simpkins H. Resistance to platinum-based chemotherapy in lung cancer cell lines. Cancer Chemother Pharmacol 2010;66:1103-11.

128. Wu J, Hu CP, Gu QH, Li YP, Song M. Trichostatin A sensitizes cisplatin-resistant A549 cells to apoptosis by up-regulating death-associated protein kinase. Acta Pharmacol Sin 2010;31:93-101.

129. Zhang P, Gao WY, Turner S, Ducatman BS. Gleevec (STI-571) inhibits lung cancer cell growth (A549) and potentiates the cisplatin effect in vitro. Mol Cancer 2003;2:1.

130. Smit EF, de Vries EG, Timmer-Bosscha H, et al. In vitro response of human small-cell lung-cancer cell lines to chemotherapeutic drugs; no correlation with clinical data. Int J Cancer 1992;51:72-8.

131. Fischer SJ, Benson LM, Fauq A, Naylor S, Windebank AJ. Cisplatin and dimethyl sulfoxide react to form an adducted compound with reduced cytotoxicity and neurotoxicity. Neurotoxicology 2008;29:444-52.

132. Yi YW, Bae I. Effects of solvents on in vitro potencies of platinum compounds. DNA Repair (Amst) 2011;10:1084-5.

133. Hall MD, Telma KA, Chang KE, et al. Say no to DMSO: dimethylsulfoxide inactivates cisplatin, carboplatin, and other platinum complexes. Cancer Res 2014;74:3913-22.

134. Vellenga E, Biesma B, Meyer C, Wagteveld L, Esselink M, de Vries EG. The effects of five hematopoietic growth factors on human small cell lung carcinoma cell lines: interleukin 3 enhances the proliferation in one of the eleven cell lines. Cancer Res 1991;51:73-6.

135. Wang K, Ubriaco G, Sutherland LC. RBM6-RBM5 transcription-induced chimeras are differentially expressed in tumours. BMC Genomics 2007;8:348.

136. Mosmann T. Rapid colorimetric assay for cellular growth and survival: application to proliferation and cytotoxicity assays. J Immunol Methods 1983;65:55-63.

137. Masramon L, Vendrell E, Tarafa G, et al. Genetic instability and divergence of clonal populations in colon cancer cells in vitro. J Cell Sci 2006;119:1477-82.

138. Voigt K, Izsvak Z, Ivics Z. Targeted gene insertion for molecular medicine. J Mol Med (Berl) 2008;86:1205-19.

139. Hernandez J, Bechara E, Schlesinger D, Delgado J, Serrano L, Valcarcel J. Tumor suppressor properties of the splicing regulatory factor RBM10. RNA Biol 2016;13:466-72.

140. Knudson AG, Jr. Mutation and cancer: statistical study of retinoblastoma. Proc Natl Acad Sci U S A 1971;68:820-3.

141. Paige AJ. Redefining tumour suppressor genes: exceptions to the two-hit hypothesis. Cell Mol Life Sci 2003;60:2147-63.

142. Ozuemba B, Masilamani TJ, Loiselle JJ, et al. Co- and post-transcriptional regulation of Rbm5 and Rbm10 in mouse cells as evidenced by tissue-specific, developmental and disease-associated variation of splice variant and protein expression levels. Gene 2016;580:26-36.